

**STUDIA  
UNIVERSITATIS BABEŞ-BOLYAI**

**PHYSICA**

**1**

**1980**

**CLUJ-NAPOCA**

**REDACTOR SEF: Prof. I. VLAD**

**REDACTORI ŞEFI ADJUNCTI: Prof. I. HAIDUC, prof. I. KOVÁCS, prof. I. A. RUS**

**COMITETUL DE REDACȚIE FIZICĂ: Prof. Z. GÁBOS, prof. V. MERCEA, membru corespondent al Academiei, prof. AL. NICULA, prof. I. POP, prof. E. TĂTARU (redactor responsabil), asist. O. COZAR (secretar de redacție)**

# STUDIA

## UNIVERSITATIS BABEŞ-BOLYAI

### PHYSICA

1

---

R e d a c t a      3400 CLUJ-NAPOCA, str M Kogălniceanu, 1 ☎ Telefon 1 34 50

---

#### SUMAR – CONTENTS – SOMMAIRE

GH CRISTEA, V IONCU, D STĂNILĂ, The varicap diodes as temperature sensors in cryogeny	3
Diode varicap-sensori de temperatură în criogenie	
C COREGA, GH ILONCA, Momente magnetice locale în aliaje ternare pe bază de nichel	7
Located magnetic moments in ternary alloys with nickel	
R I CÂMPEANU, The use of the Kohn method in a re-arrangement problem	11
Metoda lui Kohn într-o problemă de rezaranjare	
O COZAR, V ZNAMIROVSCHI, Studul R E S al $[\text{Cu}(\text{NH}_2\text{CH}_2\text{CH}_2\text{OH})_4]\text{Cl}_2$ adsorbit pe $\text{SiO}_2$ și $\text{Al}_2\text{O}_3$	18
E S R study of adsorbed $[\text{Cu}(\text{NH}_2\text{CH}_2\text{CH}_2\text{OH})_4]\text{Cl}$ on $\text{SiO}_2$ and $\text{Al}_2\text{O}_3$	
Z GABOS, Asupra ecuațiilor de mișcare ale particulelor cu masa de repaos zero	22
Sur les équations de mouvement des particules de masse de repos zéro	
L COCIU, A MARTON, AL NICULA, Study on the ageing of stratified electro-insulating materials by the electron spin resonance method	26
Studiul îmbătrâinirii materialelor electroizolatoare prin metoda rezonanței electronice de spin	
D AUSLANDER, A ČIUPE, The change in the dimension distribution of solid particles in a suspension following ultrasonic dispersion	29
Modificarea distribuției de dimensiuni a particulelor solide dintr-o suspensie dispersată ultrasonic	
I LENART, D AUSLANDER, Absorbția structurală a ultrasunetului în soluții apoase de acizi organici	33
Structural absorption of ultrasound in aqueous solutions of organic acids	
M CRIȘAN, AL ANGHEL, Analytic S-matrix theory of critical phenomena for the $\phi^3$ and $\phi^4$ models	39
Teoria fenomenelor critice pentru modelele $\phi^3$ și $\phi^4$ pe baza proprietăților analitice a matricei S	
KARACSONY J, Effect of return current on the high frequency oscillations of a relativistic electron beam-plasma system	48
Efectul curentului invers asupra oscilațiilor de frecvențe ridicate ale sistemului plasmă-fascicul relativist de electroni	
C BĂLEANU, Effect of ion dynamics on the parametric instabilities of an unmagnetized plasma (I)	55
Efectul dinamicii ionilor asupra instabilităților parametrice ale unei plasme nemagnetizate (I)	
S COLDEA, Interdiffusion of gases in liquid metals	59
Interdifuzia gazelor în metale lichide	

S SIMON, AL NICULA, Effect of some paramagnetic ions on the structure of some borate vitreous matrices • Efectul unor ioni paramagneticici asupra structurii unor matrice vitroase pe bază de bor	63
D AUSLANDER, E DARVASI, A AUSLANDER, Investigations ultrasoniques sur l'alcool polyvinilique • Cercetări ultrasonice asupra alcoolului polivinilic	68
<b>Note — Notes</b>	
F KOCH, ESR and thermoluminescent response of $\text{CaSO}_4/\text{Mn}$ • RES și termoluminiscența $\text{CaSO}_4/\text{Mn}$	72
E MOTIU, C CODREANU, M VANCEA, C GH MACAROVICI, La conductivité électrique et la tension thermoélectromotrice du système $\text{Cr}_2\text{O}_3-\text{ZrO}_2$ • Conductivitatea electrică și tensiunea electromotoare în sistemul $\text{Cr}_2\text{O}_3-\text{ZrO}_2$	74
R I CÂMPEANU, Simple matter-antimatter systems • Sisteme simple de materie cu antimaterie	77
<b>Recenzii — Books — Livres parus</b>	
M Vasiliu, Electrodinamica și teoria relativității (J KARÁCSONY)	80

THE VARICAP DIODES AS TEMPERATURE SENSORS  
IN CRYOGENY

GH. CRISTEA, V. IONCU and D. STĂNILĂ

**Introduction.** The measurement and temperature control is the main operation in any cryogenic research as well as in industrial cryogenic equipment. For this purpose a number of devices, with temperature effects, have already been reported in literature, such as the temperature dependence of the voltage on the diode junction at constant current [1], the temperature dependence of the voltage on the transistor [2], the temperature dependence of the resistivity of semiconducting materials [3], and so on. The basic requirements which these devices should satisfy are the stability and reproducibility of their temperature dependent properties. In order to meet these requirements elaborated technologies, both for obtaining of semiconducting materials as well as for welding of the electric contacts have been worked out. To avoid these difficult technologies, which can be carried out only in high specialized laboratories, we have tested as temperature sensors some Romanian made varicap diodes. So, we have investigated the BB105-109 diodes, designed mainly for tuning in the VHF and UHF bands. The manufacturing technology for these diodes is well known. They are made in associated-groups of three or four in such a way that parameter dispersion within the group is low. This is necessary in order to satisfy the requirements of high quality temperature sensors.

**The temperature coefficient.** As it is well-known, for a directly biassed diode, the dependence of the current intensity through the diode junction, on the diode voltage, is

$$I_D = I_s (e^{\frac{nq U_D}{kT}} - 1), \quad (1)$$

where  $I_s$  is the saturation current at the given temperature,  $U_D$ -the diode voltage,  $n$ -a numerical constant whose value depends on the manufacturing technology ( $n=0.5-1$ ),  $q$ -the electron charge,  $k$ -the Boltzmann's constant,  $T$ -the diode temperature. Since the power of  $e$  must be dimensionless, the quantity  $kT/q$  should have the dimension of voltage. Its value, at the room temperature, is

$$U_T = \frac{kT}{q} \simeq 26 \text{ mV}$$

Replacing  $U_T$  in (1) it becomes

$$I_D = I_s (e^{\frac{U_D}{U_T}} - 1) \simeq I_s e^{\frac{U_D}{U_T}} \quad (2)$$

In normal working conditions  $U_D \approx 1V$ , so the error introduced by neglecting 1 in (2) is less than  $10^{-8}$  of the current value through the diode. The diode voltage is then easily obtained from (2), this being

$$U_D = \frac{U_T}{n} \ln \left( \frac{I_D}{I_s} \right) \quad (3)$$

For the calculation of the temperature coefficient of the diode voltage we must know the temperature dependence of the saturation current through the diode junction. If  $I_{so}$  is the saturation current at a reference temperature  $T_0 (= 273 \text{ K})$  then the saturation current at any temperature  $T$  is [4]

$$I_s = I_{so} \left( \frac{T}{T_0} \right)^m e^{\frac{qU_c}{k} \left( \frac{1}{T_0} - \frac{1}{T} \right)}$$

where  $U_c$  is the internal contact potential difference at junction. Replacing (4) in (3) we receive

$$I_D = U_c + T \left[ \frac{k}{nq} \ln \left( \frac{I_D}{I_{so}} \right) - \frac{U_c}{T_0} + \frac{k}{nq} m \ln \left( \frac{T}{T_0} \right) \right] \quad (5)$$

For  $T = 77 \text{ K}$ ,  $n = 0.5$  and  $m = 1/2$ , the last term in the square brackets is approximately  $10^{-4}$ , thus (5) can be approximated to

$$U_D \approx U_c - \left( \frac{U_c}{T_0} - \frac{k}{nq} \ln \frac{I_D}{I_{so}} \right) T \quad (6)$$

This equation shows that diode voltage must be a linear function of temperature. By taking the derivative versus temperature it follows

$$\alpha_T = \frac{dU}{dT} = \frac{k}{nq} \ln \frac{I_D}{I_{so}} - \frac{U_c}{T_0} \quad (7)$$

The BB105 diode has the values  $I_{so} \approx 10^{-10} \text{ A}$ ,  $I_D \approx 10^{-4} \text{ A}$  and  $U_c \approx 1 \text{ V}$ . Replacing these in (7), the value of temperature coefficient of the diode voltage will be

$$\alpha_T = \frac{dU}{dT} = -1646 \text{ mV/K} \quad (8)$$

**The measurement of temperature coefficient.** To verify the linearity of the equation (6), as well as for experimental determination of the temperature coefficient  $\alpha_T$ , we have made use of circuit shown in figure 1. We have chosen such a  $U_1$  value that on the one hand the diode current should be small enough to avoid selfheating effects, and on the other hand the current should be high enough to ensure a voltage drop on the diode of the order of one millivolt. First, the bridge is balanced by  $P_1$  potentiometer to compensate the diode voltage at a given temperature. We have done this at  $T_0 = 77 \text{ K}$ , so that measured  $U_D$  value was proportional to the difference  $T - T_0$ , between working and reference temperature. Of course, any temperature which can be precisely controlled and measured, can be chosen as reference temperature. We have investigated the BB105 and BB125 varicap diodes.

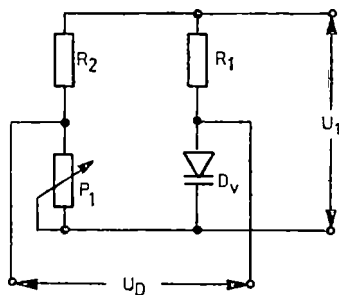


Fig. 1 The diagram of the bridge used for diode voltage measuring

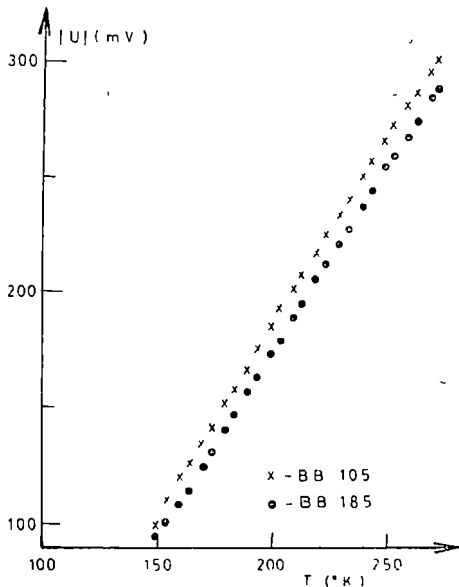


Fig. 2 The temperature dependence of the diode voltage

For the measurement of the temperature characteristics each diode was wrapped, by means of a copper band, together with one of the weldings of a Copper-Constantane thermocouple (of special composition) and stuck to a massive metallic electrod. The electrod was then immersed in a dewar vessel, containing liquid nitrogen. To avoid the condensation of water vapours a nitrogen atmosphere was created in the vessel. The other welding of the thermocouple was kept in water with ice.

A digital RFT, G-1212-010 type voltmeter, having the input resistance of  $30\text{ M}\Omega$ , was used for the measurement of the thermoelectric voltage. The diode voltage was measured by a TR-1452 type electronic microvoltmeter of  $1\text{ M}\Omega$  input resistance. This equipment enabled us to trace the temperature dependence of  $U_D$  with an accuracy of  $10^{-3}\text{ K}$ .

The temperature characteristics of  $U_D$  voltage for the investigated diodes are shown in figure 2. As it is seen the characteristics are linear within the investigated temperature range. The slope of the lines in the graphs gives us the following values for the temperature coefficients of the diode voltage.

$$\alpha_T(\text{BB}105) = 1.63 \text{ mV/K}$$

and

$$\alpha_T(\text{BB}125) = 1.57 \text{ mV/K}$$

These are in excellent agreement with the calculated value, eq (8). These results recommend the varicap diodes as temperature sensors for the measurement and control of the temperature.

(Received March 12, 1979)

## REF E R E N C E S

- 1 N. S. Bezverhnaja et al, *Pribori i tehnika experimenta*, **5**, 278 (1976)
- 2 D V Kucinsky, V M Lomako, *Pribori i tehnika experimenta*, **4**, 261 (1976)
- 3 J R Klement et al, in *Advances in Cryogenic Engineering*, vol 2, p 104, Editor K. D. Timmerhous, Plenum Press Inc, New York, 1960
- 4 M Drăgănescu, *Electronica corpului solid*, Ed tehnică, Bucureşti, 1972

## DIODE VARICAP-SENSORI DE TEMPERATURĂ ÎN CRIOGENIE

(Rezumat)

În lucrare se studiază proprietățile unor diode varicap de fabricație românească, ca termometre la temperaturi criogene. Se calculează valoarea coeficientului de temperatură al tensiunii pe diodă și se determină experimental valoarea lui. Linearitatea caracteristicilor de temperatură și valoarea mare a coeficientului de temperatură ale acestor diode le recomandă ca senzori de temperatură cu înaltă sensibilitate.

## MOMENTE MAGNETICE LOCALE ÎN ALIAJE TERNARE PE BAZĂ DE NICHEL

C. COREGA și GH. ILONCA

**Introducere.** Articole din ultima vreme impun necesitatea revizuirii anumitor considerații asupra comportării magnetice, în domeniul dezordonat al nichelului feromagnetic și a unor din aliajele sale. Se știe că principala deosebire dintre modelul localizat și cel de bandă se referă la saltul de entropie pe care le prezic acestea, la tranziția ordine-dezordine. Cum diferența dintre valorile prezise de cele două modele este aproape nesemnificativă în cazul nichelului, Beck și Flynn [1] au arătat posibilitatea existenței momentelor magnetice locale în Ni deasupra temperaturii de tranziție. Printr-o analiză pe calculator a datelor experimentale de susceptibilitate magnetică statică au reușit să le fiteze cu o lege de tip Curie-Weiss afectată de o contribuție în susceptibilitate independentă de temperatură, peste 1 000 K. Constanta Curie astfel determinată implică un moment magnetic efectiv  $\mu_{ef} = gS(S + 1)^{1/2} = 1,36 \mu_B$ , unde  $\mu_B$  este magnetonul Bohr iar  $S$  numărul cuantic de spin. Considerind  $g = 2$  se obține  $\mu^N = gS = 0,698 \mu_B$ .

Ideea a fost preluată de S. Arajs și J. R. Kelly [2], care analizând comportarea magnetică a aliajelor NiAl, ajung la aceeași concluzie.

Scopul lucrării de față este de a aduce noi argumente în sprijinirea acestei idei, studiind aliajele ternare NiCrAl, NiCrTi și NiMnTi. Alegerea acestor aliaje nu s-a făcut întâmplător ci datorită faptului că în cadrul aproximăției CPA (Coherent potential approximation), folosită curent în studiul aliajelor magnetice dezordonate, acordul cantitativ între calcule și datele experimentale nu este cel mai satisfăcător în cazul aliajelor binare NiCr și NiMn, la concentrația de peste 5% at impuritate (Cr Mn) [3, 4], necesitând deci o altă metodă de studiu.

**Rezultate și discuții.** Aliajele studiate au fost obținute prin topire în arc electric în atmosferă de argon. Investigarea proprietăților magnetice s-a făcut pe baza măsurătorilor de susceptibilitate magnetică statică, efectuate cu o balanță de tip Faraday, având o sensibilitate de ordinul a  $10^{-8}$  u em/g.

În cazul sistemului de aliaje  $NiCr_xAl_y$ , unde  $0 \leq x \leq 4$ ,  $0 \leq y \leq 9$ , datele experimentale au putut fi fitate satisfăcător cu o lege de forma  $x = x_0 + \frac{C}{T - \theta_F}$  pentru temperaturi superioare cu aproximativ 200 K temperaturilor de tranziție. Momentele magnetice efective astfel determinate respectă o lege de variație liniară față de concentrația medie de extraelectroni, aduși de elemente impuritate (fig. 1). Pentru aliajele conținând 3% at Cr și 0–9% at Al momentele magnetice  $\mu$  pe atom de nichel, calculate cu ajutorul momentelor magnetice efective  $\mu_{ef}$ , variază liniar în funcție de concentrația atomilor de aluminiu. După cum se vede în figura 2, dreapta astfel obținută este paralelă cu cea care rezultă din măsurători de saturare, primele valori fiind superioare cu aproximativ 0,2  $\mu_B$  față de ultimele. Luând în considerare efectul antiferomagnetic al cuplajului electronilor localizați cu cei de conducție folosindu-ne de valorile

obținute pentru Ni de către Arans și col [2] în aliajele de NiAl cu concentrația de Ni egală cu cea din aliajele noastre (Ni—Cr—Al) am recalculat momentele magnetice obținând în final dreapta din mijloc, figura 2. Se observă că diferența dintre valorile de pe această dreaptă și cele obținute din măsurători de saturatie este de aproximativ  $0,1 \mu_B$ , valoare ce poate fi comparată cu cea

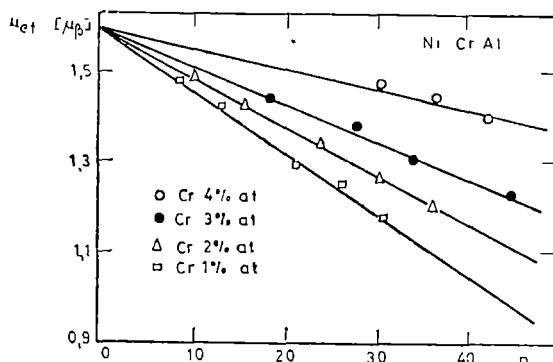


Fig. 1 Variația momentului magnetic efectiv în funcție de concentrația medie de extraelectroni aduși de elementele impuritate Cr și Al

Fig. 2 Dependența momentului magnetic efectiv de concentrația atomilor de aluminiu pentru aliajul Ni—Cr—Al

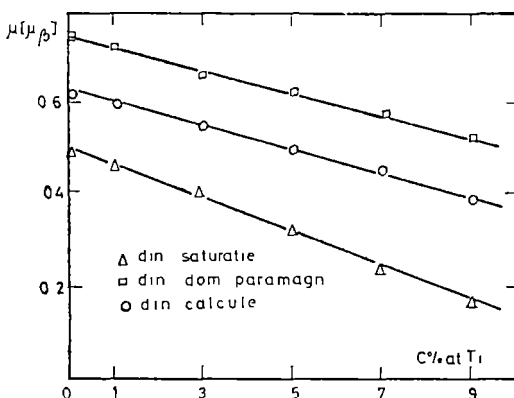
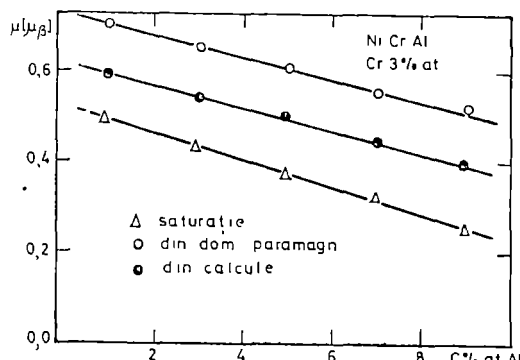


Fig. 3 Dependența momentului magnetic efectiv de concentrația atomilor de titan pentru aliajul Ni—Cr—Ti

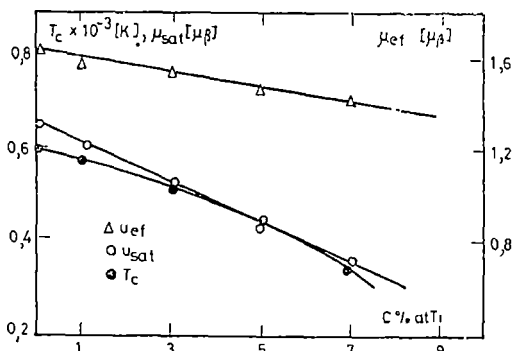


Fig. 4 Dependenta temperaturii Curie de concentratia atomilor de titan pentru aliajul Ni-Cr-Ti

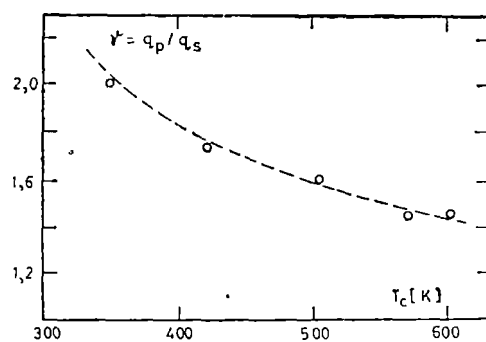


Fig. 5 Variația factorului  $\gamma$  în funcție de temperatura Curie

pusă în evidență în lucrările [1] și [2], și care este interpretată cu o polarizare negativă a gazului electronilor de conducție.

Rezultatele asemănătoare s-au obținut și în cazul aliajelor NiCrTi conținând 3% at Cr și de la 0–9% at Ti (fig. 3). S-au considerat, în calcule, că Ti își aduce o contribuție doar în cadrul amestecului s-d. Efectele de ordonare magnetică de „short-range” existente și în cazul aliajelor NiCrAl [5] sunt mai puternice în acest sistem de aliaje, lucru ce rezultă din diferența de 0,1–0,2  $\mu_B$  între valorile calculate și momentele de la saturație. Variația diferenței  $\mu_{\text{recalculat}} - \mu_{\text{saturație}}$  în funcție de concentrația de Ti se poate pune pe baza modificării polarizării negative a gazului electronic ca urmare, în principal, a modificării densității de stări prin adiția atomilor de titan.

Efectele de ordonare magnetică de „short-range” sunt mult mai puternice în cazul aliajelor NiMnTi, conținând 3% at Mn și de la 0–9% at Ti, fapt care face ca modelul folosit mai sus să nu poată fi utilizat cu succes la acest sistem de aliaje. Din figura 4 se observă că punctele Curie feromagnetice se aşază pe un arc de curbă în timp ce momentele magnetice efective și cele de saturație prezintă o dependență liniară față de concentrația atomilor de titan. Întrucînt și în cazul aliajelor NiTi [6] temperaturile critice se aşază pe un arc de curbă rezultă că atomii de Ti sunt cei care determină, în principal, forma dependenței acestora de concentrația elementului impuritate. Se cere a fi menționată buna concordanță între rezultatele noastre și cele din literatură. Astfel, momentul magnetic mediu pe atom de mangan variază de la 2,32 la 1,83  $\mu_B$  cînd concentrația atomilor de titan crește de la 0 la 75%. Dependența raportului dintre numărul de purtători magnetici din starea paramagnetică și cei din starea feromagnetică, de temperaturile critice feromagnetice, prezentată în figura 5, atestă faptul că explicarea comportării magnetice a acestor aliaje în cadrul unui model de bandă rigidă nu este satisfăcătoare.

**Concluzii.** În urma studiului celor trei sisteme de aliaje pe bază de Ni, se pune în evidență existența momentelor magnetice localizate și în aliajele ternare în acord cu ideile lui Beck și Flynn [1], punîndu-se totodată în evidență prezența pînă la temperaturi suficient de înalte efectele de ordonare magnetică de „short-range”.

Presupunem că modelul LEBV generalizat de două benzi ar descrie mai bine din punct de vedere cantitativ rezultatele experimentale în cadrul sistemelor ternare pe bază de nichel.

(Received March 14, 1979)

#### B I B L I O G R A F I E

- 1 P A Beck, C P Flynn, Sol State Comm., **18**, 1, 127 (1976)
- 2 S Arajs, J R Kelly, 21-st Ann Conf Magn, Philadelphia, 1975
- 3 R Hasegawa, M Kanamori, J Phys Soc, Japan, **31**, 2, 380 (1970)
- 4 R Hasegawa, M Kanamori, J Phys Soc Japan, **33**, 1599 (1973)
- 5 Gh Ilonca, C Corega, *Lucrările Simpozionului Național de Fizica Solidului*, Cluj-Napoca, 1978, p 38
- 6 V Marian, Ann Phys, **7**, 459 (1956)
- 7 V A Ivanov, Fiz Metalov i Metalovedenie, **43**, 1148 (1977)

#### LOCATED MAGNETIC MOMENTS IN TERNARY ALLOYS WITH NICHEL

(Summary)

It was determined the temperature dependence of magnetic susceptibility NiCrAl, NiCrTi and NiMnTi ternary alloys in the concentration range of 1–2% at Cr, Ti, Mn, respectively, between 80–1200 K. Magnetic susceptibility data satisfied Curie-Weiss modified law

The study of these systems have put in evidence the existence of the located magnetic moments in ternary alloys with nickel in agreement with the ideas of Beck and Flynn [1]

# THE USE OF THE KOHN METHOD IN A RE-ARRANGEMENT PROBLEM

R. I. CÂMPEANU

**Introduction.** The use of the Kohn method in elastic collision calculations was proven to be very fruitful. Initially used in nuclear few bodies problems [1, 2], the method was then extended to atomic collisions, where it gave excellent elastic phase shifts when employed with a sufficiently elaborate trial function [3, 4]. In spite of this success in the elastic case, the Kohn method was never employed in an atomic inelastic collision calculation. We believe that this is due to the extension of the calculation rather than some mathematical difficulties. However, modern, fast computers can cope with the amount of numerical work required in a few bodies inelastic collision calculation.

The re-arrangement processes are of particular interest among the inelastic collisions. In atomic physics, such a process is the positronium formation, which appears as an interesting feature of the positron collision on both atoms and molecules. The positronium ( $Ps$ ) is a bound state of an electron with a positron and has a lifetime before mutual annihilation of about  $10^{-10}$  sec. when their spins are antiparallel (para- $Ps$ ) and  $10^{-17}$  sec. when their spins are parallel (ortho- $Ps$ ). These lifetimes are long compared to the collision time, which is of the order of  $10^{-17}$  sec. Thus, it is meaningful to talk about positronium formation by collision.

Calculations on positronium formation by positrons colliding with hydrogen atoms are not as numerous as on elastic scattering. Earlier work includes the Born approximation of Masssey and Mohr [5] and the impulse approximation of Cheshire [6]. Bransden and Judd [7] obtained formation cross sections in the two state approximation and considered then the effect of adding various multipoles of the polarization potential in each of the hydrogen and  $Ps$  channel. Similar calculations have also been performed by Fels and Mittelman [8] and Cody et al [9]. More accurate results were obtained by Dirks and Hahn [10] and by Chan et al [11], [12], both formulations giving lower bounds on the R-matrix elements. The work of Chan et al used the close coupling algebraic method with trial functions with up to 26 Hylleraas terms and gave the best s and p-wave results to date. We intend to use a similar s-wave trial function but within the two channel Kohn method. In the case of the elastic collision the two methods gave very similar results [4].

**The trial function.** At energies above the  $Ps$  formation threshold the positron-hydrogen system wave function  $\psi(\vec{r}_1, \vec{r}_2)$  can have two distinct asymptotic forms

$$\begin{aligned} \psi(\vec{r}_1, \vec{r}_2) &\underset{r_1 \rightarrow \infty}{\sim} \Phi_H(r_2)F(r_1) \\ \psi(\vec{r}_1, \vec{r}_2) &\underset{\rho \rightarrow \infty}{\sim} \Phi_{Ps}(r_{12})G(\rho) \end{aligned} \quad (1)$$

where  $r_1$  and  $r_2$  are the positron and respectively the electron coordinates relative to the proton, which is considered infinitely massive and fixed at the origin of the coordinate system,  $\bar{\rho} = \frac{1}{2}(\bar{r}_1 + \bar{r}_2)$  is the centre of mass coordinate of the positronium atom,  $\Phi_H(r_2)$  and  $\Phi_{Ps}(r_{12})$  are the hydrogen and the positronium ground state wave functions. They satisfy the Schrödinger equations (atomic system of units)

$$\begin{aligned} \left( -\nabla_{r_2}^2 - \frac{2}{r_2} + 1 \right) \Phi_H(r_2) &= 0 \\ \left( -2\nabla_{r_{12}}^2 - \frac{2}{r_{12}} + \frac{1}{2} \right) \Phi_{Ps}(r_{12}) &= 0 \end{aligned} \quad (2)$$

and are explicitly given by

$$\begin{aligned} \Phi_H(r_2) &= \pi^{-1/2} \exp(-r_2) \\ \Phi_{Ps}(r_{12}) &= (8\pi)^{-1/2} \exp\left(-\frac{r_{12}}{2}\right) \end{aligned} \quad (3)$$

The functions  $F(r_1)$  and  $G(\rho)$  satisfy asymptotically the free particle equations

$$\begin{aligned} (\nabla_{r_1}^2 + k^2) F(r_1) &= 0 \\ \left( \frac{1}{2} \nabla_\rho^2 + \frac{1}{2} K^2 \right) G(\rho) &= 0 \end{aligned} \quad (4)$$

where  $k$  and  $K$  are the positron and  $Ps$  momenta respectively

The total energy of the system is shared differently in the two asymptotic situations

$$E = k^2 + E_H = \frac{1}{2} K^2 + E_{Ps} \quad (5)$$

and therefore  $K^2 = 2(k^2 + E_H - E_{Ps}) = 2k^2 - 1$

The s-wave Schrödinger equation of the system  $(H - E)\psi = 0$  can take two alternative forms due to the asymptotic relations (1)

$$\begin{aligned} \left( -\nabla_{r_1}^2 - \nabla_{r_2}^2 - \frac{2}{r_2} - \frac{2}{r_{12}} + \frac{2}{r_1} + 1 - k^2 \right) \psi(\bar{r}_1, \bar{r}_2) &= 0 \\ \left( -\frac{1}{2} \nabla_\rho^2 - 2\nabla_{r_{12}}^2 - \frac{2}{r_{12}} - \frac{2}{r_2} + \frac{2}{r_1} + \frac{1}{2} - \frac{1}{2} K^2 \right) \psi(\bar{r}_1, \bar{r}_2) &= 0 \end{aligned} \quad (6)$$

They can be rewritten by using (1) and (2) as

$$\begin{aligned} \left( -\nabla_{r_1}^2 - \frac{2}{r_{12}} + \frac{2}{r_1} - k^2 \right) \psi(\bar{r}_1, \bar{r}_2) &= 0 \\ \left( -\frac{1}{2} \nabla_\rho^2 - \frac{2}{r_2} + \frac{2}{r_1} - \frac{1}{2} K^2 \right) \psi(\bar{r}_1, \bar{r}_2) &= 0 \end{aligned} \quad (7)$$

We denote two linearly independent solutions of (7) by  $\psi_n$ ,  $n = 1, 2$ . Since  $F$  and  $G$  satisfy asymptotically (4) we can write the s-wave components of  $\psi_n$  as

$$\begin{aligned}\psi_{1t} &= \sqrt{\frac{k}{4\pi}} [\jmath_0(kr_1) - R_{11t}n_0(kr_1)(1 - e^{-\lambda r_1})] \Phi_H(r_2), \\ &\quad - \sqrt{\frac{K}{2\pi}} R_{21t}n_0(K\rho)(1 - e^{-\zeta\rho}) \Phi_{Ps}(r_{12}) + \frac{1}{\sqrt{4\pi}} \sum_{i=1}^N e_i \chi_i \quad (8)\end{aligned}$$

$$\begin{aligned}\psi_{2t} &= - \sqrt{\frac{k}{4\pi}} R_{12t}n_0(kr_1)(1 - e^{-\lambda r_1}) \Phi(r_2) + \sqrt{\frac{K}{2\pi}} [\jmath_0(K\rho) - R_{22t}n_0(K\rho)(1 - e^{-\zeta\rho})] \times \\ &\quad \times \Phi_{Ps}(r_{12}) + \frac{1}{\sqrt{4\pi}} \sum_{i=1}^N d_i \chi_i\end{aligned}$$

where  $\jmath_0$  and  $n_0$  are the Bessel and Neumann wave functions, describing the correct asymptotic behaviour of the system and the binomials multiplying the functions  $n_0$  ensure that every term in (8) is finite at  $r_1 = 0$  or  $\rho = 0$ . The trial functions (8) differ from the exact wave functions only because of their incomplete inclusion of the short range effects. A measure of the accuracy of  $\psi_n$  is given by the number of short range Hylleraas terms  $\chi_i$ :

$$\chi_i = \exp(-\alpha r_1 - \beta r_2) r_1^{k_i} r_2^{l_i} r_{12}^{m_i} \quad (9)$$

with  $k_i + l_i + m_i \leq w$ , all non-negative integers

$R_{mn}$  ( $m$  and  $n = 1, 2$ ) are the  $R$  matrix elements (the trial symmetric reactance matrix). The exact  $R$  matrix is related to the  $S$  and  $T$ -matrix by the relations

$$T = \frac{-2\imath R}{1 - \imath R}, \quad S = 1 - T \quad (10)$$

and to the cross section for the reaction from the channel  $m$  to the channel  $n$  by.

$$\sigma_{mn} = \frac{4}{k_m^2} \left| \left( \frac{R}{1 - \imath R} \right)_{mn} \right|^2 \quad (11)$$

where  $\sigma_{mn}$  is in units of  $\pi a_0^2$  and  $k_1 = k$ ,  $k_2 = K$

**The Kohn procedure.** The Kohn variational invariant may be written as [13].

$$\bar{R}_{mn} = R_{mn} - \langle \psi_{mt} | H - E | \psi_{nt} \rangle, \quad m, n = 1 \text{ or } 2 \quad (12)$$

where the variational  $\bar{R}_{mn}$  differ from the exact values  $R_{mn}$  by a second order error term

One can simplify the notation by writing

$$\begin{aligned} s_1 &= \sqrt{\frac{k}{4\pi}} j_0(kr_1) \Phi_H(r_2) & s_2 &= \sqrt{\frac{K}{2\pi}} j_0(K\rho) \Phi_{Ps}(r_{12}) \\ c_1 &= -\sqrt{\frac{k}{4\pi}} n_0(kr_1)(1 - e^{-\lambda r_1}) \Phi_H(r_2) & c_2 &= -\sqrt{\frac{K}{2\pi}} n_0(K\rho)(1 - e^{-\zeta\rho}) \Phi_{Ps}(r_{12}) \end{aligned} \quad (13)$$

Using (13) the variational expression (12) becomes

$$\begin{aligned} \bar{R}_{mn} = R_{mn} - & \{ \delta_{1m} \delta_{1n} < s_1 L s_1 > + R_{1mt} R_{1nt} < c_1 L c_1 > + \delta_{1n} R_{1mt} < c_1 L s_1 > + \\ & + \delta_{1m} R_{1nt} < s_1 L c_1 > + \delta_{2n} R_{2mt} < c_2 L s_2 > + \delta_{2m} R_{2nt} < s_2 L c_2 > + \\ & + \delta_{2m} \delta_{2n} < s_2 L s_2 > + R_{2mt} R_{2nt} < c_2 L c_2 > + (\delta_{1m} \delta_{1n} + \delta_{2m} \delta_{1n}) < s_2 L s_1 > + \\ & + (\delta_{1m} R_{2nt} + \delta_{1n} R_{2mt}) < c_2 L s_1 > + (\delta_{2m} R_{1nt} + \delta_{2n} R_{1mt}) < s_2 L c_1 > + \\ & + (R_{1mt} R_{1nt} + R_{2mt} R_{2nt}) < c_2 L e_1 > + (\delta_{1m} \delta_{2n} + \delta_{2m} \delta_{1n}) (\sum_i e_i < s_2 L \chi_i > + \\ & + \sum_j d_j < s_1 L \chi_j >) + 2 \delta_{1m} \delta_{1n} \sum_i e_i < s_1 L \chi_i > + 2 \delta_{2m} \delta_{2n} \sum_j d_j < s_2 L \chi_j > + \\ & + (\delta_{1m} R_{2nt} + R_{2mt} \delta_{1n}) \sum_i e_i < c_2 L \chi_i > + (R_{1mt} \delta_{2n} + \delta_{2m} R_{1nt}) \sum_j d_j < c_1 L \chi_j > + \\ & + (\delta_{1m} R_{1nt} + R_{1mt} \delta_{1n}) \sum_i e_i < c_1 L \chi_i > + (\delta_{2m} R_{2nt} + R_{2mt} \delta_{2n}) \sum_j d_j < c_2 L \chi_j > + \\ & + 2 \delta_{1m} \delta_{1n} \sum_i \sum_j e_i e_j < \chi_i L \chi_j > + 2 \delta_{2m} \delta_{2n} \sum_i \sum_j d_i d_j < \chi_i L \chi_j > + \\ & + 2 (\delta_{1m} \delta_{2n} + \delta_{2m} \delta_{1n}) \sum_i \sum_j e_i d_j < \chi_i L \chi_j > \}, \end{aligned} \quad (14)$$

where  $L = H - E$

The Kohn method considers the variations with the linear parameters in the variational invariants (12) which are to the first order equal to zero

$$\frac{\partial \bar{R}_{mn}}{\partial R_{mn}} = 0, \frac{\partial \bar{R}_{mn}}{\partial e_i} = 0, \frac{\partial \bar{R}_{mn}}{\partial d_j} = 0 \quad (15)$$

with  $i$  and  $j = 1, 2, \dots, N$

One can show that the total number of independent equations is equal to  $2N + 4$ . For instance, one can apply Kohn's procedure (15) to the stationary forms  $\bar{R}_{11}$  and  $R_{22}$  and it is then easy to show that any equation coming from  $\bar{R}_{12}$  and  $\bar{R}_{21}$  is a linear combination of the first  $2N + 4$  equations.

A convenient way of writing the  $2N + 4$  equations is the matrix equation  $AX = B$ , where  $X$  is a column vector containing the variational parameters

and  $A$  and  $B$  are a square and respectively a column matrix containing the integrals appearing in (14).

$$\left| \begin{array}{ccccccccc} \langle c_1 L c_1 \rangle & 0 & \langle c_2 L c_1 \rangle & 0 & \langle c_1 L \chi_1 \rangle & \langle c_1 L \chi_N \rangle & 0 & 0 & R_{11t} \\ \langle c_2 L c_1 \rangle & 0 & \langle c_2 L c_2 \rangle & 0 & \langle c_2 L \chi_1 \rangle & \langle c_2 L \chi_N \rangle & 0 & 0 & R_{12t} \\ 0 & \langle c_2 L c_1 \rangle & 0 & \langle c_2 L c_2 \rangle & 0 & 0 & \langle c_2 L \chi_1 \rangle & \langle c_2 L \chi_N \rangle & R_{21t} \\ 0 & \langle c_1 L c_1 \rangle & 0 & \langle c_2 L c_1 \rangle & 0 & 0 & \langle c_1 L \chi_1 \rangle & \langle c_1 L \chi_N \rangle & R_{22t} \\ \langle c_1 L \chi_1 \rangle & 0 & \langle c_2 L \chi_1 \rangle & 0 & \langle \chi_1 L \chi_1 \rangle & \langle \chi_1 L \chi_N \rangle & 0 & 0 & e_N \\ \vdots & \vdots \\ \langle c_1 L \chi_N \rangle & 0 & \langle c_2 L \chi_N \rangle & 0 & \langle \chi_N L \chi_1 \rangle & \langle \chi_N L \chi_N \rangle & 0 & 0 & d_N \\ 0 & \langle c_1 L \chi_1 \rangle & 0 & \langle c_2 L \chi_1 \rangle & 0 & 0 & \langle \chi_1 L \chi_1 \rangle & \langle \chi_1 L \chi_N \rangle & e_N \\ \vdots & \vdots \\ 0 & \langle c_1 L \chi_N \rangle & 0 & \langle c_2 L \chi_N \rangle & 0 & 0 & \langle \chi_N L \chi_1 \rangle & \langle \chi_N L \chi_N \rangle & d_N \end{array} \right| = \left| \begin{array}{c} -\langle c_1 L s_1 \rangle \\ -\langle c_2 L s_1 \rangle \\ -\langle c_2 L s_2 \rangle \\ -\langle s_2 L c_1 \rangle \\ -\langle s_1 L \chi_1 \rangle \\ \vdots \\ \vdots \\ -\langle s_1 L \chi_N \rangle \\ -\langle s_2 L \chi_1 \rangle \\ \vdots \\ \vdots \\ -\langle s_2 L \chi_N \rangle \end{array} \right| \quad (16)$$

After solving the matrix equation (16), the solution  $\tilde{X}$  can be used in the equations (14) to obtain the variational values  $\bar{R}_{mn}$ .

In writing (14) and (16) we have used the equations.

$$\begin{aligned} \langle s_m L s_n \rangle &= \langle s_n L s_m \rangle & \langle s_m L c_n \rangle &= \langle c_n L s_m \rangle \\ \langle c_m L c_n \rangle &= \langle c_n L c_m \rangle & \langle s_n L c_n \rangle &= \langle c_n L s_n \rangle + 1, \\ \text{with } m \neq n & & \text{and } m, n = 1, 2 & \end{aligned} \quad (17)$$

which are proven in the appendix and can be used as a check on the numerical accuracy.

In the second paper on this subject we shall give the results obtained with this method for the positronium formation cross sections in hydrogen, together with the numerical procedure, accuracy and convergence of the results.

I would like to thank Drs. J. W. Humberston and A. H. A. Moussa for a few useful discussions on this subject.

**Appendix.** The integral relations (17) are basically of two types: the first one shows the interchangeability of the two long range functions when they come from different channels and the second type concerns integrals containing asymptotic functions of the same channel.

For the first category let us take the integral relation.

$$\langle s_2 L c_1 \rangle - \langle c_1 L s_2 \rangle = 0 \quad (A1)$$

The only part which might not be zero in (A1) is

$$\langle s_2, -\sum_{m=1}^2 \nabla_{r_m}^2 c_1 \rangle - \langle c_1, -\sum_{m=1}^2 \nabla_{r_m}^2 s_2 \rangle \quad (A2)$$

with  $s_2$  and  $c_1$  defined in (13)

Applying the Green theorem, the expression (A2) can be written as

$$\begin{aligned} & -\frac{1}{2\pi} \sqrt{\frac{kK}{2}} \int_V d\bar{r}_2 \int_S d\bar{s}_1 \left\{ \Phi_H J_0(K\rho) \Phi_{Ps} \frac{\partial}{\partial r_1} [n_0(kr_1)(1 - e^{-\lambda r_1})] - \right. \\ & \left. - \Phi_H n_0(kr_1)(1 - e^{-\lambda r_1}) \frac{\partial}{\partial r_1} [J_0(K\rho) \Phi_{Ps}] \right\}_{r_1 \rightarrow \infty} - \frac{1}{2\pi} \sqrt{\frac{kK}{2}} \times \\ & \times \int_V d\bar{r}_1 \int_S d\bar{s}_2 \left\{ n_0(1 - e^{-\lambda r_1}) J_0(K\rho) \Phi_{Ps} \frac{\partial}{\partial r_2} \Phi_H - \Phi_H n_0(1 - e^{-\lambda r_1}) \frac{\partial}{\partial r_2} [J_0(K\rho)_P \Phi_s] \right\}_{r_2 \rightarrow \infty} \end{aligned} \quad (\text{A3})$$

where

$$d\bar{s}_m = \hat{n} r_m^2 \sin \theta_m d\theta_m d\varphi_m \quad (m = 1, 2)$$

The expression (A3) is zero because in any term involved there is an exponential function  $\Phi_H$  or  $\Phi_{Ps}$  which will be zero as  $r_m \rightarrow \infty$

From the two integral relations of the second type let us take

$$\langle s_1 L c_1 \rangle = \langle c_1 L s_1 \rangle + 1 \quad (\text{A4})$$

The integrals  $\langle s_1 L c_1 \rangle - \langle c_1 L s_1 \rangle$  can be written after the use of the equation (2a) and the integration on  $r_2$  as

$$-\int_V d\bar{r}_1 \left\{ J_0 \nabla_{r_1}^2 n_0 - n_0 \nabla_{r_1}^2 J_0 \right\} \frac{k}{4\pi} \quad (\text{A5})$$

where the factor  $(1 - e^{-\lambda r_1})$  was dropped as it is not influencing the result. We can apply the Green theorem in (A5)

$$-\int_S d\bar{s}_1 \frac{k}{4\pi} \left\{ J_0 \frac{\partial n_0}{\partial r_1} - n_0 \frac{\partial J_0}{\partial r_1} \right\}_{r_1 \rightarrow \infty} \quad (\text{A6})$$

and taking only the leading terms as  $r_1 \rightarrow \infty$ , (A6) becomes

$$\begin{aligned} & -\frac{1}{4\pi} \int_S \hat{n} r_1^2 \sin \theta_1 d\theta_1 d\varphi_1 \left\{ -\frac{\sin^2 kr_1}{r_1^2} - \frac{\cos^2 kr_1}{r_1^2} \right\} = \\ & = \frac{1}{4\pi} \int_0^{2\pi} d\varphi_1 \int_0^\pi \sin \theta_1 d\theta_1 = 1 \end{aligned} \quad (\text{A7})$$

(Received June 6, 1979)

## R E F E R E N C E S

1. J. W. Humberston, Nucl. Phys., **69**, 291 (1965)
2. L. M. Delves, *Advances in Nuclear Physics*, Vol. 5, pag. 1, Plenum Press, 1972
3. R. I. Cămpleanu, J. W. Humberston, J. Phys., B **10**, L153 (1977)
4. R. I. Cămpleanu, PhD Thesis, Univ. of London, 1977

- 5 H S W Massey, C B O Mohr, Proc Phys Soc, **A67**, 695 (1954)
- 6 I M Cheshire, Proc Phys Soc (London) **83**, 227 (1964)
- 7 B H Bransden, Z Jundi, Proc Phys Soc, **92**, 880 (1967)
- 8 M F Fels, M H Middleman, Phys Rev, **163**, 129 (1967)
- 9 W J L Cody, L Lawson, H S W Masey, K Smith, Proc Roy Soc **A278**, 479 (1964)
10. J F Dirks, Y Hahn, Phys Rev, **A3**, 310 (1971)
- 11 Y F Chan, P A Fraser, J Phys, **B 6**, 2504 (1973)
- 12 Y F Chan, R P McEachran, J Phys, **B 9**, 1 (1976)
- 13 W Eissner, M J Seaton, J Phys, **B 5**, 2187 (1972)

### METODA LUI KOHN ÎNTR-O PROBLEMĂ DE REARANJARE

(Rezumat)

Metoda lui Kohn are un deosebit succes în rezolvarea problemelor de ciocnire elastică, dar nu a fost niciodată utilizată într-o problemă de ciocnire inelastică. Se folosește un caz tipic de proces de rearanjare — formarea pozitroniului prin impact pozitronic pe atomul de hidrogen — pentru a se testa calitățile metodei lui Kohn într-o problemă inelastică. În această primă lucrare se formulează metoda pentru o funcție de incercare conținând funcții de rază de acțiune scurtă de tip Hylleraas și se reduce problema la rezolvarea unei ecuații matriciale.

**STUDIUL R.E.S. AL  $[\text{Cu}(\text{NH}_2\text{CH}_2\text{CH}_2\text{OH})_4]\text{Cl}_2$  ADSORBIT  
PE  $\text{SiO}_2$  ŞI  $\text{Al}_2\text{O}_3$**

O. COZAR și V. ZNAMIROVSCHI

În lucrarea de față ne-am propus un studiu al influenței suprafăcetelor  $\text{SiO}_2$  și  $\text{Al}_2\text{O}_3$  asupra complexului albastru [1] de  $\text{Cu}(\text{II})$ -monoetanolamină

Silicagelul folosit este fabricat de Mallinckrodt Chemical Works și notat prin ARCC-4/100—200, cu suprafață specifică de  $600 \text{ m}^2/\text{g}$ , iar alumina este de tip Carlo Erba cu suprafață specifică de  $75 \text{ m}^2/\text{g}$

Probele s-au obținut prin impregnarea pulberilor respective timp de o oră în soluții apoase având concentrația de  $5 \text{ mg}/\text{cm}^3$ . După uscare în aer la  $70$ — $80^\circ\text{C}$  pentru înlăturarea excesului de apă, acestea au fost închise în tuburi de sticlă cu diametrul de  $1,5$ — $2 \text{ mm}$ .

Spectrul R.E.S. obținut la temperatura camerei pentru probele cu  $\text{SiO}_2$  având un conținut de  $\sim 2$  monostraturi apă (fig. 1a), indică coexistența a două tipuri de complecși: unii legați de suprafața suport, ce dău un spectru caracteristic fazei solide, înghețate, și alții care pătrund în porii sau cavitățile silicagelului unde rămîne apă în exces, spectrul dat de aceștia fiind asemănător fazei lichide, soluțiilor apoase. Spre deosebire de spectrul obținut pentru  $[\text{Cu}(\text{tri(en)})\text{SCN}] \text{SCN}$  absorbit pe silicagel [2], în cazul monoetanolaminei, componenta datorată complecșilor cu mobilitate ridicată este destul de slabă, numărul acestora fiind mic, probabil datorită dimensiunilor mari ale moleculelor de ligand, fapt ce îngreunează pătrunderea lor în cavitățile suportului.

Printr-o deshidratare suplimentară a probei în aer la  $70$ — $80^\circ\text{C}$ , spectrul devine tipic fazei solide, cu linii hiperfine din banda paralelă rezolvate, ceea ce indică o imobilizare a tuturor moleculelor de complex.

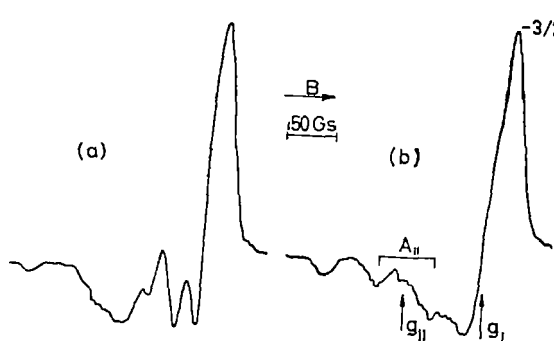


Fig. 1 Spectrele R.E.S. ale  $\text{Cu}(\text{II})$ -monoetanolaminei pe  $\text{SiO}_2$ , la temperatura camerei: (a) — probă cu  $\sim 2$  monostraturi apă, (b) — după deshidratare suplimentară ( $\sim 1$  monostrat).

Forma și parametrii acestui spectru (fig. 1b) rămân neschimbați prin înghețare la  $77 \text{ K}$ , ceea ce înseamnă că structura și pozițiile complecșilor nu se mai modifică semnificativ.

În cazul utilizării aluminei ca suport, spectrele R.E.S. obținute la temperatura camerei prezintă o anizotropie clară, linii hiperfine din banda paralelă fiind complet rezolvate fără o deshidratare suplimentară (fig. 2a). Acest fapt arată că în cazul aluminei toate moleculele de complex sunt fixate de suport datorită suprafetei specifice reduse și a reținerii

unei cantități mici de apă ( $\leq 1$  monostrat)

Spre deosebire de spectrul din fig. 1b, în cazul  $\text{Al}_2\text{O}_3$  apare o separare clară între semnalul  $m_I = -3/2$  din absorbția paralelă și cel caracteristic absorbției perpendiculare (fig. 2a). Forma spectrului rămîne asemănătoare și la 77 K (fig. 2b), modificîndu-se doar raportul intensității celor două semnale menționate mai sus.

Pe lîngă diferențele observate în forma spectrelor, se constată de asemenea și modificări ale valorilor tensorului  $\tilde{g}$  și de structură hiperfină  $\tilde{A}$ , în funcție de suportul utilizat (tabel 1).

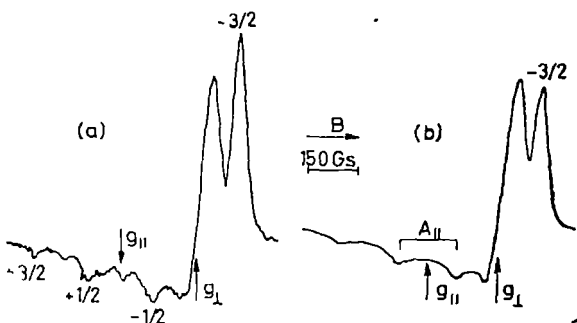


Fig. 2 Spectrele RES ale  $\text{Cu}(\text{II})$ -monoetanolamină pe  $\text{Al}_2\text{O}_3$  (a) – la temperatură camerei, (b) – la 77 K

Tabel 1

Suprafața suport	$g_{  }$	$g_{\perp}$	$A_{  }$ ( $10^{-4} \text{ cm}^{-1}$ )	$A_{\perp}$ ( $10^{-4} \text{ cm}^{-1}$ )	$\alpha^2$	$\beta^2$	$\delta^2$
$\text{SiO}_2$	2,186	2,040	163	19	0,70	0,60	0,52
$\text{Al}_2\text{O}_3$	2,245	2,068	188	19	0,86	0,64	0,72

Spectrele RES obținute, precum și valorile parametrilor  $g_{||} > g_{\perp} > 2,002$ , arată că simetria dominantă a complecșilor adsorbiți pe cele două suprafețe este axială ( $D_{4h}$ ) cu electronul paramagnetic în orbitalul  $d_{x^2-y^2}$ . În aceste considerente, orbitalii moleculari de antilegătură caracteristici stării fundamentale și celor excitate ale electronului  $3d$  sănt [3]

$$|B_{1g}\rangle = \alpha d_{x^2-y^2} - \alpha' \Phi_{\sigma}(x^2 - y^2) \quad (1)$$

$$|B_{2g}\rangle = \beta d_{xy} - (1 - \beta^2)^{\frac{1}{2}} \Phi_{\pi}(xy) \quad (2)$$

$$|E_g\rangle = \begin{cases} \delta d_{zz} - (1 - \delta^2)^{\frac{1}{2}} \Phi_{\pi}(xz) \\ \delta d_{yz} - (1 - \delta^2)^{\frac{1}{2}} \Phi_{\pi}(yz) \end{cases} \quad (3)$$

Parametrii de legătură ce intervin în (1)–(3) pot fi evaluați [1, 3] din relațiile

$$\alpha^2 = \frac{|A_{||}|}{P} + (g_{||} - 2,002) + \frac{3}{7} (g_{\perp} - 2,002) + 0,04 \quad (4)$$

$$\beta^2 = -\frac{(g_{||} - 2,002)}{8\lambda\alpha^2} \Delta_{xy} \quad (5)$$

$$\delta^2 = -\frac{(g_{\perp} - 2,002)}{2\lambda\alpha^2} \Delta_{xz} \quad (6)$$

unde  $\Delta_{xy} = \Delta_{xz} = 15\,000 \text{ cm}^{-1}$  [1]

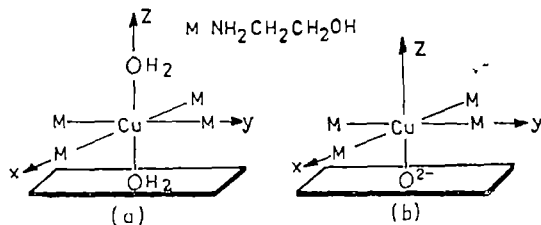


Fig 3 Model structural pentru complecșii adsorbiți pe  $\text{SiO}_2$  (a) și  $\text{Al}_2\text{O}_3$  (b)

Diferențele care apar între parametrii RES și cei de legătură caracteristici complecșilor adsorbiți pe cele două suprafete pot fi explicate prin suprapunerea în cazul aluminei a unei componente de simetrie  $C_{4v}$  peste cea  $D_{4v}$  (fig. 3). Datorită suprafetei specifice reduse, alumina prin uscare reține o cantitate de apă și radicali OH, fixați în general deasupra ionilor  $\text{Al}^{3+}$ , rămânind totodată ionii  $\text{O}^{2-}$  în stratul superior descoperiți [4]. Aceștia constituie poziții favorabile de fixare ale moleculelor de complex pe suprafața suport, astfel încât alumina participă la structura complecșilor adsorbiți printr-un ion  $\text{O}^{2-}$ , care le împriimă acestora o componentă de simetrie  $C_{4v}$  (fig. 3b).

Spre deosebire de  $\text{Al}_2\text{O}_3$ , silicagelul reține la o uscare normală  $\sim 2$  monostraturi apă, fiind astfel posibilă coordinarea a cîte unei molecule  $\text{H}_2\text{O}$  pe direcția Oz [5], atît sub planul  $xOy$ , cît și deasupra lui (fig. 3a).

Faptul că în cazul adsorbției pe alumină complecșii au o componentă de simetrie  $C_{4v}$  este demonstrat de valorile mai mari ale constantei de structură hiperfină  $A_{||}$  [6], precum și de rezolvarea netă a semnalului  $m_I = -3/2$  din banda paralelă (fig. 2). Acest semnal este „împins” spre valori mai mari ale cîmpului magnetic, iar absorbția perpendiculară este deplasată spre cîmpuri mai joase, comportare analogă cu cea întîlnită la complecșii de vanadil ce au în general o configurație  $C_{4v}$  [7], rezultînd astfel  $g_{\perp}$  (pentru  $\text{Al}_2\text{O}_3$ )  $> g_{\perp}$  (pentru  $\text{SiO}_2$ ).

Fixarea mai puternică a complecșilor pe  $\text{Al}_2\text{O}_3$  decît pe  $\text{SiO}_2$  este favorizată și de apariția unor posibile legături între moleculele de ligand bogate în electroni și ionii de aluminiu din straturile inferioare. Datorită acestor legături în moleculele de complex are loc o extensie a distanței Cu—N, ceea ce duce la slabirea gradului de covalență al legăturii  $\sigma$  prin creșterea lui  $\alpha^2$  de la 0,70 (pentru  $\text{SiO}_2$ ) la 0,86 (pentru  $\text{Al}_2\text{O}_3$ ).

(Intrat în redacție la 10 septembrie 1979)

#### B I B L I O G R A F I E

- 1 O Cozar, V Znamirovschi, I Haiduc, Studia UBB, Physica, **23**, 1, 6 (1978)
- 2 O Cozar, V Znamirovschi, Studia UBB, Physica, **24**, 1, 41 (1979)
- 3 D Kivelson, R Neiman, J Chem Phys, **35**, 149 (1961)
- 4 J B Peri, J Phys Chem, **69**, 220 (1965)

- 5 D M Clementz, Th J Pinnavaria, M M Mortland, J Phys Chem, **77**, 196 (1973)
- 6 P A Berger, J F Roth, J Phys Chem, **71**, 4307 (1967)
- 7 D Kivelson, S K Lee, J Chem Phys, **41**, 1896 (1964)

ESR STUDY OF ADSORBED [Cu(NH<sub>2</sub>CH<sub>2</sub>CH<sub>2</sub>OH)<sub>4</sub>]Cl<sub>2</sub> ON SiO<sub>2</sub> AND Al<sub>2</sub>O<sub>3</sub>  
(Summary)

It has been shown the existence of two complexes on SiO<sub>2</sub> surface, one of them is bounded by surface and another which moves in the cages of SiO<sub>2</sub>. In the case of Al<sub>2</sub>O<sub>3</sub> only the first type of the complex is formed.

On SiO<sub>2</sub> surface, the complexes are bounded by OH<sub>2</sub> having D<sub>4h</sub> symmetry, while on the Al<sub>2</sub>O<sub>3</sub> surface these are bounded by O<sup>2-</sup> having a component of C<sub>4h</sub> symmetry. The bonding is stronger on this last surface.

**ASUPRA ECUAȚIILOR DE MIȘCARE ALE PARTICULELOR  
CU MASA DE REPAOS ZERO**

Z. GĂBOS

În teoria cuantică a particulelor libere cu masa de repaos zero și spinul mai mare ca  $1/2$  pe lîngă ecuațiile de mișcare propriu-zise se folosesc unele relații care servesc la selectarea stărilor de polarizare posibile. Astfel de condiții au fost date de O. Laporte, G. E. Uhlenbeck și R. H. Good, Jr [1, 2, 5] pentru particulele cu spinul 1 și 2. În această lucrare vom scrie condițiile referitoare la particulele libere cu spinul  $3/2$ , utilizând ecuațiile de mișcare de tip Joos-Weinberg.

1°. Pentru particulele cu masă de repaos zero și spinul  $s$  avem ecuațiile [4]

$$\gamma_{\mu_1 \mu_2 \dots \mu_{2s}} \frac{\partial \Psi}{\partial x_{\mu_1}} = 0, \quad (1)$$

unde matricele  $\gamma_{\mu_1 \mu_2 \dots \mu_{2s}}$  au următoarea structură [3]

$$\gamma_{i_1 i_2 \dots i_{2s}} = \begin{pmatrix} 0 & (-1)^s M_{i_1 i_2 \dots i_{2s}} \\ M_{i_1 i_2 \dots i_{2s}} & 0 \end{pmatrix} \quad (2)$$

Vectorul de stare  $\Psi$  este compus din vectorii  $\varphi$  și  $\chi$  cu cîte  $2s + 1$  componente. Dintre relațiile (1) numai ecuațiile

$$\gamma_{\mu_1 \mu_2 \dots \mu_{2s}} \frac{\partial \Psi}{\partial x_{\mu_1}} = 0, \quad \gamma_{\mu_1 \mu_2 \dots \mu_{2s}} \frac{\partial \Psi}{\partial x_{\mu_2}} = 0 \quad (3)$$

sînt independente. Prima relație de sub (3) prin utilizarea expresiilor [3]

$$M_{4 \dots 4} = (-1)^{2s+1} I, \quad M_{k4 \dots 4} = i(-1)^{2s+1} \frac{1}{s} S_k,$$

unde  $I$  este matricea unitate și  $S_k$  sînt matricele de spin, ne conduce la ecuațiile

$$\left[ \frac{\partial}{\partial x_4} + \frac{i}{s} \left( \vec{S}, \frac{\partial}{\partial \vec{x}} \right) \right] \chi = 0 \quad (4)$$

$$\left[ \frac{\partial}{\partial x_4} - \frac{i}{s} \left( \vec{S}, \frac{\partial}{\partial \vec{x}} \right) \right] \varphi = 0 \quad (5)$$

Pentru soluția de undă plană cu impuls  $\vec{p}$  bine determinat

$$\Psi_p = \begin{pmatrix} \varphi_0(\vec{p}) \\ \chi_0(\vec{p}) \end{pmatrix} \exp \left( \frac{i}{\hbar} \vec{p} \cdot \vec{x} \right) = \begin{pmatrix} \varphi \\ \chi \end{pmatrix} \quad (6)$$

din (4) și (5) rezultă

$$(\vec{S}, \vec{e}) \varphi_0 = s \varphi_0, \quad (\vec{S}, \vec{e}) \chi_0 = -s \chi_0, \quad \text{cu } \vec{e} = \frac{\vec{p}}{|\vec{p}|} \quad (7)$$

prin urmare, pentru  $\varphi_0 \neq 0$ ,  $\chi_0 = 0$  avem soluția cu helicitatea pozitivă, pe cind pentru  $\varphi_0 = 0$ ,  $\chi_0 \neq 0$  avem soluția cu helicitate negativă. Prima ecuație de sub (3) este deci ecuația de mișcare care ne conduce la cele două soluții admise pentru particulele cu masă de repaos zero. Deoarece prima ecuație de sub (3) ne furnizează proprietățile particulelor, a doua ne dă unele condiții suplimentare.

Având în vedere că  $\gamma_{4j4} - 4 = \gamma_{j4} - 4$  și

$$M_{kj4} - 4 = (-1)^{2s+1} \frac{1}{2s-1} \left[ \frac{1}{s} (S_k S_j + S_j S_k) - I \delta_{kj} \right]$$

în urma eliminării cu ajutorul lui (4) și (5) a derivatei în raport cu  $x_4$  din relația a două de sub (3), se ajunge la condiția

$$\left[ \frac{s-1}{s^2(2s-1)} S_k S_j - \frac{1}{s(2s-1)} S_j S_k + \frac{1}{2s-1} I \delta_{kj} \right] \frac{\partial}{\partial x_4} \Phi = 0 \quad (8)$$

unde  $\Phi$  poate fi sau  $\varphi$ , sau  $\chi$ .

În cazul  $s = 1$ , cind

$$S_1 = \begin{pmatrix} 0 & 0 & 0 \\ 0 & 0 & -i \\ 0 & i & 0 \end{pmatrix}, \quad S_2 = \begin{pmatrix} 0 & 0 & i \\ 0 & 0 & 0 \\ -i & 0 & 0 \end{pmatrix}, \quad S_3 = \begin{pmatrix} 0 & -i & 0 \\ i & 0 & 0 \\ 0 & 0 & 0 \end{pmatrix} \quad (9)$$

pentru cele trei componente ale lui  $\varphi$  și  $\chi$  avem

$$\varphi_t = E_t + iB_z, \quad \chi_t = E_t - iB_z \quad (10)$$

Vectorii  $\vec{E}$  și  $\vec{B}$  satisfac ecuațiile de mișcare

$$\text{rot } \vec{E} = -\frac{1}{c} \frac{\partial \vec{B}}{\partial t}, \quad \text{rot } \vec{B} = \frac{1}{c} \frac{\partial \vec{E}}{\partial t} \quad (11)$$

și condițiile

$$\text{div } \vec{E} = 0, \quad \text{div } \vec{B} = 0 \quad (12)$$

(4), (5) și (8) ne furnizează deci rezultatele stabilite de O. Laporte, G. E. Uhlenbeck și R. H. Good, Jr [1, 2].

Pentru particulele cu spinul 2 avem

$$S_1 = \begin{pmatrix} 0 & 0 & 0 & -i & 0 \\ 0 & 0 & i & 0 & 0 \\ 0 & -i & 0 & 0 & 0 \\ i & 0 & 0 & 0 & i\sqrt{3} \\ 0 & 0 & 0 & -i\sqrt{3} & 0 \end{pmatrix}, \quad S_2 = \begin{pmatrix} 0 & 0 & -i & 0 & 0 \\ 0 & 0 & 0 & -i & 0 \\ i & 0 & 0 & 0 & -i\sqrt{3} \\ 0 & i & 0 & 0 & 0 \\ 0 & 0 & i\sqrt{3} & 0 & 0 \end{pmatrix}, \quad S_3 = \begin{pmatrix} 0 & -2i & 0 & 0 & 0 \\ 2i & 0 & 0 & 0 & 0 \\ 0 & 0 & 0 & -i & 0 \\ 0 & 0 & i & 0 & 0 \\ 0 & 0 & 0 & 0 & 0 \end{pmatrix} \quad (13)$$

$$\varphi = \begin{pmatrix} g_{11} - g_{22} \\ 2g_{12} \\ -2g_{13} \\ -2g_{23} \\ 3g_{33} \end{pmatrix}, \quad \chi = \varphi^*, \quad g_{11} + g_{22} + g_{33} = 0, \quad g_{11} = g_{22} \quad (14)$$

Utilizând (8) și introducind notația  $g_{ij} = e_{ij} + ib_{ij}$ , se ajunge la condițiile

$$\frac{\partial e_{ij}}{\partial x_j} = 0, \quad \frac{\partial b_{ij}}{\partial x_j} = 0, \quad i, j = 1, 2, 3 \quad (15)$$

Din (4), (5) și (15) se obțin ecuațiile de mișcare

$$\varepsilon_{ikl} \frac{\partial e_{lj}}{\partial x_k} = -\frac{1}{c} \frac{\partial b_{lj}}{\partial t}, \quad \varepsilon_{ikl} \frac{\partial b_{lj}}{\partial x_k} = \frac{1}{c} \frac{\partial e_{lj}}{\partial t} \quad (16)$$

Relațiile (15) și (16) au fost stabilite de R. H. Good, Jr [5]

2°. În cele ce urmează vom stabili condiții și ecuații de mișcare pentru particule cu spinul 3/2. Avem

$$S_1 = \frac{1}{2} \begin{pmatrix} 0 & \sqrt{3} & 0 & 0 \\ \sqrt{3} & 0 & 2 & 0 \\ 0 & 2 & 0 & \sqrt{3} \\ 0 & 0 & \sqrt{3} & 0 \end{pmatrix}, \quad S_2 = \frac{i}{2} \begin{pmatrix} 0 & -\sqrt{3} & 0 & 0 \\ \sqrt{3} & 0 & -2 & 0 \\ 0 & 2 & 0 & -\sqrt{3} \\ 0 & 0 & \sqrt{3} & 0 \end{pmatrix},$$

$$S_3 = \frac{1}{2} \begin{pmatrix} 3 & 0 & 0 & 0 \\ 0 & 1 & 0 & 0 \\ 0 & 0 & -1 & 0 \\ 0 & 0 & 0 & -3 \end{pmatrix} \quad (17)$$

(8) ne conduce la

$$\left( \frac{1}{9} S_i S_j - \frac{1}{3} S_j S_i + \frac{1}{2} I \delta_{ij} \right) \frac{\partial}{\partial x_j} \Phi = 0, \quad (18)$$

care ne furnizează condițiile

$$\left( \frac{\partial}{\partial x_1} + i \frac{\partial}{\partial x_2} \right) \Phi_1 - \frac{1}{\sqrt{3}} \left( \frac{\partial}{\partial x_1} - i \frac{\partial}{\partial x_2} \right) \Phi_3 - \frac{2}{\sqrt{3}} \frac{\partial \Phi_2}{\partial x_3} = 0 \quad (19)$$

$$\left( \frac{\partial}{\partial x_1} - i \frac{\partial}{\partial x_2} \right) \Phi_4 - \frac{1}{\sqrt{3}} \left( \frac{\partial}{\partial x_1} + i \frac{\partial}{\partial x_2} \right) \Phi_2 + \frac{2}{\sqrt{3}} \frac{\partial \Phi_3}{\partial x_3} = 0 \quad (20)$$

în care  $\Phi$  poate fi înlocuit fie cu  $\varphi$ , fie cu  $\chi$ . Utilizând aceste condiții pe baza relației (5) se ajunge la ecuațiile de mișcare

$$\left( \frac{\partial}{\partial x_4} - i \frac{\partial}{\partial x_3} \right) \varphi_1 - \frac{i}{\sqrt{3}} \left( \frac{\partial}{\partial x_1} - i \frac{\partial}{\partial x_2} \right) \varphi_2 = 0 \quad (21)$$

$$\left( \frac{\partial}{\partial x_4} + i \frac{\partial}{\partial x_3} \right) \varphi_4 - \frac{i}{\sqrt{3}} \left( \frac{\partial}{\partial x_1} + i \frac{\partial}{\partial x_2} \right) \varphi_3 = 0 \quad (22)$$

$$\left( \frac{\partial}{\partial x_4} - i \frac{\partial}{\partial x_3} \right) \varphi_2 - i \left( \frac{\partial}{\partial x_1} - i \frac{\partial}{\partial x_2} \right) \varphi_3 = 0 \quad (23)$$

$$\left( \frac{\partial}{\partial x_4} + i \frac{\partial}{\partial x_3} \right) \varphi_2 - i \sqrt{3} \left( \frac{\partial}{\partial x_1} + i \frac{\partial}{\partial x_2} \right) \varphi_1 = 0 \quad (23')$$

$$\left( \frac{\partial}{\partial x_4} + i \frac{\partial}{\partial x_3} \right) \varphi_3 - i \left( \frac{\partial}{\partial x_1} + i \frac{\partial}{\partial x_2} \right) \varphi_2 = 0 \quad (24)$$

$$\left( \frac{\partial}{\partial x_4} - i \frac{\partial}{\partial x_3} \right) \varphi_3 - i \sqrt{3} \left( \frac{\partial}{\partial x_1} - i \frac{\partial}{\partial x_2} \right) \varphi_4 = 0 \quad (24')$$

pentru componenteile lui  $\varphi$ . Dintre ultimele patru ecuații putem folosi fie (23), (24), fie (23'), (24'). Ecuațiile pentru componenteile lui  $\chi$  se obțin în urma unor transformări simple. Presupunind că legătura între  $\chi$  și  $\varphi$  este dată prin  $\chi = M\varphi^*$ , unde  $M$  este o matrice  $4 \times 4$  din (4) și (5) se ajunge la condițiile

$$MS_1M^{-1} = -S_1, \quad MS_2M^{-1} = S_2, \quad MS_3M^{-1} = -S_3 \quad (25)$$

de unde pentru  $M$  rezultă

$$M = \begin{pmatrix} 0 & 0 & 0 & -1 \\ 0 & 0 & 1 & 0 \\ 0 & -1 & 0 & 0 \\ 1 & 0 & 0 & 0 \end{pmatrix} \quad (26)$$

(Intrat în redacție la 19 septembrie 1979)

#### B I B L I O G R A F I E

- 1 O Laporte, G E Uhlenbeck, Phys Rev, **37**, 1380 (1931)
- 2 R H Good, Jr, Phys Rev, **105**, 1914 (1956)
- 3 Z Gábos, Studia Univ Babeș-Bolyai, ser Math-Phys, f 2, p 85 (1968)
- 4 Z Gábos, D Dumitrescu, Studia Univ Babeș-Bolyai, ser Physica, f 2, p 33 (1972)
- 5 R H Good, Jr, Annals of Phys, **63**, 590 (1971)

#### SUR LES ÉQUATIONS DE MOUVEMENT DES PARTICULES DE MASSE DE REPOS ZÉRO

(R é s u m é)

On donne les équations de mouvement de type Joos-Weinberg pour les particules libres de spin  $3/2$  et on écrit les conditions qui servent à la sélection des états de polarisation pour les particules de masse de repos zéro.

## STUDY ON THE AGEING OF STRATIFIED ELECTRO-INSULATING MATERIALS BY THE ELECTRON SPIN RESONANCE METHOD

LAVINIA COCIU, A. MARTON\* and AL. NICULA

**Introduction.** In the composition of stratified electro-insulating material used in the construction of high voltage electric machines, beside the inorganic skeleton also enter organic substances that suffer degradation in time due to the external stresses

In the present paper the results of electron spin resonance (ESR) measurements concerning the P 701 electro-insulating material, aged by means of thermic stress, are presented. The P 701-NID 3376—73 material, made by I.C.M.E.-Bucharest, a product based upon mica-paper on delicate glass tissue support impregnated with an epoxidic thermorigid resin builds up, by means of a proper technology, a heatresisting insulation employed in the construction of high voltage electric machines

**Experimental results.** Using the ESR method we have ascertained the appearance of free radicals in the structure of the investigated material, as a direct effect of thermic treatment. The ESR spectra were recorded with a JES-3B spectrometer

Before the ageing, the samples of insulating material exhibits an ESR spectrum, shown in the figure 1, which consists of a single line at  $g = 4.2$ . This line can be attributed to iron ions [1, 2]. The same spectrum is characteristic for the mica-paper and glass support both before and after their heating

The samples were aged at  $225^{\circ}\text{C}$ , a temperature higher than the operating temperature of the electric machines. After every cycle of 5 or 10 hours of thermic treatment and cooling of the samples to room temperature, the ESR spectra of the samples were recorded. As it is seen from the figure 2, it consists of the line at  $g = 4.2$ , and a new narrow signal at  $g = 2.001 \pm 0.001$  which is typical of free radicals [3]

The intensity of the resonance at  $g = 2.001$  rises with the duration of the thermal treatment. Because the spectra were recorded at different gains, we chose as a criterion of watching the intensification of the free radicals signal, the ratio between its intensity,  $I$ , and the intensity  $I'$  of the  $g = 4.2$  line of the

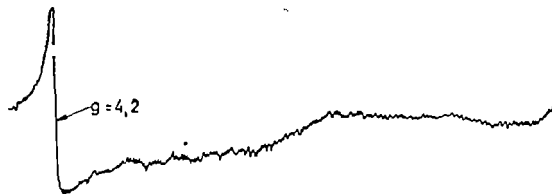


Fig 1 ESR spectrum of the insulating material before the thermic treatment

\* Institutul de subîngineri, Reșița

same sample. The dependence of the logarithm of this ratio in terms of thermal treatment duration is presented in the figure 3

**Discussion.** 1 As the signal of the free radicles is not to be found in the ESR spectra of the inorganic components of the P 701 material, we came to the conclusion that the free radicles appear due to the degradation of the structure of the epoxidic polymerized resin, as a consequence of ageing because of the heat stress

2 The increase of free radicle concentration with the time interval of the heat stress is exponential, three slopes being distinguished (that change), tending towards saturation

3 We consider that the slope changes from the linear variation of  $\ln I/I'$  depending on the stress duration is due to phase transition of the amorphous polymers [4]. Such a transition may occur when the temperature is proper for the molecule to suffer an additional motion, while the heat expansion creates a sufficient free volume so that this motion can take place. The transitions do not happen instantaneously but after a certain time necessary for the polymer to reach the equilibrium state, corresponding to the new situation

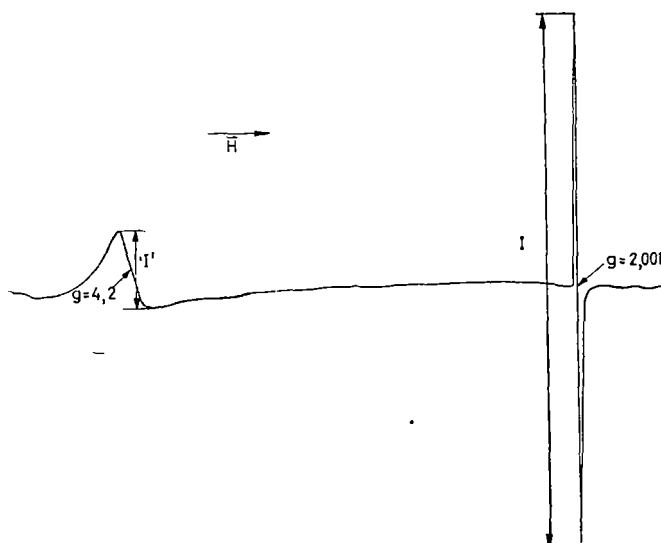


Fig. 2 ESR spectrum of the aged insulating material

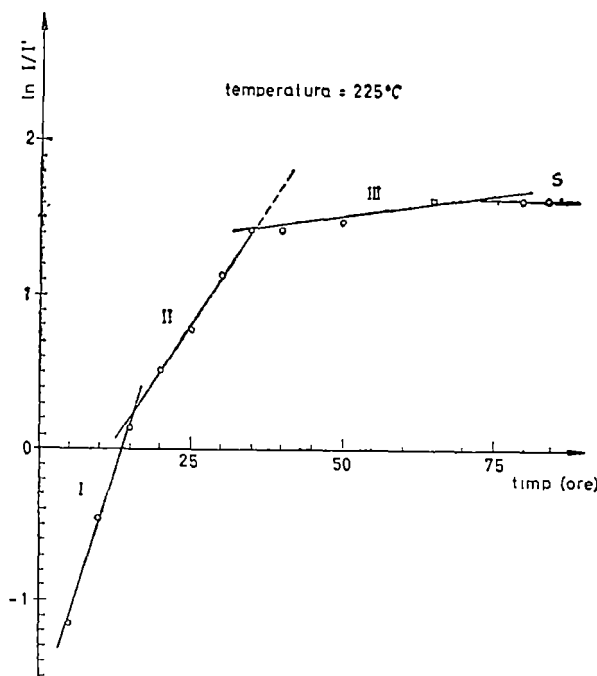


Fig. 3 Temperature dependence of the  $g = 2,00$  line intensity

4 In coal the stable free radicle concentration increases together with the growing of carbon proportion in the material [5], with the heat ageing of the polymers, the carbon contained in the electro-insulating material increases and leads to the worsening of its dielectric properties

5 Taking into account the above-mentioned facts we consider that the saturation of the free radicles concentration may be chosen as a criterion of deterioration, in order to determine the lifetime of electro-insulating materials by the accelerated ageing method

(Received November 16, 1979)

#### R E F E R E N C E S

- 1 D Loveridge, Phys Chem Glasses, **12**, 19 (1971)
- 2 Al Nicula, M Peteanu, Studia Univ Babeş-Bolyai, Phys., **42** (1976)
- 3 D J Ingram, *Free Radicals as Studied by Electron Spin Resonance*, Butterworth, London, 1958
- 4 M Leca, Buletin de Fizică și Chimie, an II, v II, p 84 (1976)
- 5 D J Ingram, Nature, **174**, 797 (1954)

#### STUDIUL ÎMBĂTRÂNIRII MATERIALELOR ELECTROIZOLATOARE PRIN METODA REZONANȚEI ELECTRONICE DE SPIN

(R e z u m a t)

Prin metoda RES s-au investigat materiale izolatoare utilizate în construcția mașinilor electrice de înaltă tensiune. În urma îmbătrânirii forțate a izolațiilor, prin tratament termic, în spectrele RES ale acestora se evidențiază semnale ale radicalilor liberi. S-a găsit că, odată cu mărirea duratei tratamentului termic la o temperatură superioară celei de funcționare normală a mașinii, concentrația radicalilor liberi crește exponențial, tînzind spre saturație.

THE CHANGE IN THE DIMENSION DISTRIBUTION OF SOLID  
PARTICLES IN A SUSPENSION FOLLOWING ULTRASONIC  
DISPERSION

D. AUSLÄNDER, AURELIA CIUPE

**Theory.** The increase of the degree of dispersion of systems by ultrasonic methods [1] is followed by a slow process of shift of the dimensions equilibrium, which takes place after the acoustic field action ceased. The estimation of these modifications, by means of the average radius of particles, is given by [2], [3]

$$\Delta r_M = \sum_i \Delta r_{ia} + \sum_j \Delta r_{jd} \quad (1)$$

where the right hand side reflects a sum of some agglomeration and dispersion processes and which increase or decrease, respectively the average radius

Attributing to the brownian motion the determining part of the agglomeration mechanism, the mean square displacement of a particle may be expressed by Einstein's relation as

$$\bar{x}_t^2 = \frac{RT}{N} \cdot \frac{t}{3\pi\eta r} \quad (2)$$

Considering that the average distance between the centers of two particles is  $\bar{L}$ , the frequency of the collisions in the volume unit containing  $n$  particles is given by

$$\nu = \frac{\bar{x}_t^2}{\bar{L}^2} \cdot n \quad (3)$$

Thus relationship (2) becomes

$$\nu = \frac{RT}{N} \cdot \frac{1}{3\pi\eta r} n^{5/3} \quad (4)$$

For a polydisperse suspension having particles with different radii  $r_1, r_2, \dots, r_s$  in corresponding concentrations  $c_1, c_2, \dots, c_s$ . the collision frequency due to the brownian motion can be expressed by

$$\nu = a \cdot A \cdot \frac{1}{r_B} \left( \sum_{i=1}^s \frac{c_i}{r_i^3} \right)^{5/3} \quad (5)$$

where  $r_B$  is the average radius of the brownian particles,

$a = \frac{R}{N} \cdot \frac{3^{2/3}}{4^{5/3} \pi^{8/3}}$  is a constant not depending on the type of suspension and  $A = T/\eta r^{5/3}$  is a characteristic constant for a certain disperse system at a given temperature

The variation of the average radius  $r_M$  of the disperse system particles by the collisions mechanism due to the brownian motion is described by the equation

$$\frac{1}{r_M} \cdot \frac{dr_M}{dt} = Bv \quad (6)$$

where  $B$  is an adherence constant which is a measure of the agglomeration efficiency through collisions

From relationships (5) and (6) we obtain the expression for the increase of the particle average radius during given periods of time

$$\Delta r_M = B \cdot a \cdot A \cdot \frac{r_M}{r_B} \Delta t_1 \left[ \frac{\sum \frac{c_i}{r_i^3} \cdot \Delta t_i}{\Delta t_1} \right]^{5/3} \quad (7)$$

**Experiemental results.** The determination of the constant  $B$  for a given suspension based on experimental data, makes possible the evaluation of relationship (7) and the comparison of the results with the measured values of the average radii

For illustration, fig 1 shows the variation of average radius in a  $ZnO - H_2O$  suspension after 10 minutes sonication in a field of  $2.15 \text{ W/cm}^2$  intensity at  $0.5 \text{ MHz}$  frequency Fig 2 shows the experimental and calculated curves for the control and the sonicated  $Pb_3O_4 - H_2O$  system, at  $1.65 \text{ W/cm}^2$  intensity and  $1 \text{ MHz}$  frequency

The satisfactory agreement of the experimental results with the values calculated using formula (7) underlines the determining role played by the brownian motion in the agglomeration process of particles in disperse systems in aqueous media.

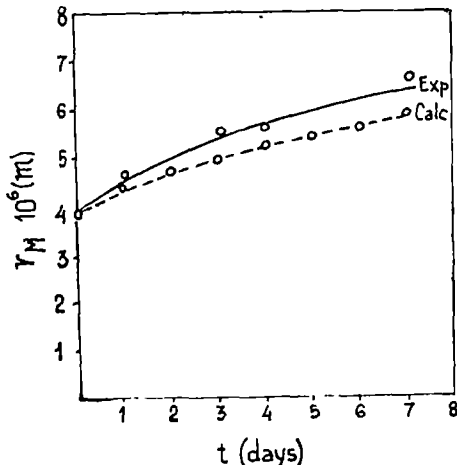


Fig 1 The change of the average radius as a function of time, for the  $ZnO - H_2O$  suspension

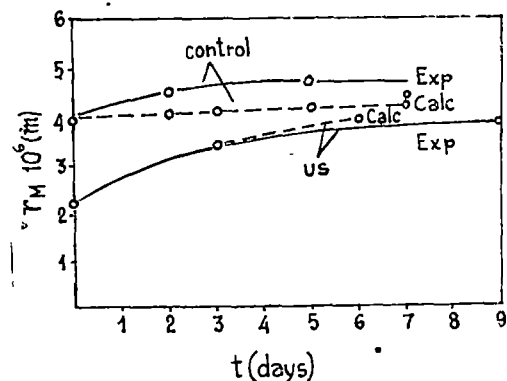


Fig 2 The change of the average radius as a function of time, for the  $Pb_3O_4 - H_2O$  suspension

A shift of the distribution equilibrium towards larger average radii might also result by one of the following mechanisms: collisions between non-spherical particles in rotational motion due to the Brownian motion, radius dependent sedimentation velocities contributions to the collisions frequency increase, and the differentiated solubility of particles according to their dimensions. This last phenomenon described by [4]

$$\frac{RT}{M} \ln \frac{s_2}{s_1} = \frac{2\sigma}{\rho} \left( \frac{1}{r_2} - \frac{1}{r_1} \right) \quad (8)$$

conveys a relative instability to the polydisperse system, the evolution of which is in the direction of decreasing the small particles concentration, thus contributing to the increase of the average radius. Simultaneously, it also has the opposite effect, as the number of Brownian particles is decreased.

The last term of equation (1) describes a process of increasing the dispersion degree, the shifting in time of the size distribution, in the direction of the reduction of the average radius of particles. It seems that the evolution of the systems, under the action of the opposite effects, depends on the properties of the dispersing medium. Thus, in aqueous medium, accumulation effects were demonstrated, while in the case of  $ZnO-C_6H_6$  and  $ZnO-C_6H_5CH_3$  systems the prevalence of dispersing factors was found (Table 1).

Table 1

The change of the average radius as a function of time,  
for the  $ZnO-C_6H_6$  and  $ZnO-C_6H_5CH_3$  suspensions

The system	$\Delta t$ (days)	$r_M \cdot 10^6$ (m)	
		control	sonicated 1 MHz, 27 W/cm <sup>2</sup>
$ZnO-C_6H_6$	0		13.7
	1		10.0
	3		9.3
	5		6.6
$ZnO-C_6H_5CH_3$	0	14.1	13.9
	3	13.4	11.4
	4	—	10.3
	5	—	10.1
	6	11.3	9.5

Among the causes of this phenomenon one may count some effects of the cavitation process. Thus, the penetration of the liquid into the microcracks created under the action of cavitation by a capillary condensation process, according to the Thomson-Kelvin relationship

$$\ln \frac{p'}{p''} = - \frac{M}{T} \frac{2\sigma}{\rho_1 - \rho_2} \left( \frac{1}{r'} - \frac{1}{r''} \right) \quad (9)$$

leads to the breakdown of some agglomerates into smaller particles. On the other hand, following the degassing effect of the ultrasounds from the particle

surface, the equilibrium of solid-liquid interface forces is modified, due to the desorption of gases with corresponding implications upon the dispersion process

**Conclusion.** The disperse systems undergo an alteration in time of the size distributions, under the action of two opposing mechanism. The evolution towards agglomeration is prevalently caused by the collision of particles in brownian motion, while the dispersion is the consequence of cavitation effects

(Received November 16, 1979)

#### R E F E R E N C E S

- 1 V M Friedman, Ultrasonics, **10**, 162 (1972)
- 2 D Auslander, A Ciupe, Proc of the 9-th Int Congress on Acoustics, K-54, Madrid, 1977
- 3 A Ciupe, Thesis, Univ Bucureşti, 1977
- 4 A V Dumanski, Colozin, Ed de Stat, Bucureşti, 1949

#### MODIFICAREA DISTRIBUȚIEI DE DIMENSIUNI A PARTICULELOR SOLIDE DINTR-O SUSPENSIE DISPERSATĂ ULTRASONIC

(Résumé)

Cercetări experimentale au pus în evidență deplasarea echilibrului distribuției de dimensiuni a particulelor unei suspensii, în absența/după încetarea iradierei ultrasonice în sensul creșterii, respectiv al scăderii razei mediș în funcție de natura dispersantului. Aglomerarea atribuită îndeosebi ciocnirilor particulelor participante la mișcarea browniană este descrisă printr-o ecuație, mecanismele de dispersare sunt explicate calitativ, pe baza unor cauze ale procesului de cavitare

# ABSORBȚIA STRUCTURALĂ A ULTRASUNETULUI ÎN SOLUȚII APOASE DE ACIZI ORGANICI

**ILEANA LENART, D. AUSLÄNDER**

**Introducere.** Tehnicile ultrasonice permit obținerea de informații utile pentru investigarea structurii lichidelor, prin intermediul constantei de atenuare și vitezei de propagare a ultrasunetului. Atenuarea undelor ultrasonice în lichide provine dintr-o însușire de efecte de absorbție în mediu, care fiind considerate independente, rezultă

$$\alpha = \alpha_{\text{vis}} + \alpha_{\text{term}} + \alpha_{\text{rel}} \quad (1)$$

unde primii doi termeni din membrul al doilea reprezintă constantele de atenuare corespunzătoare absorbției clasice de viscozitate și conductibilitate termică, iar  $\alpha_{\text{rel}}$ , constanta de atenuare de relaxare, este consecința fenomenelor de absorbție structurală

$$\alpha_{\text{vis}} + \alpha_{\text{term}} = \frac{2\pi^2}{\rho c^3} \left( \frac{4}{3} \eta + \frac{\chi - 1}{C_p} k \right) f^2 \quad (2)$$

În cazul lichidelor cu conductibilitate termică redusă,  $\alpha_{\text{term}}$  este neglijabil, deci:

$$\alpha_{\text{vis}}/f^2 = \frac{2\pi^2}{\rho c^3} \frac{4}{3} \eta \quad (3)$$

unde  $f$  este frecvența ultrasunetului,  $\rho$  densitatea mediului,  $c$  viteza de propagare a undei și  $\eta$  coeficientul de viscozitate a lichidului

Cercetările au demonstrat că în realitate raportul  $\alpha/f^2$  este mult mai mare decât valoarea rezultată din calculul relației (3), nefiind satisfăcută nici independența raportului de frecvență cu excepția lichidelor monoatomicice.

Absorbția de exces, numită absorbție „suprastokes” provine din procese moleculare de disipare a energiei acustice, descrise prin intermediul constantei de atenuare de relaxare

$$\alpha_{\text{rel}} = 2\pi \frac{n(q^2 - 1)}{1 + q^2 n^2} \quad (4)$$

unde  $q = c_\infty/c_0$  reprezintă gradul de dispersie a vitezei de propagare a ultrasunetului, iar  $n = \omega/\omega_0 = f/f_0$  este raportul dintre frecvența ultrasunetului și frecvența de relaxare de rotație, respectiv de vibrație

Pentru studiul fazelor lichide este esențială componenta structurală a absorbției a cărei determinare este posibilă prin două metode:

a) Măsurarea absorbției în domeniul frecvenței corespunzătoare dispersiei anormale la care se pune în evidență absorbția structurală, respectiv în domeniul îndepărtate de această valoare, caracterizate prin corespondența cu teoria hidro-

dinamică clasice a absorbției, diferența valorilor obținute reprezintă absorbția de relaxare la frecvența respectivă

b) Calcularea diferenței dintre absorbția experimentală și cea exprimată prin relația (2) cu ajutorul constantelor respective

Utilizând ultima metodă, s-a cercetat comportarea unor acizi organici în soluții apoase pentru evaluarea absorbției de relaxare în funcție de procesele de disociere moleculară care afectează frecvența proprie de vibrație a componentelor moleculare.

**Rezultate experimentale.** S-a determinat vîscozitatea, densitatea și viteza de propagare a ultrasunetului în soluții apoase de acizi mono-, bi-, și tricarboxilici, la diferite concentrații din domeniul 0–1 M care au permis calcularea raportelor  $\alpha/f^2$  din relația (3)

Măsurarea constantei experimentale de atenuare s-a efectuat prin metoda impulsului la distanță fixă pe baza ecourilor repetate, la frecvența de 10 MHz, pe baza relației

$$\alpha = \frac{\Delta L}{20 \cdot \log e - 21} \quad (5)$$

unde  $L = 20 \log \frac{P}{P_0}$ , iar 1 este distanța emițător-reflector.

Rezultatele pun în evidență valori apreciabile ale absorbției structurale, o creștere foarte pronunțată cu concentrația în domeniul diluțiilor mari și una mai lentă în restul intervalului, panta fiind în întregul interval superioară celei corespunzătoare absorbției clasice

Saltul constantei de atenuare de relaxare îl atribuim componentelor de disociere caracterizate prin noi valori de frecvență de vibrație, pe baza reacției de echilibru



Pentru verificarea acestui mecanism au fost măsurate valorile absorbției în condițiile frînării procesului de disociere prin creșterea concentrației ionilor de hidrogen în urma adăosului de HCl diluat

În acest scop s-au efectuat măsurători de absorbție în soluții apoase de HCl, la temperatura determinărilor anterioare, la diferite concentrații, s-a stabilit astfel că într-o soluție apoasă de HCl, pînă la concentrația de 0,2 M, absorbția nu diferă de cea a apei. În consecință, s-au preparat soluțiile de acizi organici utilizînd ca solvent HCl 0,1 M, asupra căror s-au repetat toate determinările anterioare

Rezultatele obținute sunt ilustrate în fig. 1, pentru acidul propionic, care este un acid monocarboxilic

Curba inferioară (I) care prezintă o variație lentă a raportului  $\alpha/f^2$  cu concentrația corespunde absorbției clasice, curba superioară (III) indică dependența absorbției totale de concentrație, iar cea intermedieră (II) s-a obținut în soluții de acid propionic în HCl 0,1 M

Variația cu concentrația a raportului  $\alpha/f^2$ , determinat în mod experimental, este prezentată pentru cei trei acizi organici studiați în fig. 2, diferențiat în cazul celor doi solvenți apă, respectiv HCl 0,1 M.

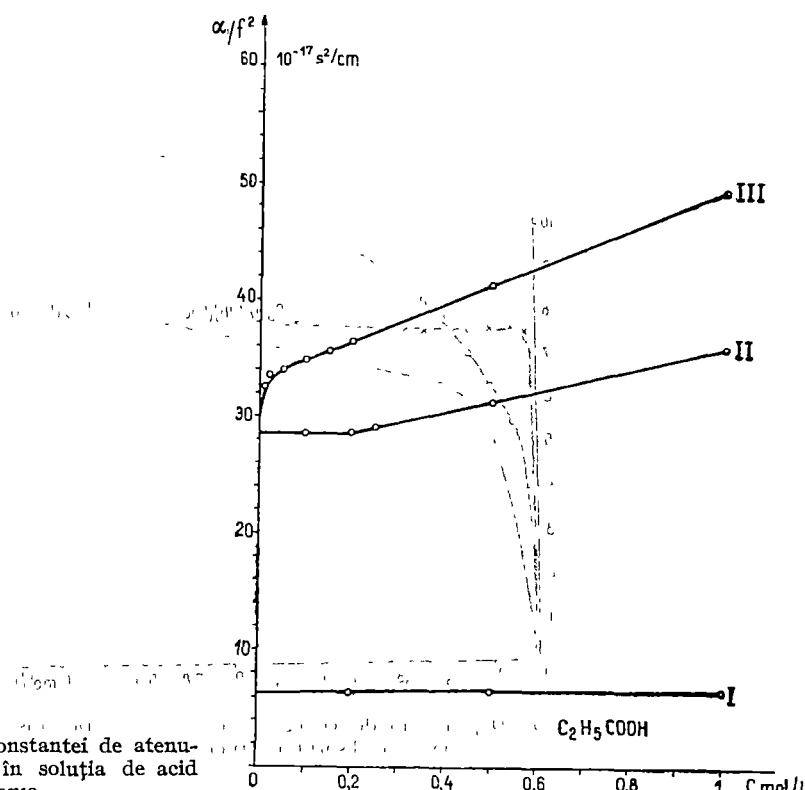


Fig. 1 Variația constantei de atenuare cu concentrația în soluția de acid propionic.

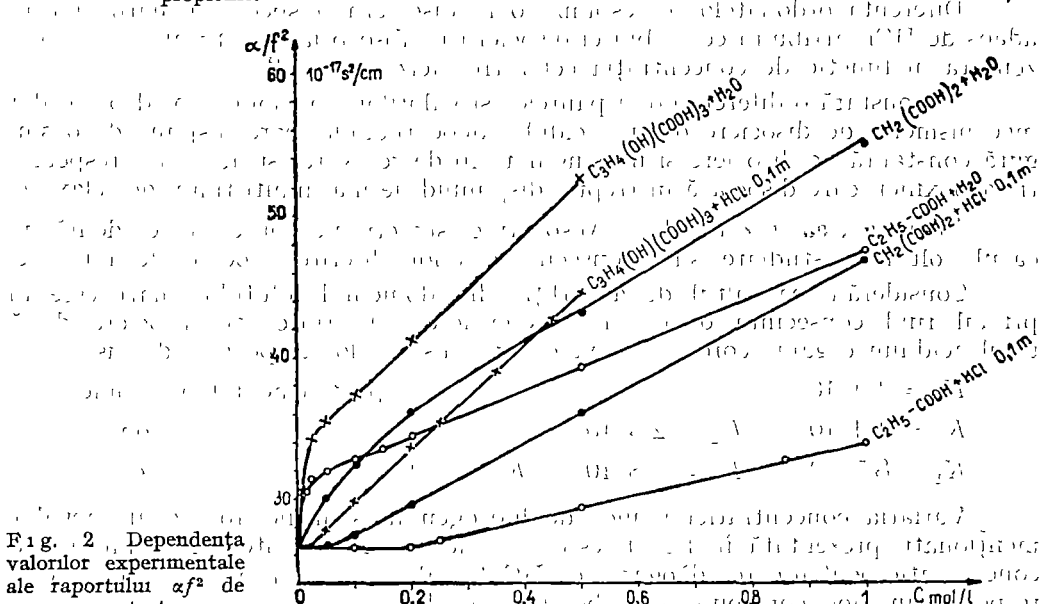


Fig. 2 Dependența valorilor experimentale ale raportului  $\alpha/f^2$  de la concentrație.

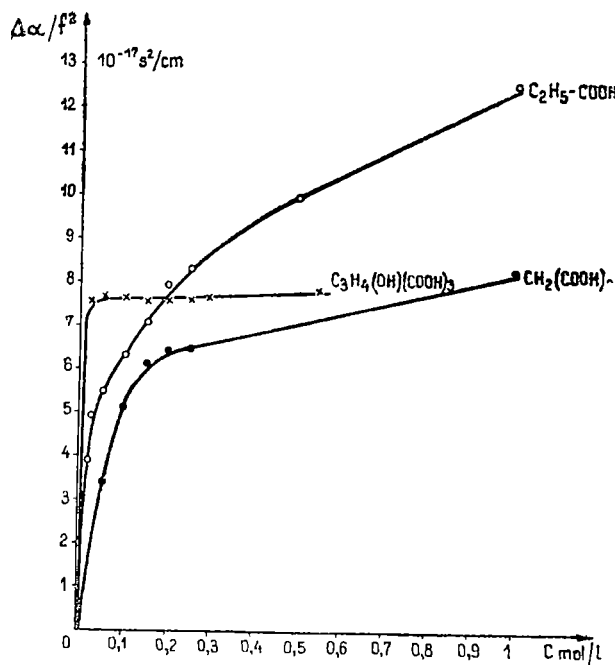


Fig. 3 Dependența de concentrație a contribuției disocierii la absorbția structurală

Diferența ordonatelor corespunzătoare disocierii, respectiv frânrării ei prin adăos de HCl, atribuită contribuției disocierii la absorbția structurală este reprezentată în funcție de concentrația celor trei acizi în fig. 3.

Se constată o diferențiere a pantelor și valorilor, corespunzător deosebirilor mecanismelor de disociere dintre acidul monocarboxilic, care dispune de o singură constantă de disociere și un singur timp de relaxare, și acizii bi, respectiv tricarboxilici, care disociază în trepte, dispunind de mai mulți timpi de relaxare.

**Interpretarea rezultatelor.** Absorbțile structurale puse în evidență în cazul soluțiilor studiate sunt consecințele unor diferite procese de relaxare.

Considerăm că saltul de absorbție din domeniul diluțiilor mari este în primul rînd consecința disocierii. Diferențierea absorbției de disociere după tipul acidului organic corespunde valorilor constantelor respective de disociere

$$K_1 = 1,4 \cdot 10^{-5} \quad \text{pentru acidul propionic}$$

$$K_1 = 1,4 \cdot 10^{-3}, \quad K_2 = 2,3 \cdot 10^{-6} \quad \text{,, ,,, malonic}$$

$$K_1 = 8,7 \cdot 10^{-4}, \quad K_2 = 1,8 \cdot 10^{-5}, \quad K_3 = 4 \cdot 10^{-6} \quad \text{,, ,,, citric}$$

Variatia concentratiei ionilor de hidrogen în solutiile apoase ale acizilor menționati, prezentată în fig. 4, este în concordanță cu intervalele diferite de concentratie pentru care adăugarea de HCl 0,1 M anulează procesul de disociere, respectiv în mod corespunzător absorbția de disociere.

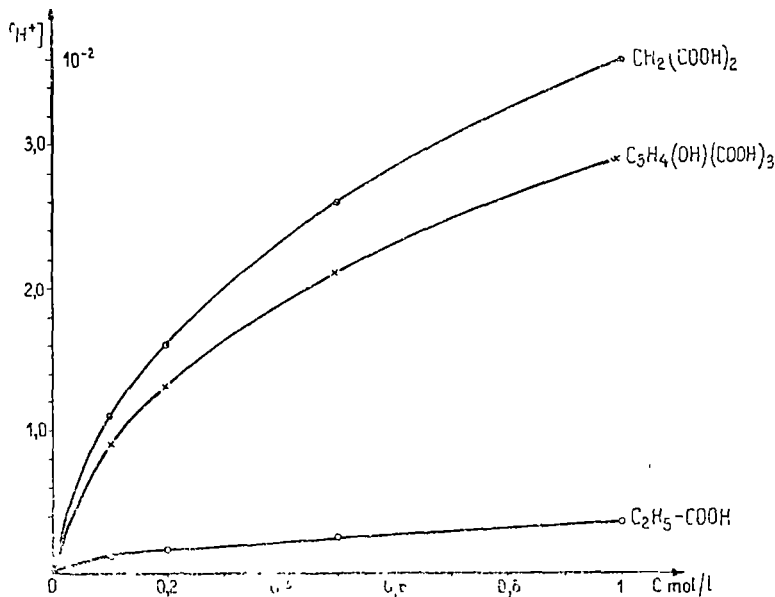


Fig. 4. Variația concentrației ionilor de hidrogen în soluțiile apoase ale acizilor propionic, malonic și citric

În domeniul respectiv, din relația (4) rezultă :

$$\frac{d\alpha_{dis}}{d\omega_0} = K \frac{q^2 n^2 - 1}{[\omega_0(1 + q^2 n^2)]^3} \quad (7)$$

unde  $K = 2\pi\omega(q^2 - 1)$

La diluții mari, viscozitatea soluțiilor fiind puțin diferită de cea a apei, se poate presupune că  $q \approx \frac{c_\infty}{c_0} = 1,01$  de unde rezultă că  $K > 0$ , deci pentru :

$$\frac{d\alpha_{dis}}{d\omega_0} > 0,$$

se obține:  $q^2 n^2 > 1$ , de unde prin aproximarea  $q \approx 1$ , se obține  $\omega_0 < \omega$ . Pe de altă parte, din măsurările experimentale rezultă că  $\frac{d\alpha_{dis}}{dc} > 0$ , astfel din condiția de mai sus:  $\frac{d\alpha_{dis}}{d\omega_0} > 0$ , rezultă  $\frac{d\omega_0}{dc} > 0$  pentru domeniul în care se poate presupune independența de concentrație a lui  $q$

Prin urmare, la disocierea acizilor carboxilici are loc creșterea frecvenței de relaxare cu concentrația, menținându-se însă la valori inferioare frecvenței de 10 MHz, diferențindu-se în funcție de constanta de disociere.

Regiunile marcate prin variații mai lente de absorbție indică limitarea procesului de disociere și prezența altor fenomene de relaxare caracterizate tot prin frecvențe inferioare valorii de 10 MHz, în creștere cu concentrația

Astfel, la concentrații mai mari este favorizată formarea de dimeri prin asociere moleculară. De exemplu, pentru  $C_2H_5-COOH$ , la  $20^{\circ}C$  frecvența de relaxare de asociere este de 2,02 MHz.

Sunt posibile de asemenea relaxări de rotații și vibrații în jurul unor legături de H, în momentul desfacerii altor legături, respectiv în jurul unor grupei atomice, cu valori diferite ale frecvențelor respective.

**Concluzii.** 1. Fenomenul de disociere a acizilor organici este însotit de un salt al absorbției.

2 Frecvența de relaxare de disociere este mai mică decât 10 MHz

3 Frecvența de relaxare de disociere crește cu concentrația

(Intrat în redacție la 20 noiembrie 1979)

#### B I B L I O G R A F I E

- 1 A L Lehninger, *Biochemistry*, Worth Publishers INC, 1976
- 2 F Eggers, Th Funck, E Grell, *7-th Int Congr Ac*, IV, 129, 1971
3. I E Elpiner, F I Brogynskaya, O M Zorina, *7-th Int Congr Ac*, IV, 153, 1971
4. S Gasse, I Emery, *9-th Int Congr Ac*, 561, 1977
- 5 O Nomoto, H Endo, *Bull Chem Soc Jap*, **44**, 1519 (1971)
- 6 L W Kessler, W D O'Brien, F Dunn, *J Phys Chem*, **74**, 4096 (1970).
7. S A Hawley, L W Kessler, F Dunn, *J Ac Soc Am*, **38**, 4, 521 (1965)

#### STRUCTURAL ABSORPTION OF ULTRASOUND IN AQUEOUS SOLUTIONS OF ORGANIC ACIDS

(Summary)

The paper presents some acoustic-molecular parameters, determined in aqueous solutions of organic acids of different concentrations. The ultrasound velocity, measured by means of an optical diffraction method, the density and the viscosity experimentally determined, resulted in the calculation of the Stokes-Kirchoff absorption. By a pulse technique was measured the absorption of the ultrasound, at a 10 MHz frequency, being then calculated the excess absorption. A leap of the structural absorption is pointed out, assigned to the dissociation processes characterized through a characteristic relaxation frequency.

## ANALYTIC S-MATRIX THEORY OF CRITICAL PHENOMENA FOR THE $\varphi^3$ AND $\varphi^4$ MODELS

M. CRIŞAN, AL. ANGHEL

**I. Introduction.** In the last years the perturbative methods have been intensively used in the theory of phase transitions

As it is well-known Wilson [1] pointed out that the critical behaviour in the phase transitions can be described in  $4 - \epsilon$  dimensions using the perturbation theory and the fixed point condition for the recurrence relations.

An equivalent treatment for the theory of phase transitions was given by the Soviet school [2—4] using the “parquet summation” and solving the D i a t l o v - S u d a k o v - T e r - M a r t i r o s i a n equations for the vertex function in 4 or  $4 - \epsilon$  dimensions G i n z b u r g [5] pointed out that using such a method and the “scaling hypothesis” the same results as in the Wilson theory can be obtained for the critical coefficients

All of these approaches are equivalent, in the sense that they are perturbative expansions of the S-matrix involved in the theory. However, it is well-known, that in the high energy physics there is also a formulation of the S-matrix theory which is in fact more general than the perturbation theory. This method proposed by Heisenberg in 1943 was developed by E d e n et al [6] and is known as the „unitarity and connectedness” theory of S-matrix.

A justified question, after the well-known success of the perturbative methods in quantum field theory and statistical physics is the following: is the analytic S-matrix theory adequate for the description of the critical behaviour of the phase transitions? And if it is so, how accurate is this method as compared with the “traditional” ones?

In a remarkable program Polyakov [7—8] has used the unitarity condition in order to analyse the asymptotic behaviour of many points correlations in the critical region

The main idea implicitly contained in this paper is that the  $N$ -point correlation functions are all elements of the S-matrix, and their analytic properties remain valid even in the critical region where the perturbative method fails.

Polyakov [7—8] calculated by this method the asymptotic behaviour of the correlation function, vertex function and discussed the scaling behaviour of these functions

In this paper another interesting aspect of this theory is pointed out. Indeed, Polyakov [8] considered that the unitarity condition is not sufficient for describing the critical behaviour in the phase transitions, but the dispersion relations for the Green function associated with the fluctuations are also necessary. Recently Bray [9] used the dispersion relation method, proposed by F e r r e l and S c a l a p i n o [10] in order to calculate the „universality function” of the two-point correlation function

The purpose of this paper is two-fold. First we intend to present, at the largest possible extent, the unitarity method in the theory of critical phenomena, since at the present time there is no such a monography available. Then

we will give a concrete method to calculate the critical indexes and the dimensions of space in which scaling behaviour is possible. The results obtained by this method are identical with the results obtained by so-called classical methods as Wilson recurrence relations [1] or summation of the "parquet diagrams"

The paper is organized as follows. In section II we reconsider the "unitarity and connectedness" principle for the  $S$ -matrix and re-write the properties of the Green function and vertex function taking into consideration this principle.

Section III is devoted to the analysis of the  $\varphi^3$ -model, and  $\varphi^4$ -models.

**II. Unitarity and Analytical Properties.** In the high energy physics the problem of calculation of the  $S$ -matrix elements is an essential one. Usually this calculation is performed using the perturbation theory and the Feynman diagrams.

However, the unitarity condition imposed to the  $S$ -matrix, gives us the possibility to write down the equations for imaginary parts of Green function and vertex function, but not as perturbative terms in the coupling constant. However, these equations will contain more or less terms and the number of these terms is function of number of intermediate states considered in the theory.

Before we apply this method in the theory of phase transition we give some results from  $S$ -matrix theory which are extensively discussed in [6].

1. Unitarity and Connectedness for  $S$ -matrix. The unitarity and connectedness-structure of the  $S$ -matrix can be analysed if we define the  $S$  operator as

$$\begin{aligned} S &= \sum_m |m, in\rangle \langle m, out| \\ S^+ &= \sum_m |m, out\rangle \langle m, in| \end{aligned} \quad (1)$$

From the orthonormality and completeness conditions of the states  $|m, in\rangle$ ,  $|m, out\rangle$  we get

$$S^+S = 1 \quad (2)$$

Because the momentum eigenstates are accessible to experiment we will concentrate with the matrix elements

$$\langle p'_1 \dots p'_m | S | p_1 \dots p_m \rangle$$

which describe the transition of a configuration of  $m$  particle each with definite momentum into one of  $m'$  particle

The basic assumption of the theory is that the total energy momentum is conserved in the interaction, then the matrix-element vanishes unless

$$\sum_{i=1}^m p'_i = \sum_{i=1}^m p_i \quad (3)$$

and the unitarity condition (2) can be written as

$$\begin{aligned} \sum_n \frac{1}{(2\pi)^{3n}} \frac{1}{n!} \int \prod_{i=1}^n d^4 q_i \delta(q_i^2 - m^2) \langle p'_1 \dots p'_m | S | q_1 \dots q_m \rangle \\ \langle q'_1 \dots q'_m | S^+ | p_1 \dots p_m \rangle = \langle p'_1 \dots p'_m | p_1 \dots p_m \rangle \end{aligned} \quad (4)$$

From the conservation of the energy-momentum we get for (3) the condition

$$\sum_i q_i = \sum_i p_i = \sum_i p'_i \quad (5)$$

and in particular

$$(nm)^2 \leq \left( \sum_i p'_i \right)^2 \quad (6)$$

where  $m$  is the mass of the particle

The diagrammatic notation is

$$\begin{aligned} \langle p'_1 & \quad p'_m | s(p_1, p_m) = \begin{array}{c} 1' \\ 2' \\ \vdots \\ m \end{array} \text{---} \begin{array}{c} 1 \\ 2 \\ \vdots \\ m \end{array} \end{aligned}$$

$$\begin{aligned} \langle p'_1 & \quad p'_m | p_1, p_m \rangle = \begin{array}{c} \text{---} \\ \text{---} \\ \text{---} \end{array} \end{aligned}$$

$$\frac{1}{(2\pi)^3 n!} \delta^3 \left( \frac{p'_1}{n} \right) \sum_{i=1}^n d^4 q \delta(q^2 - m^2) = \begin{array}{c} 1 \\ 2 \\ \vdots \\ m \end{array}$$

Fig 1

Using this notation we can write (3) as

$$\begin{array}{c} \text{---} \\ \text{---} \end{array} \text{---} \text{---} = \begin{array}{c} \text{---} \\ \text{---} \end{array}$$

Fig 2

if

$$(2m)^2 \leq (\Sigma p)^2 \leq (3m)^2 \quad (7)$$

and similar diagrams given in [6-8] for different conditions (6)

The connectedness structure of S-matrix is introduced by writing the equation for S-matrix of two-particle scattering as

$$\begin{array}{c} \text{---} \\ \text{---} \end{array} \text{---} = \begin{array}{c} \text{---} \\ \text{---} \end{array} + \begin{array}{c} \text{---} \\ \text{---} \end{array} \text{---} \text{---}$$

Fig 3

and similar equations for  $n$ -particle interaction.

Using this relation and the condition (1) we get

$$\left( \begin{array}{c} \text{---} \\ \text{---} \end{array} + \begin{array}{c} \text{---} \\ \text{---} \end{array} \text{---} \right) \left( \begin{array}{c} \text{---} \\ \text{---} \end{array} - \begin{array}{c} \text{---} \\ \text{---} \end{array} \text{---} \right) = \begin{array}{c} \text{---} \\ \text{---} \end{array}$$

Fig 4

or the unitarity condition

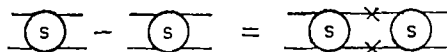


Fig 5

where each integral line is  $(2\pi)^{-3} \int d^4q \delta(q^2 - m^2)$

The unitarity condition gives the possibility to study also the analyticity of the  $S$ -matrix introduced in this way

A complete study given by Eden et al [6] showed that as a function of number of intermediate state the  $S$ -matrix has

- single pole singularities
- the normal threshold branch-points

These properties will be used in the phase transition theory, because the Green functions and vertex functions are the  $S$ -matrix elements

*2 Unitarity Condition for Green function and vertex function* In the theory of phase-transitions the Green function  $G(q)$  is

$$G(q) = [q^2 + \tau]^{-1} \quad (8)$$

$\tau = (T - T_0)/T$ , and it is in fact the Fourier transform of the correlation function

In order to use the unitarity condition Polyakov [7-8] performed the analytical continuation  $q^2 \rightarrow -q^2$ ,  $\tau \rightarrow r(\tau) = \tau^{-\beta}$  and (8) becomes

$$G(q^2) = [q^2 - m^2]^{-1} \quad (9)$$

where  $m^2 = r^{-2}(\tau)$ .

The singularities of the Green function (9) are given by

$$q^2 = -nm^2, \tau_m = (-q^2/n^2)^{1/2} \quad (10)$$

where  $n$  is the number which characterizes the branch-point. In the limit  $n \rightarrow \infty$  we get  $\tau_\infty = \tau = 0$  and (9) has the asymptotic form  $G(q) = 1/q^2$ .

Now, if we apply the equation (7) for the Green function  $G(q^2)$ , and the vertex function  $\Gamma_3$  and  $\Gamma_4$  we get the equations

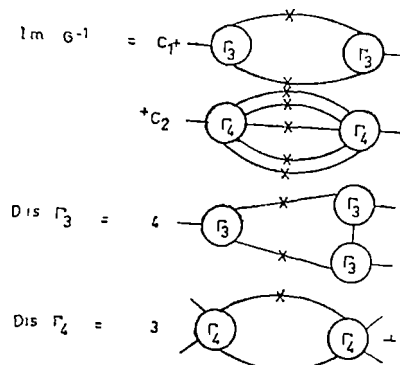


Fig 6

where  $\text{---} * \text{---} = 2\pi\Theta(q_0)\delta(q^2 - m^2) = \text{Im } G(q^2)$

These equations are exact and we can use a larger number of intermediate states if this is necessary.

In the next section we will calculate the critical index defined as

$$G(q^2) = q^{-2+\eta} \quad (11)$$

for different models, using the „scale invariance” which is supposed to be valid in the critical point  $\tau = 0$ .

**III The Critical Behaviour of Different Models** In order to study the critical behaviour of the different models we can use the unitarity condition for the Green function and to look for the „scale invariant” solutions of the integral equations.

Polyakov [8] studied the asymptotic behaviour of many points correlation functions using the „scale invariance” hypothesis, but we are going to point out on  $\phi^3$  and  $\phi^4$  models that the critical index „ $\eta$ ” can be calculated by this method.

1 *The  $\phi^3$ -model.* This model treated in the field theory only to point out the different methods of renormalization is of great interest in the phase transition theory. Recently Ginzburg [11] pointed out that the percolation theory is in fact a  $\phi^3$ -theory which has the ground state.

In this framework the  $\phi^3$ -model is interesting to be studied and we are going to apply the method presented in section II in order to obtain the critical behaviour of this model. The Green function

$$G(p^2) = p^{-2+\eta} \quad (12)$$

has the imaginary part written as

$$\text{Im } G(p^2) = - (p^2)^{\eta/2-1} \sin \frac{\pi\eta}{2} \quad (13)$$

where  $\eta$  is the critical index of the correlation function. The unitarity conditions for Green function on vertex function are given in fig. 7.

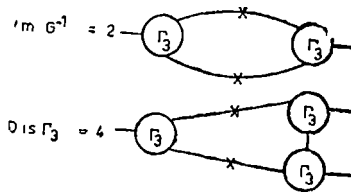


Fig 7

and are rewritten analytically as

$$\text{Im } G^{-1}(q^2) = 2g_3^2 \int |\Gamma_3(p^2, p^2, (p-q)^2)|^2 \text{Im } G(p^2) \text{Im } G[(q-p)^2] d^D p \quad (14)$$

$$\text{Disc } \Gamma_3(q^2, q_1^2, q_2^2) = 4g_3^2 \int \Gamma_3[q^2, p^2, (q-p)^2] \Gamma_3(q^2) \Gamma_3(p^2)$$

$$\text{Im } G(p^2) \text{Im } G(q^2) G[(q-p)^2] d^D q \quad (15)$$

In the scaling approximation

$$\Gamma_3 = (\dot{p}^2)^{\gamma_3} \quad (16)$$

and using (15) we get from (16)

$$(q^2)^{1-\frac{\eta}{2}} \sin \frac{\pi \eta}{2} = \frac{g_3^2}{(2\pi)^D} \int (q^2)^{2\gamma_3} [(q - \dot{p})^2]^{\frac{\eta}{2}-1} \sin^2 \frac{\pi \eta}{2} \frac{(q^2)^{D/2} \pi^{\frac{D-1}{2}}}{\Gamma \left[ \frac{D-1}{2} \right] 2^{D-2}} dx dy \quad (17)$$

where  $x = \frac{\dot{p}^2}{q^2}$ ,  $y = \frac{(\dot{p} - q)^2}{q^2}$ ,  $\max (\dot{p} - q)^2 \approx q^2$ ,

and

$$d^D \dot{p} = d\dot{p}_0 d|\dot{p}|^{D-2} \Omega_{D-2} = \frac{(q^2)^{D/2} \pi^{\frac{D-1}{2}}}{\Gamma \left[ \frac{D-1}{2} \right] 2^{D-2}} \quad (18)$$

From equation (19) we get

$$2\gamma_3 + \frac{3}{2} \eta + \frac{D-6}{2} = 0 \quad (19)$$

and

$$\sin \frac{\pi \eta}{2} = \frac{g_3^2}{(2\pi)^D} \int_0^1 x^{\frac{\eta}{2}-1} y^{\frac{\eta}{2}-1} \sin^2 \frac{\pi \eta}{2} \frac{\pi^{\frac{D-1}{2}}}{\Gamma \left[ \frac{D-1}{2} \right] 2^{D-2}} dx dy \quad (20)$$

This equation will give for  $\eta$  the value

$$\frac{\eta}{2} = \frac{\pi^{D+1}}{\Gamma \left[ \frac{D-1}{2} \right] 2^{D-2}} \frac{g_3^2}{(2\pi)^D} \quad (21)$$

In order to calculate the value  $\gamma_3$  we will use the equation (17) in the approximation which is shown in fig 8

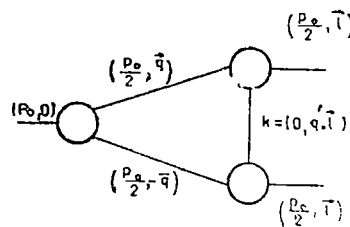


Fig. 8.

and using

$$k^2 = -(\vec{q} - \vec{l})^2 = -\frac{p_0^2}{2}(1 - \cos \theta) \quad (22)$$

where  $\Theta$  is angle between  $\vec{q}$  and  $\vec{l}$  we will perform the integral in (17) with the substitution

$$d^D p = dp_0 d|\vec{p}| |\vec{p}|^{D-2} \Omega_{D-3} \sin^{D-3} \Theta d\Theta$$

However, in order to introduce the variables  $x$  and  $y$  the angular part will be

$$= 2 \int \frac{\sin^{D-3} \Theta}{1 - \cos \Theta} d\Theta \quad (23)$$

and finally if (22) is also considered, we get from (17)

$$\frac{\sin \pi \gamma_3}{\pi} = -4 \frac{\eta/2}{\int \sin^{D-3} \Theta d\Theta} \left[ \int \frac{\sin^{-3} \Theta d\Theta}{1 - \cos \Theta} \right] \quad (24)$$

From (21) and (24) we get in  $D = 6$  the following expressions for  $\eta$  and  $\gamma_3$

$$\eta = \frac{1}{6} \frac{\pi^3}{(2\pi)^6} g_3^2 \quad (25)$$

$$\gamma_3 = -\frac{1}{2} \frac{\pi^3}{(2\pi)^6} g_3^2$$

and using (21) we get

$$g_3^2 = \frac{2}{3} \frac{(2\pi)^6}{\pi^3} (6 - D) \quad (26)$$

which is in fact the fixed point in the  $\varphi^3$ -theory. Indeed if we use the notation  $\varepsilon = 6 - D$ ,

$$(g_3^*)^2 = \frac{4}{3} (2\pi)^3 \varepsilon \quad (27)$$

and in this way we have demonstrated that (19) is in fact the equation for the fixed point. In the transition point the coupling constant is (27) and  $\eta$  will be,

$$\eta = \frac{1}{72\pi^3} \varepsilon \quad (28)$$

## 2. The $\varphi^4$ -model.

The  $\varphi^4$ -model was intensively studied by different authors [1, 5, 9] and is in fact the most realistic model for the second order phase transitions.

The unitarity relations for the Green function and vertex function are

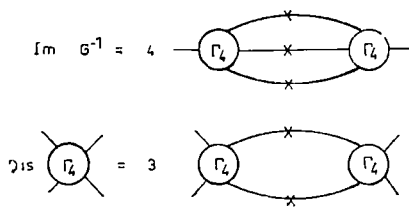


Fig 9

and if we consider  $\Gamma_4 = (p^2)^{\gamma_4}$  and  $\text{Im } \Gamma_4 = -\sin \pi \gamma_4 (p^2)^{\gamma_4}$  we can write down the equation for vertex function as

$$-\sin \pi \gamma_4 (p^2)^{\gamma_4} g_4 = \frac{g_4^2}{(2\pi)^D} \int |\Gamma_4|^2 \sin^2 \frac{\pi \eta}{2} (k^2)^{\frac{\eta}{2}-1} [(k-p)^2]^{\frac{\eta}{2}-1} d^D k \quad (30)$$

Following the same way as for the equation (16) with the substitutions

$$x = \frac{k^3}{p^3}, \quad y = \frac{(k-p)^3}{p^2}$$

we get the equation for the fixed point as

$$\gamma_4 + \eta + \frac{D-4}{2} = 0 \quad (31)$$

and the equation for  $\gamma_4$  as

$$\frac{\sin \pi \gamma_4}{\pi} = -c g_4$$

where

$$C = \int \frac{\pi^{D-1} dx dy}{(2\pi)^{D-1} 2^{D-1} \Gamma([D-1]/2)} \quad x \in [0, 1], y \in [0, 1]$$

From this relation we see that  $\gamma_4$  depends linearly on the coupling constant and the equation (31) for the fixed point will be

$$g_4^* = \frac{16\pi^2}{3} \varepsilon \quad (32)$$

where  $\varepsilon = D - 4$

With this result we start the calculation of  $\eta$  from the first equation (31) which will be written analytically as

$$\text{Im } G^{-1}(p^2) = 4g_4^2 \int d^D p d^D q |\Gamma_4(p, k, q)|^2 \text{Im } G(p) \text{Im } G(q) \text{Im } G(p+q-k) \quad (33)$$

From the beginning we remark that the index  $\eta$  will be dependent on the  $(g_4^*)^2$  and following the same method we get

$$\eta = \frac{\varepsilon^2}{54} \quad (34)$$

as in the Wilson theory.

**IV. Conclusions.** The unitarity condition for Green function, and vertex function, applied by Polyakov in order to obtain the asymptotic behaviour of physical quantities in the critical region, has been developed for the calculation of the fixed points and critical indexes in the  $\varphi^3$  and  $\varphi^4$  models. The method was also applied by Bray [9] in order to calculate the universality function in the  $\varphi^4$ -theory. These results prove that this method, which was successfully applied in high energy physics, can also be used in the theory of phase transitions and is in fact equivalent with the „parquet summation or RNG theory.

(Received November 20, 1979)

#### REFERENCES

- 1 K G Wilson, Phys Rev Lett, **28**, 548 (1972)
- 2 V V Sudakov, Dokl Akad Nauk SSSR, **111**, 338 (1956)
- 3 I T Diatlov, V V Sudakov, K A Ter-Martirosian, Zh Eksp Teor Fiz, **32**, 767 (1957)
- 4 A A Migdal, Zh Eksp Teor Fiz, **55**, 1964 (1968)
- 5 S L Ginzburg, Zh Eksp Teor Fiz, **76**, 697 (1974)
- 6 R J Eden, P V Landshoff, D L Olive, J C Polkinghorne, *The Analytic S-Matrix*, Cambridge Univ Press, Cap IV, 1965
- 7 A M Polyakov, Zh Eksp Teor Fiz, **35**, 1026 (1968)
- 8 A M Polyakov, Zh Eksp. Teor Fiz, **57**, 271 (1969)
- 9 A Bray, Phys Rev, **14**, 1248 (1976)
- 10 R A Ferrel, D J Scalapino, Phys Rev Lett, **34**, 200 (1974).
- 11 S L Ginzburg, Zh Exsp Teor Fiz, **68**, 273 (1975)

#### TEORIA FENOMENELOR CRITICE PENTRU MODELELE $\varphi^3$ SI $\varphi^4$ PE BAZA PROPRIETATILOR ANALITICE A MATRICEI S

(Rezumat)

Analiticitatea matricei  $S$  este folosită pentru calculul indicilor critici în cazul fenomenelor critice în modelele  $\varphi^3$  și  $\varphi^4$ .

EFFECT OF RETURN CURRENT ON THE HIGH FREQUENCY  
OSCILLATIONS OF A RELATIVISTIC ELECTRON BEAM-PLASMA  
SYSTEM

KARÁCSONY JÁNOS

**I Introduction.** As it is well-known electromagnetic waves can be excited by an electron beam penetrating through a uniform, cold, extended stationary plasma immersed in a uniform magnetic field  $\vec{B}_0$ . In this plasma-beam system, (the beam being assumed in motion in a direction parallel to the applied magnetic field  $\vec{B}_0$ ) the electromagnetic waves whose direction of propagation makes an angle  $\theta \neq 0$  with respect to  $\vec{B}_0$  are, in general, neither transverse nor longitudinal [1]. Particularly, when the velocity of propagation of the electromagnetic waves are small enough, i.e., when the refractive index  $n = ck/\omega$  is very large ( $c$  denoting here the velocity of light,  $k$  the wave number and  $\omega$  the frequency) „almost longitudinal” waves may occur [1–3]. For these waves the electric vector  $\vec{E}$  is nearly parallel to the wave vector  $\vec{k}$  [1].

The interaction between a nonrelativistic electron beam and a charge equilibrated one-component electronic plasma has already been investigated in the quasistatic (electrostatic) approximation by K. N. Stepanov and A. B. Kitzenko [2]. A more general case involving a two component electron-ion plasma interacting with a relativistic electron beam has been also considered by H. Wright and coworkers [3]. But, in their model an inconsistency occurs, since in unperturbed configuration the selfmagnetic field of the relativistic beam is neglected, which is in contradiction with Maxwell's equations. For short wavelengths, however, this inconsistency can be released by assuming a homogeneous return current to flow in the plasma. In certain circumstances, this representation seems to correspond to physical reality [4–6].

The purpose of the present paper is to investigate the influence of the return current in the quasistatic approximation earlier considered by H. Wright. As we will be concerned only with high frequency oscillations, we will assume the positive ions at rest, forming a stationary background of positive charge which neutralizes at each point the unperturbed electron gas. As it is known, the role of ion motion becomes important in the low frequency spectrum only. This case will be investigated by us in a forthcoming paper.

**II Dispersion equation.** We restrict the analysis to regions far enough behind the beam front in order that both electrostatic and magnetic neutralization should be insured. We will consider a relativistic electron beam with number density  $n_{bo}$  and we will assume that the average velocity of beam electrons  $\vec{v}_0$  is parallel to the external magnetic field  $\vec{B}_0$  oriented along the positive  $Oz$  axis. The plasma electrons producing the return current have a mean velocity

$$\vec{v}_1 = - (n_{bo}/n_0) \vec{v}_0 \quad (1)$$

where  $n_0$  denotes the plasma electron density satisfying the condition  $n_0 \gg n_{bo}$ .

Expression (1) for the plasma electron mean velocity follows from the current neutralization condition

$$\vec{j}_{bo} + \vec{j}_{po} = 0 \quad (2)$$

where  $\vec{j}_{bo} = -en_{bo}\vec{v}_0$  and  $\vec{j}_{po} = -en_0\vec{v}_1$  denote the unperturbed beam current density and plasma current density, respectively.

Considering small perturbations of the system from a steady state and for the situations in which all perturbations from uniformity vary as  $\exp[i(\vec{k}\vec{r} - \omega t)]$ , the general dispersion equation for longitudinal waves can be written as [2, 3].

$$\epsilon_{11} \sin^2 \theta + \epsilon_{33} \cos^2 \theta + 2 \epsilon_{13} \cos \theta \sin \theta = 0 \quad (3)$$

where  $\epsilon_{ij}$  ( $i, j = 1, 3$ ) are the dielectric tensor components of the system and  $\theta$  represents the angle between the wave vector  $\vec{k}$  and the direction of the external magnetic field  $\vec{B}_0$  (One assumes that the wave vector  $\vec{k}$  lies in the  $xOz$  plane).

The dielectric tensor can be expressed by means of the conductivity tensor  $\sigma$  in the following way [1, 7]

$$\epsilon_{ij} = \delta_{ij} + \frac{4\pi i}{\omega} \sigma_{ij} \quad (4)$$

In order to find the conductivity tensor components for the plasma-beam system we used the linearized relativistic equation of motion for the beam electron [7]

$$\left( \frac{\partial t}{\partial} + \vec{v}_0 \cdot \nabla \right) \left[ \gamma_0 \vec{v}' + \gamma_0^3 \frac{\vec{v}_0 (\vec{v}_0 \vec{v}')}{c^2} \right] = - \frac{e}{m} \left( \vec{E} + \frac{1}{c} \vec{v}' \times \vec{B}_0 + \frac{1}{c} \vec{v}_0 \times \vec{B}' \right) \quad (5)$$

and a nonrelativistic equation of motion for plasma electrons

$$\frac{\partial \vec{v}_1'}{\partial t} + (\vec{v}_1 \cdot \nabla) \vec{v}_1' = - \frac{e}{m} \left( \vec{E} + \frac{1}{c} \vec{v}_1 \times \vec{B}' + \frac{1}{c} \vec{v}_1' \times \vec{B}_0 \right) \quad (6)$$

together with the continuity equations. In these equations  $\vec{v}'$  and  $\vec{v}_1'$  are the perturbed velocities of the beam and plasma electrons,  $\vec{E}$  and  $\vec{B}'$  are the perturbed electric and magnetic fields, respectively, while  $\gamma_0 = (1 - v^2/c^2)^{-1/2}$ .

Finally, we obtained for the components  $\epsilon_{11}$ ,  $\epsilon_{13}$  and  $\epsilon_{33}$  of the dielectric tensor the following expressions:

$$\epsilon_{11} = 1 - \frac{1}{\omega^2} \left[ \frac{\omega_{b\perp}^2 (\omega - \vec{k} \vec{v}_0)^2}{(\omega - \vec{k} \vec{v}_0)^2 - \omega_{cR}^2} + \frac{\omega_p^2 (\omega - \vec{k} \vec{v}_1)^2}{(\omega - \vec{k} \vec{v}_1)^2 - \omega_c^2} \right] \quad (7)$$

$$\epsilon_{13} = - \frac{1}{\omega^2} \left[ \frac{\omega_{b\perp}^2 (\omega - \vec{k} \vec{v}_0) k_x v_0}{(\omega - \vec{k} \vec{v}_0)^2 - \omega_{cR}^2} - \frac{\omega_p^2 (\omega - \vec{k} \vec{v}_1) k_x |\vec{v}_1|}{(\omega - \vec{k} \vec{v}_1)^2 - \omega_c^2} \right] \quad (8)$$

$$\epsilon_{33} = 1 - \frac{1}{\omega^2} \left[ \frac{\omega_{b||}^2 k_x^2 v_0^2}{(\omega - \vec{k} \vec{v}_0)^2 - \omega_{cR}^2} + \frac{\omega_{b||}^2 \omega^2}{(\omega - \vec{k} \vec{v}_0)^2} + \frac{\omega_p^2 k_x^2 v_1^2}{(\omega - \vec{k} \vec{v}_1)^2 - \omega_c^2} + \frac{\omega_p^2 \omega^2}{(\omega - \vec{k} \vec{v}_1)^2} \right] \quad (9)$$

where  $\omega_p^2 = 4\pi n_0 e^2/m$  and  $\omega_{b||}^2 = \omega_{b\perp}^2/\gamma_0 = 4\pi n_{b0} e^2/(m\gamma_0^3)$  are the electron plasma frequency and the beam electron plasma frequency, respectively, while  $\omega_{cR} = \omega_c/\gamma_0 = \frac{eB_0}{mc\gamma_0}$ .

The substitution of (7)–(9) into (3) leads to the electrostatic dispersion equation:

$$1 - \frac{\omega_p^2 \cos^2 \Theta}{(\omega - \vec{k}\vec{v}_1)^2} - \frac{\omega_p^2 \sin^2 \Theta}{(\omega - \vec{k}\vec{v}_1)^2 - \omega_c^2} - \frac{\omega_{b||}^2 \cos^2 \Theta}{(\omega - \vec{k}\vec{v}_0)^2} - \frac{\omega_{b\perp}^2 \sin^2 \Theta}{(\omega - \vec{k}\vec{v}_0)^2 - \omega_{cR}^2} = 0 \quad (10)$$

**III. Excitation of longitudinal waves.** With the purpose to investigate the dispersion equation (10), we will follow the procedure used by H. W. R. G. and coworkers in [3]. At first we will put this equation in the form

$$F_p - \varepsilon \omega_p^2 \left[ \frac{\cos^2 \Theta}{\gamma_0 (\omega - \vec{k}\vec{v}_1)^2} - \frac{\sin^2 \Theta}{\gamma_0 [(\omega - \vec{k}\vec{v}_1)^2 - \omega_{cR}^2]} \right] = 0 \quad (11)$$

where

$$F_p(\vec{k}, \omega) = 1 - \frac{\omega_p^2 \cos^2 \Theta}{(\omega - \vec{k}\vec{v}_1)^2} - \frac{\omega_p^2 \sin^2 \Theta}{(\omega - \vec{k}\vec{v}_1)^2 - \omega_c^2} \quad (12)$$

and  $\varepsilon = n_{b0}/n_0 \ll 1$

As  $F_p$  does not depend of the parameters of the beam, it follows that the equality

$$F_p(\vec{k}, \omega) = 0 \quad (13)$$

represents the dispersion equation for a plasma in a drift motion with the velocity  $\vec{v}_1 = -\varepsilon\vec{v}_0$ . The last term in equation (11) represents the perturbation produced by the beam. For beams of small density, unless the quantity within the brackets is very large, this term is very small and consequently negligible. However, for frequencies in the neighborhood of frequencies that are singularities of bracketed term, the quantity in the brackets is very large and the contribution of the beam term in equation (11) becomes significant even when  $\varepsilon$  is extremely small. As one immediately sees the singularities of the bracketed term in (11) are  $\omega_1 = \vec{k}\vec{v}_0$  and  $\omega_{2\pm} = \vec{k}\vec{v}_0 \pm \omega_{cR}$ .

On the basis of the above arguments we will seek solutions of the electrostatic dispersion equation in the neighborhood of frequencies  $\omega_1$  and  $\omega_{2\pm}$ . The roots of (11) will be represented in the form

$$\omega = \omega_1 + \delta_1 \quad (14)$$

and

$$\omega = \omega_{2\pm} + \delta_{2\pm} \quad (15)$$

where  $\omega_1$  and  $\omega_{2\pm}$  must be both positive real numbers in order to ensure the interaction of the beam with plasma waves. Besides we must have

$$\lim_{\varepsilon \rightarrow 0} \delta_i = 0 \quad i = 1, 2 \quad (16)$$

Instability occurs when  $\text{Im } \delta < 0$ , where  $|\text{Im } \delta|$  denotes the rates of growth of an excited wave

*A. Excitation of longitudinal Cerenkov waves.* The wave which corresponds to the singularity of the first term in brackets in equation (11) is called the longitudinal Cerenkov wave [3]. In order to calculate the growth rate of the excited wave we insert (14) into (11). We observe that under the assumption that  $|\delta_1| \ll \omega_{cR}$  and  $\theta \neq \pi/2$ , the second term in brackets can be neglected. Expanding  $F_p$  in Taylor series about  $\omega_1$  and retaining only the first two terms, the dispersion equation becomes.

$$(\partial F_p / \partial \omega)_{\omega=\omega_1} \delta_1^3 + F_p(\omega_1) \delta_1^2 - \omega_{b11}^2 \cos^2 \theta = 0 \quad (17)$$

This equation has complex roots and consequently an instability occurs when the discriminant of (17) is positive. This happens if

$$4 [F_p(\omega_1)]^3 < 27 \epsilon \frac{\omega_p^3}{\gamma_0^3} \cos^2 \theta (\partial F_p / \partial \omega)_{\omega=\omega_1} \quad (18)$$

Here we used the definition  $\omega_{b11}^2 = \epsilon \omega_p^2 / \gamma_0^2$

As  $\epsilon$  is very small, (18) is satisfied only if

$$F_p(\omega_1) \approx 0 \quad (19)$$

or

$$F_p(\omega_1) < 0 \quad (20)$$

Condition (19) reveals that an instability will occur if  $\omega_1$  lies in the neighborhood of the frequency of a normal mode of the drifting electron plasma. In this case the dispersion equation has the following complex roots:

$$\delta_1 = \left( -\frac{1}{2} \pm i \frac{\sqrt{3}}{2} \right) \frac{\omega_{b11}^{2/3} \cos^{2/3} \theta}{[(\partial F_p / \partial \omega)_{\omega=\omega_1}]^{1/3}} \quad (21)$$

In order to calculate the growth rate for a certain well determined excited wave, the factor  $\partial F_p / \partial \omega$  must be evaluated for the frequency of excited wave. Due to (19), the excited wave frequencies correspond to the solutions of the plasma dispersion equation for plasma electrons drifting with velocity  $\vec{v}_1$ . These frequencies are the Doppler shifted normal mode frequencies of the stationary plasma:

$$\omega_{\pm} = \frac{\sqrt{2}}{2} (\omega_p^2 + \omega_c^2)^{1/2} \left[ 1 \pm \sqrt{1 - \frac{4\omega_p^2 \omega_c^2 \cos^2 \theta}{(\omega_p^2 + \omega_c^2)^2}} \right]^{1/2} + \vec{k} \cdot \vec{v}_1 = \omega_{p\pm} + \vec{k} \vec{v}_1 \quad (22)$$

Differentiating equation (12) with respect to  $\omega$  we immediately get

$$\frac{\partial F_p}{\partial \omega} = \frac{2}{(\omega - \vec{k} \vec{v}_1)} \left\{ \frac{\omega_p^2 \cos^2 \theta}{(\omega - \vec{k} \vec{v}_1)^2} + \frac{\omega_p^2 \sin^2 \theta (\omega - \vec{k} \cdot \vec{v}_1)^2}{[(\omega - \vec{k} \vec{v}_1)^2 - \omega_c^2]^2} \right\} \quad (23)$$

By inserting here  $\omega_{\pm}^2$  from (22), (23) becomes:

$$\left( \frac{\partial F_p}{\partial \omega} \right)_{\omega=\omega_{\pm}} = \frac{2}{\omega_{p\pm}^2} \left[ \frac{\omega_p^2 \cos^2 \theta}{\omega_{p\pm}^2} + \frac{\omega_p^2 \omega_{p\pm}^2 \sin^2 \theta}{(\omega_{p\pm}^2 - \omega_c^2)^2} \right] \quad (24)$$

This expression is identical with those that we should have obtained for a stationary plasma without return current. Therefore, from this result it follows that the return current has no influence on the growth rate of the excited waves which satisfy the condition (19). It yields only a Doppler shift of the excited wave frequencies, because instead of  $\omega_{p\pm}$  we must use  $\omega_{\pm}$  to calculate them.

Longitudinal Cerenkov waves can be excited outside the resonance frequency [3], when the condition (19) is not satisfied, but only the condition  $F_p(\omega_1) < 0$ . If condition (20) together with the following condition

$$|(F_p)_{\omega=\omega_1}| \gg |(\partial F_p / \partial \omega)_{\omega=\omega_1} \delta_1| \quad (25)$$

are fulfilled the term in equation (17) involving  $\delta_1^3$  can be neglected. Thus, it results

$$\delta_1 = \frac{\omega_{b||} \cos \theta}{[F_p(\omega_1)]^{1/2}} = \omega_{b||} \cos \theta \left\{ \frac{(\vec{k} \vec{v}_0 - \vec{k} \vec{v}_1)^* [(\vec{k} \vec{v}_0 - \vec{k} \vec{v}_1)^* - \omega_c^*]}{(\vec{k} \vec{v}_0 - \omega_+) (\vec{k} \vec{v}_0 - \omega_-)} \right\}^{-1/2} \quad (26)$$

Inspecting this expression we immediately see that if  $\vec{k} \vec{v}_0 < \omega_p + \vec{k} \vec{v}_1$  or if  $\omega_c + \vec{k} \vec{v}_1 < \vec{k} \vec{v}_0 < \omega_{p+} + \vec{k} \vec{v}_1$ , respectively, we will obtain a purely imaginary root

If the plasma return current would be neglected, we obtained for  $\delta_1$  the following expression

$$\delta_1 = \omega_{b||} \cos \theta \left\{ \frac{(\vec{k} \vec{v}_0)^* [(\vec{k} \vec{v}_0)^* - \omega_c^*]}{(\vec{k} \vec{v}_0 - \omega_{p+}) (\vec{k} \vec{v}_0 - \omega_{p-})} \right\}^{-1/2} \quad (27)$$

This last expression becomes purely imaginary for  $\vec{k} \vec{v}_0 < \omega_{p-}$  or  $\omega_c < \vec{k} \vec{v}_0 < \omega_{p+}$ . Now, if we compare this result with the previous one, we see that the return current produces a Doppler shift of the excited nonresonant Cerenkov waves. As  $\vec{v}_1 = -\vec{v}_0$ , the brackets in (26) differs from that in (27) by certain terms of first and higher order in  $\epsilon$ . Noting that  $\delta_1$  given by (26) is of order  $\epsilon^{1/2}$ , we conclude that the effect of return current on growth rate of nonresonant Cerenkov waves is quite weak.

*B. Excitation of the longitudinal cyclotron wave* The wave which corresponds to the singularity in the second term in brackets in equation (11) is called the longitudinal cyclotron wave [3]. In order to calculate the growth rate of this wave, we insert (15) into (11). Subsequently assuming  $|\delta_{2\pm}| \ll \omega_{cR}$  and  $\theta \neq 0$  the first term in brackets can be neglected. Expanding  $F_p$  in Taylor series about  $\omega_{2\pm}$  and retaining only the first two terms, the dispersion equation becomes:

$$(\partial F_p / \partial \omega)_{\omega=\omega_{2\pm}} \delta_{2\pm}^3 + F_p(\omega_{2\pm}) \delta_{2\pm} \mp \frac{\omega_{b||}^2 \sin^2 \theta}{2\omega_{cR}} = 0 \quad (28)$$

If the discriminant of this equation is negative, the equation has complex roots. On account of the expression (23) of  $\partial F_p / \partial \omega$  and as  $\omega = \omega_{2\pm} > 0$  it can be seen that the discriminant is always positive if the last term in equation

(28) is negative, i.e., for wave with frequency  $\omega = \omega_{2+}$ . Therefore the wave whose frequency is  $\omega = \vec{k} \vec{v}_0 + \omega_{cR}$  is stable for a cold beam.

On the contrary when the last term in (28) is positive, instability does occur if and only if

$$(F_p)_{\omega=\omega_2-}^2 < 2\epsilon \frac{\omega_p^2 \sin^2 \Theta}{\gamma_0 \omega_{cR}} (\partial F_p / \partial \omega)_{\omega=\omega_2-} \quad (29)$$

Here, we have used the notation  $\omega_{b\perp}^2 = \epsilon \omega_p^2 / \gamma_0$

As  $\epsilon$  is very small, (29) implies

$$(F_p)_{\omega=\omega_2-} \approx 0 \quad (30)$$

This means that instability may occur only for frequencies in the neighborhood of normal mode frequencies of the drifting electron plasma

Substituting (30) into (28), we immediately obtain the imaginary roots of this equation

$$\delta_{2-} = \pm i \left[ \frac{\omega_{b\perp}^2 \sin^2 \Theta}{2\omega_{cR} (\partial F_p / \partial \omega)_{\omega=\omega_2-}} \right]^{1/2} \quad (31)$$

where  $\omega_{2-} \approx \omega_{\pm}$ . It has been shown above that for  $\omega = \omega_{\pm}$ ,  $\partial F_p / \partial \omega$  involves no return current effect, therefore the growth rate of excited longitudinal cyclotron waves is not affected by the existence of the return current in the plasma. On the other hand, if the return current is taken into account only a Doppler shift of the excited wave frequencies appears, since we must use  $\omega_{\pm}$  instead of  $\omega_{p\pm}$  in the evaluation of the excited wave frequencies.

**IV. Conclusion.** In the present paper we have investigated the high frequency electrostatic oscillations in a relativistic electron beam-magnetized plasma system, taking into account the induced return current in the plasma. We were concerned with the effect of return current on high frequency oscillations of the beam-plasma system and therefore ion motion has been neglected. We find that the inclusion of return current in the calculations does not affect the growth rate values of resonant longitudinal Cerenkov and cyclotron waves and it has a quite weak effect on the growth rate of nonresonant Cerenkov waves. If the return current is taken into account a change in the frequencies of the excited wave appears, due to the drift motion of the plasma electrons which produces a Doppler shift of these frequencies.

A more significant effect of the return current is to be expected in the low frequency spectrum domain, where the drift motion of the electron relatively to the plasma ion background may excite a new instability. This will be investigated in a forthcoming paper.

(Received December 3, 1979)

#### R E F E R E N C E S

1. A. I. Ahiezer, *Elektrodinamika plazmy*, Nauka, Moscow, 1974
2. K. N. Stepanov, A. B. Kitzenko, *Zh. Tekhn. Fiz.* **31**, 167 (1961)
3. H. Wright, C. L. Wigington, J. Neufeld, *Phys. Fluids*, **8**, 1375 (1965)
4. J. L. Cox, W. H. Bennett, *Phys. Fluids*, **13**, 182 (1970)

- 5 D A Hammer, N Rostoker, Phys Fluids, **13**, 1831 (1970)
- 6 R. Lee, R. N. Sudan, Phys Fluids, **14**, 1213 (1971)
7. P. C Clemmow, J. P Dougherty, *Electrodynamics of Particles and Plasmas*, London, Addison-Wesley Publ. Comp., 1969

**EFFECTUL CURENTULUI INVERS ASUPRA OSCILAȚIILOR DE FRECVENTE RIDICATE  
ALE SISTEMULUI PLASMĂ-FASCICUL RELATIVIST DE ELECTRONI**

(Rezumat)

Se studiază influența curentului invers asupra oscilațiilor instabile ale unui sistem de plasmă-fascicul relativist de electroni. Se constată că din cauza curentului invers frecvența oscilațiilor excitate prezintă o deplasare Doppler, în timp ce coeficientul de amplificare nu este influențat în mod sensibil.

# EFFECT OF ION DYNAMICS ON THE PARAMETRIC INSTABILITIES OF AN UNMAGNETIZED PLASMA (I)

C. BĂLEANU

We have consacrated the present paper to the study of the parametric oscillations in an unmagnetized two — components plasma immersed in an external oscillatory electric field

$$\vec{E}_0 \cos(\vec{k}_0 \cdot \vec{r} - vt) \approx \vec{E}_0 \cos vt \quad (1)$$

considering the ions as statistically moving particles and by making use of R Prasad's method [4]. This topic has been already investigated by R Prasad [5] for cold plasma, yet by applying a method given by N N. Bogoliubov and Yu A Mitropolskii [2]. At the same time C S Chen and G J Lewak [3] considered the same problem for an unmagnetized plasma by taking into account the thermal motion and making use of the multi time scales method. We have in our turn discussed in a previous paper [1] this problem, but for a magnetized plasma imbedded in an external circularly right — hand polarized electric field by taking into account the thermal motion too.

Denoting by  $f^e$  and  $f^i$  the distribution functions of electrons and ions respectively we may write the collisionless Boltzmann equations for both these functions under the form

$$\frac{\partial f^e}{\partial t} + \vec{v}^e \frac{\partial f^e}{\partial \vec{r}^e} - \frac{e}{m} \left( \vec{E} + \frac{\vec{v}^e}{c} \times \vec{B} \right) \frac{\partial f^e}{\partial \vec{v}^e} = 0 \quad (2)$$

$$\frac{\partial f^i}{\partial t} + \vec{v}^i \frac{\partial f^i}{\partial \vec{r}^i} + \frac{e}{M} \left( \vec{E} + \frac{\vec{v}^i}{c} \times \vec{B} \right) \frac{\partial f^i}{\partial \vec{v}^i} = 0 \quad (3)$$

One may derive from Maxwell equations the second-order differential equation for the first-order perturbation of the electric field.

$$\left( \text{grad div} - \nabla^2 + \frac{1}{c^2} \frac{\partial^2}{\partial t^2} \right) \vec{E}_1(\vec{r}, t) = - \frac{4\pi}{c^2} \frac{\partial}{\partial t} \vec{j}(\vec{r}, t) \quad (4)$$

where  $\vec{j}(\vec{r}, t)$  is the first order perturbation of the total current density and is represented by

$$\vec{j}(\vec{r}, t) = - e \int \vec{v}^e f_1^e d\vec{v}^e + e \int \vec{v}^i f_1^i d\vec{v}^i \quad (5)$$

By making the following assumptions

$$\vec{E}_0 = E_0 \hat{e}_z \quad (6)$$

$$\vec{k} = k \hat{e}_z \quad (7)$$

$$\vec{E}^T(\vec{k}, t) = e^{-i\omega t} \sum_{n=-\infty}^{\infty} \vec{E}_n^T(\vec{k}) e^{-imvt} \quad (8)$$

one obtains the following infinite system of equations for the spatial Fourier transforms of the transversal electric field.

$$a_{n-1} \frac{\vec{E}_{n-1}^T(\vec{k})}{\omega + n - 1 v} + \frac{\vec{E}_n^T(\vec{k})}{\omega + nv} + b_{n-1} \frac{\vec{E}_{n+1}^T(\vec{k})}{\omega + n + 1 v} = 0 \quad (9)$$

where:

$$a_n = \frac{\eta^e [F^e(\omega + nv) - F^e(\omega + \overline{n+1}v) + PF^e(v)]}{\frac{c^2 k^2}{v^2} - \left(\frac{\omega}{v} + n + 1\right)^2 - \frac{\omega_{pe}^2}{v^2} F^e(\omega + \overline{n+1}v) - \frac{\omega_{ps}^2}{v^2} F^e(\omega + \overline{n+1}v)} - \frac{\eta^s [F^s(\omega + nv) - F^s(\omega + \overline{n+1}v) + PF^s(v)]}{\frac{c^2 k^2}{v^2} - \left(\frac{\omega}{v} + n + 1\right)^2 - \frac{\omega_{pe}^2}{v^2} F^s(\omega + \overline{n+1}v) - \frac{\omega_{ps}^2}{v^2} F^s(\omega + \overline{n+1}v)} \quad (10)$$

$$b_n = \frac{\eta^e [F^e(\omega + nv) - F^e(\omega + \overline{n-1}v) + PF^e(-v)]}{\frac{c^2 k^2}{v^2} - \left(\frac{\omega}{v} + n - 1\right)^2 - \frac{\omega_{pe}^2}{v^2} F^e(\omega + \overline{n-1}v) - \frac{\omega_{ps}^2}{v^2} F^e(\omega + \overline{n-1}v)} - \frac{\eta^s [F^s(\omega + nv) - F^s(\omega + \overline{n-1}v) + PF^s(-v)]}{\frac{c^2 k^2}{v^2} - \left(\frac{\omega}{v} + n - 1\right)^2 - \frac{\omega_{pe}^2}{v^2} F^s(\omega + \overline{n-1}v) - \frac{\omega_{ps}^2}{v^2} F^s(\omega + \overline{n-1}v)} \quad (11)$$

$$F^{e,s}(\Omega) = \Omega \Psi_0^{e,s}(\Omega) \quad (12)$$

$$\Psi_0^{e,s} = \frac{v}{(2\pi\theta_{e,s})^{1/2}} \int_{-\infty}^{\infty} \frac{e^{-u^2/2\theta_{e,s}}}{ku - z} du \quad (13)$$

$$\eta^e = \frac{i\omega_{pe}^2}{v^2} \frac{e_e(\vec{k})}{2}, \quad \eta^s = \frac{i\omega_{ps}^2}{v^2} \frac{e_s(\vec{k})}{2} \quad (14)$$

$$\omega_{pe}^2 = \frac{4\pi n_0 e^2}{m} \quad (15)$$

$$\omega_{ps}^2 = \frac{4\pi n_0 e^2}{M} \quad (16)$$

$$e_e(\vec{k}) = \frac{e \vec{k} \vec{E}_0}{mv^2} \quad (17)$$

$$e_s(\vec{k}) = \frac{e \vec{k} \vec{E}_0}{Mv^2} \quad (18)$$

The infinite system of equations (9) leads to the dispersion relation represented by an infinite periodic determinant of period  $\omega/v = 1$ , namely

$$\Delta \left( \frac{\omega}{v} \right) = \begin{vmatrix} 1 & b_1 & 0 & 0 \\ a_0 & 1 & b_2 & 0 \\ 0 & a_1 & 1 & b_3 \\ 0 & 0 & a_2 & 1 \end{vmatrix} = 0 \quad (19)$$

The determinant (19) has been evaluated for the two following cases

a) Both the electronic and ionic plasma are cold, that is  $\theta_e \rightarrow 0$  and  $\theta_i \rightarrow 0$  ( $\theta_{ei}$  being the kinetic temperatures of electrons respectively ions). From dispersion relation (19) we get

$$\sin^2 \pi z = \sin^2 \pi \alpha \left[ 1 + \left( \frac{\omega_{pe}^2 \epsilon_e(\vec{k})}{v^2} - \frac{\omega_{pi}^2 \epsilon_i(\vec{k})}{v^2} \right)^2 \frac{2\pi \cot \pi \alpha}{\alpha(4\alpha^2 - 1)} \right] \quad (20)$$

where .

$$z = \frac{\omega}{v}, \quad \alpha^2 = \frac{c^2 k^2 + \omega_{pe}^2 + \omega_{pi}^2}{v^2} \quad (21)$$

b) The electronic plasma is hot, while the ionic plasma cold, besides the following conditions hold .

$0 << \frac{2k^2 \theta_e}{v^2} << 1$ . The dispersion relation for this case is

$$-\frac{\left[ \eta^e \left( 1 + \frac{k^2 \theta_e}{v^2} \right) - \gamma^2 \right]^2}{(2\gamma_1 \cotg \pi \gamma_1 - \gamma_2 \cotg \pi \gamma_2)(\gamma_1^2 - \gamma_2^2)} \left( \frac{\gamma_1 \sin 2\pi \gamma_1}{\sin^2 \pi z - \sin^3 \pi \gamma_1} - \frac{\gamma_2 \sin 2\pi \gamma_2}{\sin^2 \pi z - \sin^3 \pi \gamma_2} \right) - \left\{ \frac{2\pi \gamma_1^2 \cotg \pi \gamma_1}{4\gamma_1^2 - 1} + \frac{2\pi \gamma_2^2 \cotg \pi \gamma_2}{4\gamma_2^2 - 1} + \frac{2\pi \gamma_1^2 \gamma_2^2}{(1 - \gamma_1^2 - \gamma_2^2)^2 - 4\gamma_1^2 \gamma_2^2} \left[ (1 - \gamma_1^2 - \gamma_2^2) \left( \frac{\cotg \pi \gamma_1}{\gamma_1} + \frac{\cotg \pi \gamma_2}{\gamma_2} \right) + 2(\gamma_1 \cotg \pi \gamma_1 + \gamma_2 \cotg \pi \gamma_2) \right] \right\} = 1 \quad (22)$$

where  $\gamma_1^2$  and  $\gamma_2^2$  are roots of the algebraic equation

$$\alpha^2 + \frac{\beta^2}{(z + n)^2} - (z + n)^2 = 0 \quad (23)$$

with :

$$\beta^2 = \frac{k^2 \theta_e \omega_{pe}^2}{v^4} \quad (24)$$

For the first case of cold plasma (20) gives the following expressions of growth rates

$$\begin{aligned}\lambda_{\max} = \lambda_{\max}^0 &= -\frac{\pi v}{8c^2} \frac{\omega_{pe}^4}{v^4} \left( \frac{E_0}{mv^2} \right)^2 \frac{\omega_{pi}^2}{n(n+1)(2n+1)} - \\ &- \frac{\pi v}{16c^2} \left( \frac{eE_0}{v^2} \right)^2 \frac{(2n+1)^2 v^2 - 4\omega_{pe}^2}{n(n+1)(2n+1)} \frac{\omega_{pe}^2 \omega_{pi}^2}{v^4 m M}\end{aligned}\quad (25)$$

when  $\alpha = n + 1/2$

and

$$\lambda_{\max} = \lambda_{\max}^0 - \frac{\pi v}{4c^2} \left( \frac{eE_0}{mv^2} \right)^2 \frac{\omega_{pe}^4}{v^4} \frac{\omega_{pi}^2}{n(4n^2 - 1)} - \frac{\pi v}{2c^2} \left( \frac{eE_0}{v^2} \right)^2 \frac{1}{v^4} \frac{n^2 v^2 - \omega_{pe}^2}{n(4n^2 - 1)} \frac{\omega_{pe}^2 \omega_{pi}^2}{m M} \quad (26)$$

when  $\alpha = n$

In (25) and (26)  $\lambda_{\max}^0$  denotes the maximum growth rates when ion dynamics is neglected. By inspecting (25) and (26) we see that if ion dynamics is taken into account decreasing effect, on the maximum growth rates will appear. This result is in agreement with that previously obtained by other authors [3], [5].

For hot electronic plasma the dispersion relation is a very cumbersome one, therefore the evaluation of  $\text{Im}(\omega/v)$  needs numerical computations.

If  $\alpha$  is taken large enough and the frequency  $v$  close to  $\sqrt{\omega_{pe}^2 + \omega_{pi}^2}$ , the approach of  $E_0 \cos(\vec{k}_0 \cdot \vec{r} - vt)$  by  $\vec{E}_0 \cos vt$  is well founded and our results are valid.

The stimulating discussions with Profesor M Drăganu are gratefully acknowledged.

(Received December 3, 1979)

#### R E F R E N C E S

- 1 C Băleanu, Bull Math de la Soc Sci Math de la RS Roumanie, **22** (70), 245, 339 (1978)
- 2 N N Bogoliubov, Yu A Mitropol'skii, *Asimptoticheskie metodi v teorii nelineinikh kolebanij*, Moskva, Izdatel'stvo Nauka, 1974
- 3 C S Chen, G J Lewak, J. Plasma Phys., **4**, 357 (1970)
- 4 R Prasad, The Phys of Fluids, **10**, 2642 (1967)
- 5 R Prasad, J Plasma Phys., **5**, 291 (1971)

#### EFFECTUL DINAMICII IONILOR ASUPRA INSTABILITĂȚILOR PARAMETRICE ALE UNEI PLASME NEMAGNETIZATE (I)

(R e z u m a t)

Folosind teoria cinetică, este studiat efectul mișcării ionilor asupra instabilităților parametrice ale unei plasme total ionizate nemagnetizate formată din electroni și ionii de o singură specie. Studiul s-a limitat la cimpul răspuns transversal care se propagă paralel cu direcția cimpului exterior (pompă).

Au fost determinați coeficienții de creștere pentru cazul plasmei reci.

## INTERDIFFUSION OF GASES IN LIQUID METALS

SPERANȚA COLDEA

The interaction of gases and liquid metals is a topic of fundamental and practical interest. The diffusion of gases in liquid metals prior to and during solidification determines the concentration of incorporated gases in the solid which in turn influences the mechanical, electrical, and chemical properties of the metal systems. Knowledge of the interdiffusion coefficients of gases in liquid metals and binary alloys, as well as of the other atomic transport coefficients contributes to the understanding of the structure and properties of liquid metals.

The interdiffusion of gases as hydrogen, oxygen and nitrogen in different liquid metals and alloys was experimentally investigated in various temperature conditions and for several compositions, including the pure components [1]—[12]. The diffusion coefficients of hydrogen in some pure liquid metals and the diffusivities of hydrogen and nitrogen in liquid iron alloys were determined [2]—[3]. Because the affinity of oxygen with metal is very strong the experiments for the measurements of oxygen interdiffusion in liquid metals are more difficult than for hydrogen and nitrogen. So, the interdiffusion coefficients of oxygen have been measured only in liquid iron, nickel [4a—b], lead [5], [6b], silver [6a—b], and copper [6b], [7a—b], [8]—[10]. The oxygen diffusion coefficients in liquid copper-lead alloys and gallium-indium alloys were recently determined [11]—[12].

However, there are only a few studies available on each gas-liquid metal-systems and when there are many, they are usually contradictory. It would be desirable to perform many other measurements of interdiffusion coefficients in a large temperature range.

Many mechanisms have been proposed in order to explain diffusion phenomena in liquid metals. Semiempirical models are in general transposed from diffusion theories appropriate to crystals and, as they make use of numerous parameters, their agreement with experimental data is not significant. On the other hand, statistical methods evolved from the theory of dense hard-sphere fluids [13] are successful, although the adjustable parameters are only the hard-sphere diameter  $\sigma$  and the radial distribution function  $g(\sigma)$  deduced from the compressibility factor  $Z$ .  $Z$  can be calculated using the Carnahan-Starling or Percus-Yevick approximations, when the packing fraction is known [14]—[15].

The temperature dependence of the interdiffusion of gases in liquid metals is very well reproduced when approximation is made for the relative softness of the repulsive potential of the fluid. This approximation leads to a temperature dependent hard-sphere diameter  $\sigma(T)$ .

In the present paper this last theoretical model is applied to the calculation of the interdiffusion coefficients.

The basic expression for the interdiffusion is that from the Enskog-Thorne theory of mutual diffusion in a binary dense fluid [13]

$$D_{12} = \frac{D_{12,0}}{g_{12}} \quad (1)$$

where  $D_{12,0}$  is the interdiffusion coefficient for diluted binary fluids

$$D_{12,0} = \frac{3}{8n} \frac{\sigma_{12}^2}{\sigma_1^2} \left[ \frac{kT(m_1 + m_2)}{2\pi n_1 m_2} \right]^{1/2} = \quad (2)$$

$$= \frac{1.5}{(n_1 + n_2)(\sigma_1 + \sigma_2)^2} \cdot \left[ \frac{kTN_A(M_1 + M_2)}{2\pi M_1 M_2} \right]^{1/2} \quad (2')$$

with  $m_i$  — the mass of the „ $i$ ”-component of the binary fluid,  $\sigma_{12}$  — the diameter of the hard-spheres mixture,  $n_i$  — the numerical density of the „ $i$ ” component,  $M_i$  — the atomic weight ( $i = 1, 2$ ),  $T$  is the temperature of the system,  $k$  — the Boltzmann's constant,  $\sigma_1, \sigma_2$  are the hard-spheres diameters of the two components of the fluid;  $g_{12}(\sigma_{12})$  in the relation (1) is the pair correlation function at contact between two dissimilar molecules, which represents the correction to the value of  $D_{12,0}$ ,  $n$  is the total atom density of the system:  $n = n_1 + n_2$

Two kinds of expressions can be used to calculate the pair correlation function  $g_{12}$ . The first is the Lebowitz pair correlation function [16] subsequently corrected in an approximate manner [17]

$$g_{12} = \frac{(2 - \eta)}{(2 + \eta)(1 - \eta)^2} \left[ 1 + \frac{\eta}{2} \left\{ 1 - 3 \frac{(\sigma_1 - \sigma_2)(\eta_1 - \eta_2)}{(\sigma_1 + \sigma_2)(\eta_1 + \eta_2)} \right\} \right] \quad (3)$$

where  $\eta_i$  are the packing fractions of the „ $i$ ”-species, defined by the following expressions [14]:

$$\eta_i = \frac{\pi}{6} n_i \sigma_i^3 \quad (4)$$

and

$$\eta = \eta_1 + \eta_2 \quad (2)$$

A better possibility is to use the Carnahan-Starling expression for the correlation function  $g_{12}$  [15]

$$g_{12} = (\sigma_1 g_{22} + \sigma_2 g_{11})/2\sigma_{12} \quad (6)$$

where

$$g_{ii} = \frac{1}{1 - \eta} + \frac{3Y_i}{2(1 - \eta)^2} + \frac{Y_i^2}{2(1 - \eta)^3} \quad (7)$$

and

$$Y_i = (\sigma_i \eta_i + \sigma_j \eta_j)/\sigma_j \quad (i, j = 1, 2) \quad (8)$$

The expression (3) for  $g_{12}$  was earlier tested for shear viscosity coefficients of binary alloys [18] and the results should allow the conclusion that this correlation function is inferior to that of Carnahan-Starling expression (6).

The most important parameters of the theory are the hard-sphere diameters  $\sigma_i$  ( $i = 1, 2$ ) of the components of binary fluid systems. The following temperature dependence of the effective hard-sphere diameter for metal atom was proposed [14].

$$\sigma_T = 1,288 \left( \frac{M}{\rho_m} \right)^{1/3} \cdot \left[ 1 - 0,112 \left( \frac{T}{T_m} \right)^{1/2} \right] (10^{-8} \text{ cm}) \quad (9)$$

where  $\rho_m$  is the mass density of the metal at the melting point  $T_m$  and  $M$  is the atomic weight of the metal.

In order to maintain a constant ratio of gas-metal diameters, at any temperature, we must postulate that the gases diameters  $\sigma_g$  depend on the liquid metal (the solvent), as follows

$$\gamma_{gas} = \sigma_c \left[ 1 - 0,112 \left( \frac{T}{T_m} \right)^{1/2} \right] (\cdot 10^{-8} \text{ cm}) \quad (10)$$

where  $\sigma_c$  is the corresponding covalent diameter of the gas

Another element of the present model is the correction which we can deduce from the molecular dynamics calculations, effectuated for binary systems diffusion [19]. Applying this correction term to the interdiffusion expression (1) we obtain the following final term.

$$D = c \cdot D_{12} = \quad (11)$$

$$= \frac{1,5C}{(n_1 + n_2)(\sigma_1 + \sigma_2)^2 g_{12}} \cdot \left[ \frac{kTN_A(M_1 + M_2)}{2\pi M_1 M_2} \right]^{1/2} \quad (11')$$

$g_{12}$ ,  $\sigma_1$  and  $\sigma_2$  can be easily calculated from the relations (6), (9) and (10).

Numerical evaluations of the interdiffusion coefficients, in several liquid metals systems will be made in order to test the expression (11). The results will be compared with the available experimental data and will be reported in a following paper

(Received December 3, 1979)

#### R E F E R E N C E S

1. E. M. Sacris and N A D Parlee, Met Trans., **1**, 3377 (1970)
- 2 P V Depuydt and N A D Parlee, Met Trans., **3**, 525 (1972)
- 3 J Y. Lee and N A D Parlee, High Temp. Sci., **4**, 147 (1972)
- 4 a) K Suzuki and K Mori, Iron Steel Inst Japan, **57**, 51 (1971),  
b) S Otsuka and Z Kozuka, Trans Japan Inst Metals, **18**, 690 (1977)
- 5 a) S Honma, N Sano and Y Matsushita, Met Trans., **2**, 1494 (1971);  
b) S Otsuka and Z Kozuka, Trans Japan Inst Metals, **6B**, 399 (1975)
- 6 a) I D Shah and N A D Parlee, Trans Met Soc AIME, **239**, 763 (1967).  
b) H Rickert and A A El-Miligy, Z Metallk., **59**, 635 (1968).
- 7 a) J Osterwald and G Schwarzlose, Z. Phys Chem N F, **62**, 119, (1968).  
b) S Otsuka and Z Kozuka, Met Trans., **7B**, 147 (1976)
- 8 S Otsuka and Z Kozuka, Trans Japan Inst Metals, **15**, 32 (1974)
- 9 K E Oberg, L M Friedman and R A Rapp, Met Trans., **4B**, 61 (1973)
- 10 M A El-Naggar and N A D Parlee, High Temp Sci., **3**, 138 (1971)
- 11 S Otsuka, M Matsuyama and Z Kozuka, Met Trans., **9B**, 21 (x1978)

- 12 S K Hahn and D A Stevenson, *High Temp Sci*, **9**, 165 (1977).
- 13 S Chapman and T G Cowling, *The Mathematical Theory of Non-uniform Gases*, Cambridge Univ Press, 1959
- 14 P Protopapas, H C Andersen and N A D Parlee, *J Chem Phys*, **59**, 15 (1973)
15. G A Mansoori, N F Carnahan, K E Starling and T W Leland, *J Chem Phys*, **54**, 1523 (1971)
- 16 T L Lebowitz, *Phys Rev* **133A**, 895 (1964)
- 17 P Protopapas and N A D Parlee, *Chem Phys*, **11**, 201 (1975)
- 18 S Coldea, *Rev Roum Phys*, **24**, 459 (1979)
- 19 B J Alder, W E Alley and J H Dymond, *J Chem Phys*, **61**, 1415 (1974)

### INTERDIFUZIA GAZELOR ÎN METALE LICHIDE

(Rezumat)

Lucrarea propune un model teoretic care permite calculul efectiv al coeficienților de interdifuzie a gazelor în metale lichide, pornind de la teoria Enskog-Thorne a difuziei mutuale în fluide binare dense. Rezultatul obținut pentru interdifuzie, folosind și elemente ale teoriei metalelor lichide, cum ar fi dependența diametrului atomilor de temperatură, î se aplică un termen de corecție determinat pe baza calculelor de dinamici moleculare.

## EFFECT OF SOME PARAMAGNETIC IONS ON THE STRUCTURE OF SOME BORATE VITREOUS MATRICES

S. SIMON, AL. NICULA

**I. Introduction.** Nuclear magnetic resonance studies contributed successfully to the elucidation of the structure and chemical bondings in binary borate glasses [1–3]. Thus it was evidenced the considerable effect of alkali oxides on the boron coordination which led to the explanation of modifications of the properties of borate glasses, with the modification of alkali oxide content

Recent NMR studies approached the problem of  $\text{SiO}_2$ ,  $\text{Al}_2\text{O}_3$  and  $\text{P}_2\text{O}_5$  effects on the fraction  $N_4$  of boron atoms in  $\text{BO}_4$  units from the vitreous system  $\text{Na}_2\text{O}-\text{B}_2\text{O}_3-\text{SiO}_2$  [4–6],  $\text{Na}_2\text{O}-\text{B}_2\text{O}_3-\text{Al}_2\text{O}_3$  [7] and  $\text{K}_2\text{O}-\text{B}_2\text{O}_3-\text{P}_2\text{O}_5$  [8] respectively.

It is known the fact that the glass colouring is realized also with paramagnetic ions introduced in different concentrations and proportions in the matrix. The aim of this paper is to study, for the first time, in what way these ions modify the coordination type of boron in binary sodium borate glasses having in view that their stability and their physical and mechanical properties are determined by the fraction  $N_4$  of four-coordinated boron atoms. Partial results of these concerns were still presented by us in other papers [9–10].

**II. Experimental results.** Two types of samples were prepared. samples of type A having the composition  $84\text{B}_2\text{O}_3-16\text{Na}_2\text{O}$  (mol %) and samples of type B with the composition  $66,66\text{B}_2\text{O}_3-33,33\text{Na}_2\text{O}$  (mol %). In both types of samples were introduced the following oxides.  $\text{Cr}_2\text{O}_3$ ,  $\text{Co}_2\text{O}_3$ ,  $\text{MnO}$ ,  $\text{MoO}_3$ ,  $\text{V}_2\text{O}_5$  and  $\text{NiO}$  in concentrations of 4 mol % and 10 mol %.

The glasses were prepared by mixing together reagent grade oxides in suitable proportions and melting at  $1000^\circ\text{C}$  for 1 h. After being kept at this temperature the glasses were poured onto a unoxidizable steel plate at room temperature.

The  $^{11}\text{B}$ -NMR spectra were registered at 9,212 MC on a JEOL spectrometer, on powder samples at room temperature. Figure 1 indicates the  $^{11}\text{B}$  NMR spectrum on  $\text{B}_2\text{O}_3$  vitreous glass, figures 2a and 2b represent the NMR spectra registered on samples of type A respectively B without paramagnetic ions, while figures 3 and 4 show the resonance signals on samples with paramagnetic ions of different types, in different concentrations. The symbols of samples, as well as the values of the ratio c/a (fig. 2a) measured from the resonance spectra for all the twenty-six prepared glasses are given in table 1.

**III. Discussions and conclusions.** It was established that the value of the nuclear quadrupole coupling constant for the case of three coordinated boron is the same nondepending of glass composition, of presence or absence of paramagnetic ions and this value coincides with that determined for the  $\text{B}_2\text{O}_3$  vitreous glass (see fig. 1–4). This conclusion is an argument to consider that the planar  $[\text{BO}_3]$  triangular units connected randomly by the sharing of

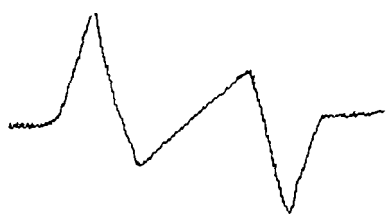


Fig 1 The  $^{11}\text{B}$ -NMR spectrum on  $\text{B}_2\text{O}_3$  vitreous glass

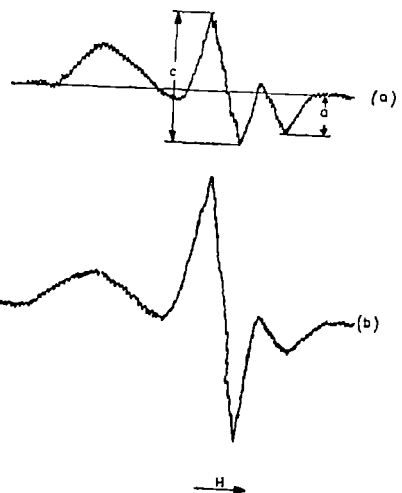


Fig 2 The  $^{11}\text{B}$ -NMR spectra on sodium borate glasses unimpurified with paramagnetic ions, 2a) sample  $\text{A}_0$ , 2b) sample  $\text{B}_0$

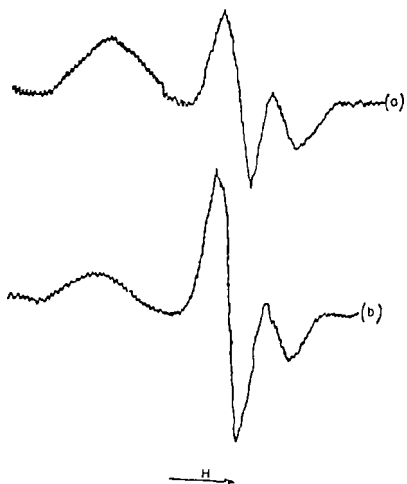


Fig 3 The  $^{11}\text{B}$ -NMR spectra on sodium borate glasses with 4 mol% paramagnetic ions, 3a) sample  $\text{A}_4$ , 3b) sample  $\text{B}_4$

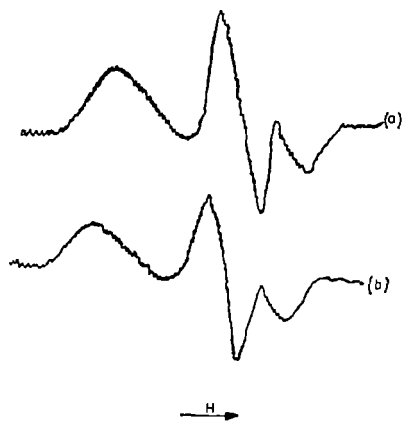


Fig 4 The  $^{11}\text{B}$ -NMR spectra on sodium borate glasses with 10 mol% paramagnetic ions, 4a) sample  $\text{A}_{10}$ ; 4b) sample  $\text{B}_{10}$

all three oxygen vertices specific of the  $\text{B}_2\text{O}_3$  glasses are maintained also in the studied glasses

The nuclei of boron atoms belonging to these units give the broad resonance line corresponding to the  $m = \frac{1}{2} \rightarrow -\frac{1}{2}$  central transition distorted in second-order by quadrupole interaction of the  $^{11}\text{B}$  nucleus.

Table 1

The value of the ratio  $c/a$  measured from the  $^{11}\text{B}$ -NMR spectra

Samples of Type A			Samples of Type B		
Symbol	Content in mol % and type of metallic oxide	$c/a$	Symbol	Content in mol % and type of metallic oxide	$c/a$
A <sub>0</sub>	—	2,44	B <sub>0</sub>	—	7,89
A <sub>4</sub> <sup>1</sup>	4% MoO <sub>3</sub>	3,06	B <sub>4</sub> <sup>1</sup>	4% MoO <sub>3</sub>	5,80
A <sub>10</sub> <sup>1</sup>	10% MoO <sub>3</sub>	3,23	B <sub>4</sub> <sup>10</sup>	10% MoO <sub>3</sub>	3,34
A <sub>2</sub> <sup>2</sup>	4% Cr <sub>2</sub> O <sub>3</sub>	3,75	B <sub>4</sub> <sup>2</sup>	4% Cr <sub>2</sub> O <sub>3</sub>	6,66
A <sub>4</sub> <sup>2</sup>	10% Cr <sub>2</sub> O <sub>3</sub>	4,37	B <sub>10</sub> <sup>2</sup>	10% Cr <sub>2</sub> O <sub>3</sub>	6,89
A <sub>3</sub> <sup>3</sup>	4% NiO	3,65	B <sub>4</sub> <sup>3</sup>	4% NiO	6,39
A <sub>10</sub> <sup>3</sup>	10% NiO <sub>2</sub>	4,16	B <sub>10</sub> <sup>3</sup>	10% NiO	6,42
A <sub>4</sub> <sup>4</sup>	4% Co <sup>2</sup> O <sub>3</sub>	2,84	B <sub>4</sub> <sup>4</sup>	4% Co <sub>2</sub> O <sub>3</sub>	7,10
A <sub>10</sub> <sup>4</sup>	10% Co <sub>2</sub> O <sub>3</sub>	2,91	B <sub>10</sub> <sup>4</sup>	10% Co <sub>2</sub> O <sub>3</sub>	6,15
A <sub>5</sub> <sup>5</sup>	4% V <sub>2</sub> O	2,66	B <sub>4</sub> <sup>5</sup>	4% V <sub>2</sub> O	6,66
A <sub>10</sub> <sup>5</sup>	10% V <sub>2</sub> O	2,58	B <sub>10</sub> <sup>5</sup>	10% V <sub>2</sub> O	4,29
A <sub>6</sub> <sup>6</sup>	4% MnO	2,33	B <sub>6</sub> <sup>6</sup>	4% MnO	4,56
A <sub>10</sub> <sup>6</sup>	10% MnO	2,04	B <sub>10</sub> <sup>6</sup>	10% MnO	4,44

The addition of alkali oxides and, as follows from the data listed in table 1, the addition of metallic oxides influences the fraction of boron atoms which take part in the building of these structural units specific of B<sub>2</sub>O<sub>3</sub> glasses, in comparison with the number of boron atoms which will participate in the building of the [BO<sub>4</sub>] tetrahedra as structural units whose  $^{11}\text{B}$  nuclei will give the narrow resonance line

It is known from the NMR theory that the number of nuclei which contribute to a resonance signal can be estimated knowing the area under the absorption curve. Since the used resonance spectrometer registers the first derivatives of the absorption curves, to determine this area, a double integration would be necessary.

The valuation of  $^{11}\text{B}$  nuclei number which participate in narrow line,  $N_4$ , and of that which determines the broad line,  $N_3$ , from the  $^{11}\text{B}$  NMR spectra obtained in the case of the studied glasses, also assumes in addition to this double integration a decomposition of the overlapping resonance. Having in view that it was not possible to simulate on computer these spectra, the above-mentioned process would be difficult to realize and would introduce a lot of errors.

A simple method to estimate the ratio  $N_4/N_3$  which does not affect the quality of the comparative studies made in this work was presented by Bray and Silver [1]. They show that

$$\frac{N_4}{N_3} = \frac{1}{K} \frac{c}{a}$$

where  $c$  is the intensity of the narrow line per mole of B<sub>2</sub>O<sub>3</sub> and is measured by the peak - to - peak signal amplitude (fig. 2a), and  $a$  is the relative intensity of the broad line per mole of B<sub>2</sub>O<sub>3</sub>, measured in our case by the height of the high - magnetic field peak because this peak is less affected by the variations in (eq Q) and ( $\eta$ ), specific of glasses.

The factor  $K$  depends only on the experimental parameters of the spectrometer such as the modulation amplitude, radio frequency oscillation level etc., and since these were maintained constant,  $K$  should be constant.

Thus, following the manner in what degree the ratio  $c/a$  modifies according to the different parameters, one will obtain information about the variation of the ratio  $N_4/N_3$  and therefore about the manner in what degree these factors influence the structure of the respective matrices.

Analysing the data listed in table I one remarks that the effect of metallic oxides has not a unitary character depending strongly on the nature of the metal. Thus, for the samples of type A one observes that the metallic oxides  $\text{MoO}_3$ ,  $\text{Cr}_2\text{O}_3$ ,  $\text{NiO}$  and  $\text{Co}_2\text{O}_3$  determine the transformation of an additional number of  $[\text{BO}_3]$  structural units into  $[\text{BO}_4]$  tetrahedra, which leads to the increase of the four-coordinated boron atoms number,  $\text{V}_2\text{O}_5$  lets rather unchanged the ratio  $c/a$ , while  $\text{MnO}$  has an opposite effect, causing a number of  $[\text{BO}_4]$  tetrahedra to return to the structural units  $[\text{BO}_3]$  specific of vitreous  $\text{B}_2\text{O}_3$ .

In the case of type B samples where the share of structural units  $[\text{BO}_4]$  is close by the maximum which can be obtained by the modification of alkali oxide content in this type of glasses, all the metallic oxides added determine a decrease of the ratio  $c/a$ , therefore they have implicitly as effect the transformation of some  $[\text{BO}_4]$  units into  $[\text{BO}_3]$  units. However, one remarks that while for the oxides  $\text{MoO}_3$ ,  $\text{V}_2\text{O}_5$  and  $\text{Co}_2\text{O}_3$  the ratio  $N_4/N_3$  continues to decrease with the increasing of metallic oxide content, in the case of  $\text{MnO}$ ,  $\text{NiO}$  and  $\text{Cr}_2\text{O}_3$  the ratio  $c/a$  is not essentially modified with the augmentation of metallic oxide from 4% mol to 10% mol.

Therefore the conclusion follows that the accurate establishment of the effect of alkali oxides on the borate glasses structure is complex, depending both on the nature of metallic oxides and on the value of the ratio  $R = (x \text{ mol \% } \text{B}_2\text{O}_3)/(y \text{ mol \% } \text{Na}_2\text{O})$  being imposed the study of this effect on more types of matrices and for more concentrations of alkali oxides.

(Received December 4, 1979)

#### REFERENCES

- 1 P J Bray and H Silver, *Modern Aspects of the Vitreous State*, vol 1, London, 1960, 0 92-119
- 2 P J Bray, M Leventhal and H O Hooper, Phys. and Chem of Glasses, **4**, 2, 47 (1963)
- 3 P C Taylor and E J Friebele, J of Non-Cryst Solids **16**, 375 (1974)
- 4 S P Zhdanov, I Kerger and E V Koromal'di, Dokl Akad Nauk, SSSR, **204**, 622 (1972)
- 5 M E Milberg, J G O'Keefe, R A Verhelst and H O Hooper, Phys Chem Glasses, **13**, 79 (1972)
- 6 Y H Yun, P J Bray, J Non-Cryst Solids, **27**, 363 (1978)
- 7 R Gresch et al, J Non-Cryst Solids, **21**, 31 (1976)
- 8 Y H Yon, P J Bray, J Non-Cryst Solids, **30**, 45 (1978)
- 9 S Simon, V Simon, Al Nicula, Studia Univ Babes-Bolyai, Phys., **1**, 77 (1979)
- 10 S Simon, I Biris, Al Nicula, Analele Univ Timisoara, **XVI**, 2, 85 (1978)
- 11 G E Jellison, Jr and P J Bray, J Non-Cryst Solids, **29**, 187 (1978)

EFFECTUL UNOR IONI PARAMAGNETICI ASUPRA STRUCTURII  
UNOR MATRICI VITROASE PE BAZĂ DE BOR

(R e z u m a t)

În lucrarea prezentă sînt expuse rezultatele obținute din studierea efectului pe care unii ionii paramagneticici îl au asupra spectrelor RMN ale  $^{11}\text{B}$  din sistemele vitroase de tipul  $x$  mol%  $\text{B}_2\text{O}_3 - y$  mol %  $\text{Na}_2\text{O}$  cărora le-au fost adăugăți în concentrații de 4% și 10% (mol) următorii oxizi metalici  $\text{MoO}_3$ ,  $\text{Cr}_2\text{O}_3$ ,  $\text{NiO}$ ,  $\text{Co}_2\text{O}_3$ ,  $\text{V}_2\text{O}_5$ ,  $\text{MnO}$ . S-a constatat astfel că acești oxizi influențează structura acestor sticle, deci și proprietățile lor fizico-mecanice, efectul oxizilor depinzînd atât de compozitîa matriciui vitroase cât și de natura oxizilor metalici utilizati.

## INVESTIGATIONS ULTRASONIQUES SUR L'ALCOOL POLYVINIQUE

D. AUSLÄNDER, E. DARVASI, A. AUSLÄNDER

**Introduction.** Les constantes de propagation de l'ultrason dans des solutions de polymères permettent d'obtenir des données relatives au degré de dépolymérisation et à la cinétique des processus de polymérisation et de dépolymérisation [1], [2], [3], [4], [5]

A un moment  $\tau$  de la dépolymérisation, la masse moléculaire est illustrée par la formule

$$M = Ae^{-K\tau} + M_\infty \quad (1)$$

où  $K$  est la constante de la vitesse de dépolymérisation tandis que  $A = M_0 - M_\infty$ ,  $M_0$  représentant la masse moléculaire initiale et  $M_\infty$  étant la valeur limite de la masse moléculaire que l'on peut obtenir dans les conditions expérimentales données, on aura

$$M_\infty = \frac{E \cdot m \cdot S_2}{q \cdot S} \quad (2)$$

où  $E$  représente l'énergie de la liaison des unités moléculaires du polymère,  $m$  — la masse moléculaire de l'unité structurale,  $S_2$  la distance interatomique limite au moment de scission de la liaison intermoléculaire, et  $q$  l'énergie de liaison des unités structurales moléculaires [6], [7], [8], [9]

**Méthodes expérimentales.** La corrélation des propriétés du polymère et des valeurs de la vitesse de propagation et d'absorption de l'ultrason a été réalisée dans des solutions aqueuses d'alcool polyvinique, à concentrations différentes, par dépolymérisations ultrasoniques, dans des conditions expérimentales variables

Ainsi s'est-on servi de champs acoustiques aux intensités variées de 4,1 W/cm<sup>2</sup> à 8,4 W/cm<sup>2</sup>, aux fréquences de 20 kHz et 1 MHz, la température de travail se situant dans l'intervalle 35 °C—65 °C, le temps d'ultrasonorisation étant de 3 à 30 minutes

On a établi, par des mesurages de densité et de viscosité, les masses moléculaires moyennes initiales et finales ainsi que le nombre de liaisons scindées par macromolécule, dans les solutions à degrés de dépolymérisation différents, obtenues pour chacune des valeurs des paramètres, dans les intervalles ci-dessus

**Résultats et discussion.** La diminution de la masse moléculaire moyenne au cours du processus de dépolymérisation corrélativement au temps d'ultrasonorisation est présentée dans la figure nr 1 pour trois valeurs d'intensité du champ de 1 MHz, dans le cas de la solution à concentration de 0,057%

La vitesse de dépolymérisation augmentant avec l'intensité, le temps de réalisation de l'équilibre, par l'arrivée à la valeur de la masse limite  $M_\infty$ , s'en trouve diminué d'autant. Dans les conditions expérimentales données, pour  $M_0 = 625\,000$ , le degré maximum de dépolymérisation se caractérise par  $M_\infty = 26\,000$

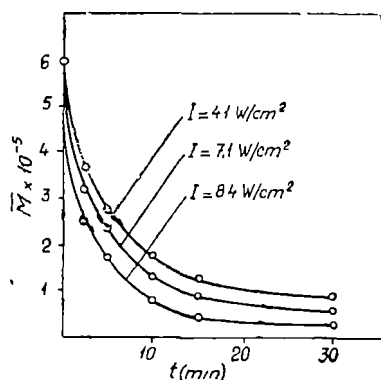


Fig 1 La dépolymérisation de l'alcool polyvinilique en fonction du temps d'ultrasonorisation

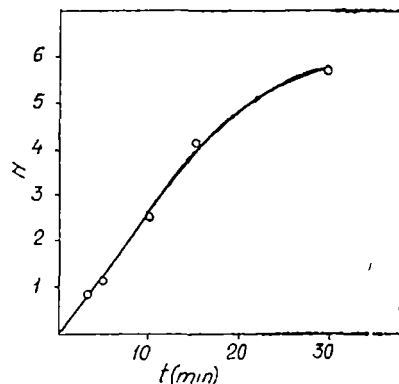
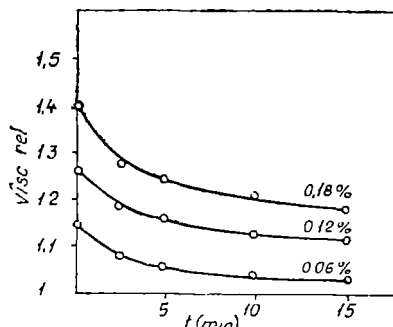


Fig 2 L'accroissement du nombre de liaisons scindées, avec le temps d'ultrasonorisation

Fig 3 Variation de la viscosité des solutions à différentes concentrations



L'accroissement du nombre de liaisons scindées  $N$ , corrélativement au temps d'ultrasonorisation est illustrée par la figure nr 2, dans le cas de la solution à concentration de 0,057%, sous l'action d'un champ de 1 MHz, à intensité 7,1 W/cm<sup>2</sup>.

De la figure nr 3 il s'ensuit que, dans les conditions expérimentales données, à savoir fréquence = 1 MHz et intensité = 8,4 W/cm<sup>2</sup>, la concentration de la solution aqueuse d'alcool polyvinilique n'influencerait pas la dépolymérisation.

Quant à la température de travail, on y relève l'existence d'une valeur optima par rapport à laquelle les valeurs inférieures et d'autant plus les valeurs supérieures s'avèrent être défavorables à la dépolymérisation.

En vue d'obtenir une caractérisation des systèmes étudiés et pour assurer le déroulement de ces processus sur la base de certaines constantes acoustiques, on a effectué le mesurage de la vitesse de propagation et d'absorption de l'ultrason dans toutes les solutions préparées, leurs constantes de dépolymérisation étant déterminées. On s'est servi à cette fin d'une méthode optique de diffraction, à fréquence de 4 MHz, respectivement d'une technique d'impulsion à fréquence de 10 MHz.

Les valeurs de la vitesse de propagation de l'ultrason et celles de la compressibilité adiabatique, calculées par la formule  $\beta_{ad} = \frac{1}{\rho c^2}$ , ont été observées dans des solutions à masse moléculaire moyenne connue.

On a calculé aussi les valeurs des constantes Rao et Wada

$$R = \frac{M}{\rho} c^{1/3}, \quad W = \frac{M}{\rho} \beta^{-1/7} \quad (3)$$

qui présentent des dépendances linéaires avec la concentration des solutions d'alcool polyvinilique

*Tableau 1*

#### Valeurs des constantes acoustiques

t us (min)	$\bar{M}$	c (m/s)	$\beta_{ad}$ ( $10^{-10} \text{ m}^2/\text{N}$ )	$R_p$	$W_p$
0	610 000	1 439,9	4,8340	497,98	2,53
5	235 000	1 439,6	4,8358	497,92	2,53
10	130 000	1 439,3	4,8370	497,85	2,53
15	95 000	1 438,8	4,8406	497,76	2,53

*Tableau 2*

#### Absorption de l'ultrason en fonction du temps d'irradiation

t us (min)	$\alpha/f^2 \cdot 10^{17} \cdot \text{cm}^{-1} \cdot \text{s}^2$
0	32,28
5	32,48
10	32,66
15	32,94
30	33,84

L'origine de ce phénomène serait la variation de la viscosité de volume au moment de scission de la chaîne de polymère et la modification correspondante des fréquences de relaxation.

**Conclusion.** Ces recherches relèvent la liaison existente entre les constantes de propagation de l'ultrason et le degré de dépolymérisation, tout comme la possibilité de caractériser le polymère par le truchement de certains incrémentes acoustiques.

(Manuscr. reçu le 11 décembre 1979)

#### B I B L I O G R A P H I E

- 1 I Perepechko, Acoustic Methods of investigating Polymers, Moscow, 1975
- 2 I Heglein, Macromol Chem, 15, 188 (1959)
- 3 A. R. Peacocke et al., Biopolymers, 6, 605 (1968)
- 4 K. Y. Sergeeva, Sov Phys Acoust, 13, 120 (1967)

- 5 K Y Sergeeva, Akust Zh, **13**, 145 (1967)
- 6 M T Shaw, F Rodriguez, J Appl Polymer Sci, **11**, 991 (1967)
- 7 J R Thomas, L Vries, J Phys chem, **63**, 254 (1959)
- 8 N H Langton, Journal of Sound and Vibration, **10**, 22 (1969)
- 9 O M Zorina, R S Nezlin, T I Vengerova, I E Elpiner, Biophysika, **13**, 595 (1968)

### CERCETĂRI ULTRASONICE ASUPRA ALCOOLULUI POLIVINILIC

(Rezumat)

În lucrare sunt prezentate unele proprietăți acustice ale soluțiilor apoase de alcool polivinilic în funcție de gradul de depolimerizare realizat prin intermediul ultrasunetelor. Prin corelarea masei moleculare medii și a numărului de legături rupte cu viteza de propagare și cu absorbția ultrasunetului, se stabilesc incrementele acustice ale unităților structurale de masă caracteristice polimerului.

NOTE

ESR AND THERMOLUMINESCENT RESPONSE OF  $\text{CaSO}_4/\text{Mn}$

F. KOCH

$\text{CaSO}_4/\text{Mn}$  is distinguished in thermoluminescent dosimetry (TLD) by relatively great and large  $\gamma$ -ray sensitivity and low thermoluminescent temperature. Metastable energy levels in crystal can be destroyed by about  $110^\circ\text{C}$  [1]. We have irradiated the  $\text{CaSO}_4/\text{Mn}$  crystals prepared with the Z Spurny method [2] with  $\text{Co}-60$   $\gamma$ -ray, tested and applied it in dosimetry [3]. It is accepted that the "light-storage" in these crystals is mainly in F and F' centers and iron transition group can act as a luminescence center, as a trap.

In 1951 Schneider and England [4] reported on ESR of Mn in luminescent ZnS powders. It is important that Lamb, Baker and Kukuchi [5] in 1959 reported for the first time a light induced ESR pattern ( $\text{Fe}^{3+}$  in a single crystal of CdS). It is stated also [6] that  $\gamma$ , n, X, UV radiations produce similar changes in monocrystals. Thus the results obtained with an irradiation may be generalized and it is evident that there are  $\gamma$  induced ESR patterns, too.

In our measurements [7], first the Mn can be identified by the appearance of the known six-line hyperfine and fine structure (fig 1). Intensity of the central ESR pattern yields direct information on the number of charge carriers trapped. In fig 2 we reproduce the central part of ESR pattern by  $1,7 \cdot 10^3$  rad(I), by  $5,1 \cdot 10^3$  rad (envelop, dotted line) II, and after  $120^\circ\text{C}$  heating (dotted line, III). The g factor calculated from these measurements in the [001] direction was 1,9827. After  $2,5 \cdot 10^4$  rad irradiation the six line hyperfine structure is in part destroyed and the ESR patterns become complicated. In fact, at these doses the crystals can't be used anymore in dosimetry.

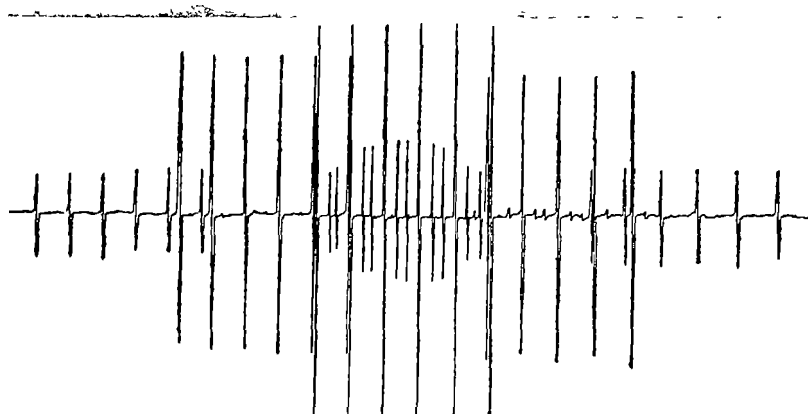


Fig 1

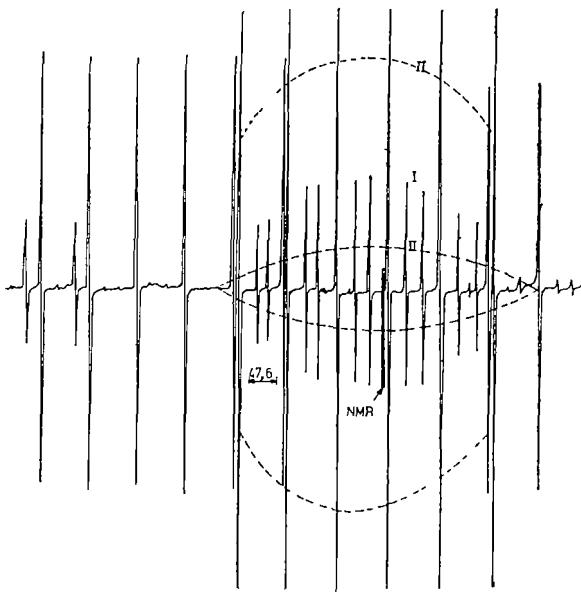


Fig 2

From fig 2 it follows that with the ESR method the great  $\gamma$  irradiations can be identified disappearance of the irradiation centres. Accordingly it can be seen the possibility of using the ESR in dosimetry and may be by archeological investigations [8]. The advantage of the ESR method compared with the TL lies in the possibility of repeating the measurements (it is not destructive).

(Received November 15, 1979)

#### R E F E R E N C E S

- 1 B B j a r n g a r d, Aktiebolaget Atomenergi (Stockholm), Report AE-118, 18 (1963)
- 2 Z Spurny, Kernenergie, 5, 611 (1962)
- 3 F Koch, C Fulea, *Solid State Symposium*, Cluj-Napoca, 1978, 65
- 4 E E Schneider, T S England, Physica, 17, 221 (1951)
- 5 J Lambe, J Baker, C Kikuchi, Phys Rev Letters, 3, 270 (1959)
- 6 C B Lusik, G G Liidjy, M A Elango, FTT, 6, 2256 (1964)
- 7 F Koch, *Program XX-th Congres Ampere, Tallinn*, Report B 1508, 1978, p 16
- 8 Motojji Ikeya, Yamaguchi Univ., Japan, Privat comun (1979)

#### RES ȘI TERMOLUMINISCENȚA $\text{CaSO}_4/\text{Mn}$

(R e z u m a t)

Cristalele  $\text{CaSO}_4/\text{Mn}$  termoluminiscente se iradiază cu radiații  $\gamma$  la doze mari. Spectrele RES înregistrate arată schimbări importante atât după iradieri, cât și după încălzirea probelor, deschizând astfel unele posibilități de folosirea RES în dozimetria cu termoluminiscență.

LA CONDUCTIVITÉ ÉLECTRIQUE ET LA TENSION  
THERMOÉLECTROMOTRICE DU SYSTÈME  $\text{Cr}_2\text{O}_3-\text{ZrO}_2$

**EMILIA MOTIU, C. CODREANU, M. VANCEA, C. GH. MACAROVICI**

On sait que dans le système  $\text{Cr}_2\text{O}_3-\text{ZrO}_2$  il y a la possibilité d'obtenir des solutions solides [1, 2]

Afin de réaliser un haut degré d'homogénéité nous avons utilisé la méthode de préparation des substances par coprécipitation des composés oxydiques, à savoir, la décomposition thermique des coprécipitats de hydroxydes [3]

On a préparé des pastilles, pressées à  $7 \cdot 10^8 \text{ N} \cdot \text{m}^{-2}$  et synthétisées à  $1500^\circ \text{C}$  sous vide. Les contacts métalliques ont été obtenus par métallisation avec platine colloïdale

A l'aide de l'installation décrite en [4] on a mesuré la résistance électrique dans le domaine de température  $20 - 1300^\circ \text{C}$ , sur des pastilles métallisées et la tension thermoélectromotrice, sur des pastilles non métallisées

Pour les onze échantillons du système, dont les propriétés électriques ont été étudiées, la composition chimique, exprimée en %mole, est présentée dans le tableau 1.

Tableau 1

**La composition chimique en mole %**

Echantillon	Zr	Cr	ZrO	CrO
1	0	100	0	100
2	10	90	18,19	81,81
3	20	80	33,33	66,66
4	30	70	46,16	53,84
5	40	60	57,14	42,86
6	50	50	66,66	33,33
7	60	40	75,00	25,00
8	70	30	82,35	17,65
9	80	20	88,99	11,11
10	90	10	94,74	5,26
11	100	0	100,00	0

L'analyse comparée des fonctions  $\log \rho = f(1/T)$ , figure 1, et de la variation thermique du coefficient de Seebeck  $\alpha = \frac{\Delta \epsilon}{\Delta T}$ , figures 2 a et b, montre que les valeurs de  $\rho$ , fonction de température, et la nature de la conductivité électrique, d'après (sign  $\alpha$ ), pour les premières compositions du système, sont comparables avec celles du  $\text{Cr}_2\text{O}_3$ , type p, ce qui nous détermine à supposer que le mécanisme de la conduction électrique est le même, c'est à dire  $\text{Cr}^{4+} \rightarrow \text{Cr}^{3+}$ , mais favorisé ici par une possible transition  $\text{Zr}^{4+} \rightarrow \text{Zr}^{3+}$

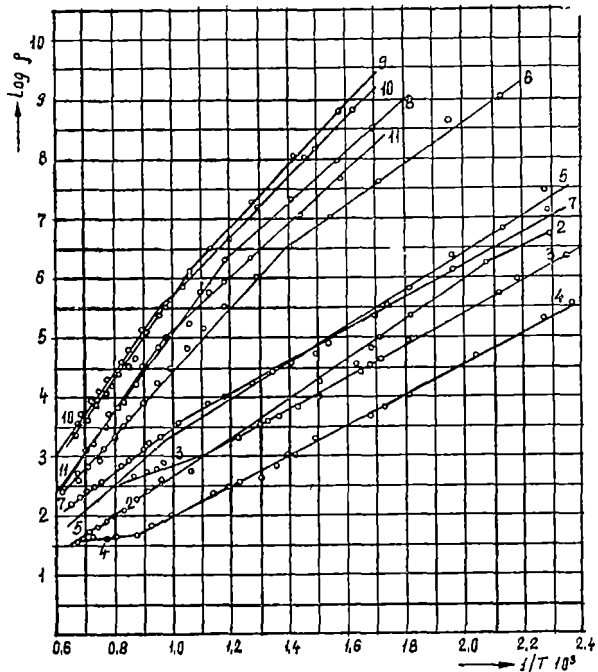


Fig 1 La variation de la résistivité fonction de  $1/T$

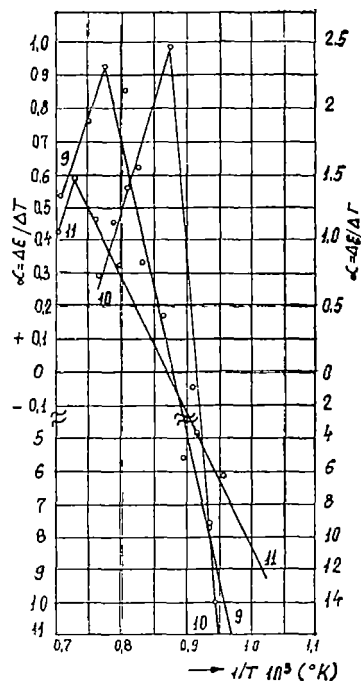
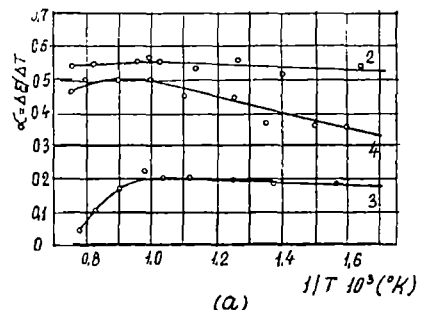


Fig 2 La variation du coefficient Seebeck fonction de  $1/T$

- a) pour les échantillons 2, 3, 4
- b) pour les échantillons 9, 11, à gauche,  
et 10, à droite

D'après les deux valeurs de l'énergie d'activation thermique, tableau 2, on voit que les compositions riches en Zr (8, 9, 10) se comportent comme le ZrO<sub>2</sub> pur, avec une conduction mixte ionique et électronique.

L'énergie d'activation thermique

Tableau 2

No	2	3	4	5	6	7	8	9	10	11
E ev	0,64	0,54	0,51	0,63	0,69	0,73	0,90	1,04	0,94	1,28

L'échantillon (4), qui présente un abaissement plus sensible de la résistivité électrique avec la température, semble être un eutechtique [5], dont la température de fusion est 2200°C, ce qui recommande cette composition comme matériau technologique pour des thermistances de haute température

(Manuscris reçu le 3 decembre 1979)

#### B I B L I O G R A P H I E

- 1 I A Toropov, L L Barzakovski, U V Lepin, N N Kurtzeva, *Diagrami sostoiania silikatnih sistem*, Izd Nauk, Moskva, 1965, p 68
- 2 D Becherescu, R Cipău, Keram Zeitsch, 11, 713 (1968)
- 3 J Paris, R Paris, Bul Soc Chim France, 1138 (1965)
4. C Codreanu, M Vancea, Studia Univ Babeş-Bolyai, Phys., 2 (1970)
- 5 E Motiu, These de doctorat, Inst de Chimie, Cluj-Napoca, 1973

#### CONDUCTIVITATEA ELECTRICĂ ȘI TENSIUNEA ELECTROMOTOARE ÎN SISTEMUL $\text{Cr}_2\text{O}_3 - \text{ZrO}_2$

(Rezumat)

În lucrare se studiază variația termică a conductivității electrice și a tensiunii electromotoare pentru o serie de probe din sistemul  $\text{Cr}_2\text{O}_3 - \text{ZrO}_2$ , preparate, pentru prima oară, prin piroliza coprecipitațiilor de hidroxizi de crom și zirconiu

## SIMPLE MATTER-ANTIMATTER SYSTEMS

R. I. CÂMPEANU

The interest in the atomic and molecular systems involving antimatter has been aroused by the analysis of bubble-chamber reactions and by recent evidence on the existence of a significant amount of antimatter (antiparticles) in cosmos. In most experiments antimatter is observed in the form of free, fast moving antiparticles. However, there are quite a large number of papers dealing with bound state systems involving antiparticles. Most of them were directed to the study of the positronium atom, the bound state of an electron with a positron. There are also few experiments which show some evidence on the bound states between a positron and various atoms and molecules. Most of the positron physics has been recently reviewed by Griffith and Heyland [1].

**The  $e^+H_2$  bound state.** We have tried in this work to show that the positron does form a bound state with the hydrogen molecule. For this purpose we have used ATMOL implemented on the IBM-360 computer of University College London. ATMOL is a package of programs which calculates molecular energies by a selfconsistent field method, using molecular functions as linear combinations of atomic wave functions.

We have obtained first the binding energy of the  $H_2$  molecule in its ground state by including in the calculation 1s, 2s and 3s electron orbitals in the  $\sigma_g$  molecular state. The electrons were represented by Slater orbitals containing a nonlinear parameter  $\alpha_1$  to be adjusted for the lowest  $H_2$  energy. We found for the internuclear distance  $R = 2$  au the lowest energy  $-1.0863$  au for  $\alpha_1 = 1.08$ , which is above the best calculated energies in the literature; in order to obtain a better result one has to include a much larger number of electron orbitals in the calculation. However we are interested in a relative calculation and in considering the ground state of the  $e^+H_2$  system we have used exactly the same wave functions for the two electrons. The positron was taken in the 2s, 3s and 4s orbitals both in the  $\sigma_u$  and  $\sigma_g$  molecular states. Having fixed  $\alpha_1 = 1.08$  we have varied  $\alpha_2$  of the positron orbitals to obtain the lowest energy.

No bound state was found for the configuration  $\sigma_g^2$  (electrons)  $\sigma_g^1$  (positron) — the energy was always above the  $H_2$  ground state energy. For the configu-

ration  $\sigma_g^2$  (electrons)  $\sigma_u^1$  (positron) and  $R = 2$  a.u. we found for  $\alpha_2 = 0.1$  the energy  $-1.2993$  a.u. which is well below  $-1.0863$  a.u. of the  $H_2$  molecule.

**Antiproton-hydrogen interaction potential.** The  $\bar{p}$ -H system is, like  $H^+$ , the simplest two-center molecular problem. It has an exact solution which was calculated by Wightman [2]. The interaction between antihydrogen and hydrogen, which has cosmological importance [3], cannot be calculated exactly and one has to choose between various approximations. Our purpose is to test two of these approximations on the  $\bar{p}$ -H system, where we have the exact answer.

A first calculation was performed using again ATMOL with a simple electron configuration  $1s$ ,  $2s$  and  $3s$ . We have taken  $\alpha_1 = 1.0$  for the H wave functions and various values  $\alpha_2 < 1.0$  for the  $e\bar{p}$  function. The best results obtained for an internuclear distance  $R = 1$  a.u. were around  $-0.5004$  a.u. well above Wightman's  $-0.51$  a.u. On the other hand, the convergence of this method seemed to be quite slow.

The second test was made by using the Rayleigh-Ritz variational method, with a trial function

$$\Psi_t = \sum_{i=1}^n c_i \lambda^{k_i} \mu^{l_i} e^{-(\alpha\lambda + \beta\mu)}$$

where  $\lambda$  and  $\mu$  are the prolate spheroidal coordinates of the electron and  $k_i$ ,  $l_i$  integers ( $l_i$  even) given by

$$k_i + l_i < \omega = 0, 1, 2, \dots$$

Table 1

$\alpha = \beta$	0.01	0.1	0.11	0.13	0.2	0.5	0.9
$-V(\text{a.u.})$	0.500212	0.501010	0.501013	0.501012	0.500925	0.498287	0.487735

In table 1 we give the variation of the interaction energy with the nonlinear parameters  $\alpha = \beta$  for  $R = 1$  a.u.,  $\omega = 8$  ( $n = 45$ ). The lowest value  $-0.501$  a.u. was obtained for  $\alpha = \beta = 0.11$ . The convergence with  $\omega$  is shown in table 2 to be very rapid. The study of this convergence allowed us to extrapolate to  $n \rightarrow \infty$ .

Table 2

$w$	0	1	2	3	4	5	6	7	8
$-V(\text{a.u.})$	0.2733	0.4307	0.4706	0.4851	0.4923	0.4962	0.4985	0.5	0.501

The extrapolated value obtained for  $R = 1$  a.u. and  $\alpha = \beta = 0.11$  was  $-0.5042$  a.u. in good agreement with Wightman's result. We shall report in a future paper the results obtained with this method for the antihydrogen-hydrogen interaction potential.

I would like to thank Dr A. Malvern for few useful discussions on the use of ATMOL.

(Received November 15, 1979)

#### REFERENCES

- 1 T C Griffith, G R Heyland, Phys Reports, **39C**, 170 (1978)
- 2 A S Wightman, Phys Rev, **77**, 521 (1950)
- 3 D L Morgan, V W Hughes, Phys Rev, **A 7**, 1811 (1973)

#### SISTEME SIMPLE DE MATERIE CU ANTIMATERIE

(Rezumat)

În prima parte a lucrării se arată că pozitronul formează cu molecula de hidrogen o stare de legătură. Apoi, având în vedere importanța cosmologică a interacțiunilor atom-antiatom, se studiază două metode de calcul al potențialului de interacție dintre antiproton și hidrogen. Rezultate foarte bune sunt obținute cu metoda Rayleigh-Ritz într-un sistem de coordonate sferoidale.

REZENZII

M. Vasile, **Electrodinamica și teoria relativității** (Electrodynamics and theory of relativity) Ed. did. și ped., București, 1979

Dr M. Vasile's book is primarily intended as a course of electrodynamics and theory of relativity. Its aim is to present an account that would give the reader a firm theoretical grounding in the subject. However, it must be emphasized that besides the theoretical problems of the electromagnetism the author presents modern applications throughout. For example, the magnetohydrodynamics, waves in plasma, magnetogravitational instability, wave-guides, electromagnetic radiation and other present-day problems of physics are treated. Some epistemological aspects of the physical phenomena from the point of view of the dialectical materialism are also analyzed.

In this volume an attempt is made to give a joint treatise of the electromagnetic field. Besides the classical macroscopic and microscopic electromagnetic field theory the author also presents a quantum mechanical point of view.

By its content and structure the book of Dr M. Vasile differs from others appeared in our country in this area. It is characterized by a clarity of ideas, its style is clear and easy to follow.

The material contained in the book has been arranged in 12 chapters and 16 appendices with a number of basic mathematical problems. At the end of each chapter there is a selection of problems which is a very useful aid to the student. For the most part these are designed to supplement the text.

The first brief chapter summarizes the fundamental relations of the macroscopic electromagnetic field theory. Maxwell's equations in free space and in material media, together with the boundary conditions are given. Finally, the basic concepts of potentials are also introduced.

The second chapter contains a short review of the classical theory of microscopic electromagnetic field.

The third chapter deals with the theory of relativity. It is worth to remark that the author, besides the theory of special relativity, gives some basic concepts of the general theory of relativity.

The following two chapters contain the four-dimensional form of the macroscopic and micro-

scopic electromagnetic field theory. Noether's theorem as well as the derivation of conservation laws from symmetry properties are also given.

The sixth chapter is devoted to the study of the electrostatic field in free space. Some general techniques for solving electrostatic problems are given and the theory of electric multipole is considered. The end of the chapter is consecrated to the electrostatic field in dielectrics.

The next chapter deals with the problems of magnetostatics. An entire chapter (VIII) is devoted to the basic equations of magnetohydrodynamics together with some applications (frozen field lines, pinch effect). The adiabatic invariants are also considered.

In the absence of sources and when a dielectric constant and permeability characterize the medium, the macroscopic Maxwell equations are linear and homogeneous. This means that wave solutions exist. The basic problems of the electromagnetic wave theory, including a model theory of the dielectric constant and a discussion of the classical dispersion relations together with the electromagnetic wave propagation in various media and inside waveguides is the subject of chapter IX.

The fundamental problems of the electromagnetic radiation is covered in chapter X. The subjects treated are among others: The retarded potentials, Electric dipole radiation, Magnetic dipole radiation, The Lienard-Wiechert potentials, Fields of an accelerated electron.

In the subsequent chapter the application of the Fourier and Laplace transforms to the study of transient phenomena in electrical circuits is shortly presented.

In the last chapter the author considers the quantum mechanical point of view. Starting from the Hamiltonian of the electromagnetic field written under the form of the sum of Hamiltonians of the harmonic oscillators, arrives at the quantisation of the free electromagnetic field. Finally, Vavilov-Cerenkov effect is considered.

Despite its shortcomings (369 pages), however, the book should prove a good basic text for the student if it is used in conjunction with the literature.

KARÁCSONYI



I. P. Cluj, Municipiul Cluj-Napoca c. 3014/1980

In cel de al XXV-lea an (1980) *Studia Universitatis Babeș-Bolyai* apare semestrial în specialitățile:

matematică  
fizică  
chimie  
geologie-geografie  
biologie  
filozofie  
științe economice  
științe juridice  
istorie  
filologie

На XXV году издания (1980) *Studia Universitatis Babeș-Bolyai* выходит два раза в год со следующими специальностями:

математика  
физика  
химия  
геология-география  
биология  
философия  
экономические науки  
юридические науки  
история  
филология

Dans sa XXV-e année (1980) *Studia Universitatis Babeș-Bolyai* paraît semestriellement dans les spécialités:

mathématiques  
physique  
chimie  
géologie-géographie  
biologie  
philosophie  
sciences économiques  
sciences juridiques  
histoire  
philologie

**43 904**

Abonamentele se fac la oficile poștale, prin factorii poștali și  
prin difuzorii de presă, iar pentru străinătate prin ILEXIM, De-  
partamentul export-import presă, P.O. Box 136—137, telex 11226,  
București, str. 13 Decembrie nr. 3.

**Lei 10**